T.R.
VAN YÜZÜNCÜ YIL UNIVERSITY
INSTITUTE OF NATURAL AND APPLIED SCIENCES
DEPARTMENT OF CHEMICAL ENGINEERING

PREPARATION OF MAGNETIC GEL-POLYMER BRUSH/METAL NANOPARTICLE HYBRID MATERIALS FOR CATALYTIC DEGRADATION OF SOME ORGANIC DYES

M.Sc. THESIS

Mohammed Abdul Kareem Shallal SHALLAL
Supervisor: Assoc. Prof. Dr. Adem ZENGİN
Second Supervisor: Asst. Prof. Dr. Necdet KARAKOYUN

VAN – 2023

T.R.
VAN YÜZÜNCÜ YIL UNIVERSITY
INSTITUTE OF NATURAL AND APPLIED SCIENCES
DEPARTMENT OF CHEMICAL ENGINEERING

PREPARATION OF MAGNETIC GEL-POLYMER BRUSH/METAL NANOPARTICLE HYBRID MATERIALS FOR CATALYTIC DEGRADATION OF SOME ORGANIC DYES

M.Sc. THESIS

Mohammed Abdul Kareem Shallal SHALLAL

VAN – 2023

ACCEPTANCE AND APPROVAL PAGE

This thesis entitled "***Preparation of Magnetic Gel-polymer Brush/Metal Nanoparticle Hybrid Materials for Catalytic Degradation of some Organic Dyes***" presented by Mohammed Abdul Kareem shallal SHALLAL under supervision of Adem ZENGIN in the department of Chemical has been accepted as a M.Sc. thesis according to Legislations of Graduate Higher Education on …...../...../..... with unanimity / majority of votes members of jury.

Chair: Signature:

Member: Signature:

Member: Signature:

This thesis has been approved by the committee of The Institute of Natural and Applied Sciences on ..……../...../…..….. with decision number of .....

Signature

…….

Director of Institute

ETHICAL DECLARATION

I declare that all the information in this thesis has been obtained and presented within the framework of ethical behavior and academic rules, and that in this thesis, which has been prepared in accordance with the thesis writing rules, all kinds of statements and information that do not belong to me have been fully cited.

Mohammed Abdul Kareem Shallal SHALLAL

ABSTRACT

PREPARATION OF MAGNETIC GEL-POLYMER BRUSH/METAL NANOPARTICLE HYBRID MATERIALS FOR CATALYTIC DEGRADATION OF SOME ORGANIC DYES

SHALLAL, Mohammed
M.Sc. Thesis, Department of Chemical Engineering
Supervisor: Assoc. Prof. Dr. Adem ZENGIN
Second Supervisor: Asst. Prof. Dr. Necdet KARAKOYUN
September 2023, 92 pages

In this study, the co-precipitation method was used to make a Pd@Polymer@$CoFe_2O_4$ catalyst that can be used again and again. The XRD analysis revealed the crystal structure of the Pd@Polymer@$CoFe_2O_4$ catalyst, confirming its composition and purity. The SEM and EDX analyses provided detailed information about the morphology and elemental composition of the sample, respectively. The phase contains Co, Fe, and Pd elements. XRD analysis confirmed the synthesis of a single-phase nanoproduct with a crystal size of 3.2 nm. VSM measurements showed the superior magnetic properties of the product; this suggests that the product has potential applications in magnetic separation processes or as a catalyst in magnetically driven reactions. Catalytic studies showed that Pd@Polymer@$CoFe_2O_4$ can catalyze the reduction of organic dyes such as methyl orange (MO), methylene blue (MB), and 4-nitrophenol (4-NP). Moreover, the magnetic catalyst showed reuse properties after several cycles. Therefore, Pd@Polymer@$CoFe_2O_4$ is a potential candidate for applying organic pollutants to wastewater treatment.

Keywords: Gel-polymer brush, Heterogeneous catalysis, Magnetic particle, Metal nanoparticle, Paint degradation

ÖZET

BAZI ORGANİK BOYALARIN KATALİTİK BOZUNMASINA YÖNELİK MANYETİK JEL-POLİMER FIRÇA/METAL NANOPARÇACIK HİBRİT MALZEMELERİN HAZIRLANMASI

SHALLAL, Mohammed
Yüksek Lisans Tezi, Kimya Mühendisliği Anabilim Dalı
Danışman: Doç. Dr. Adem ZENGIN
İkinci Danışman: Dr. Öğr. Üyesi Necdet KARAKOYUN
Eylül 2023, 92 sayfa

Bu çalışmada, tekrar tekrar kullanılabilecek bir Pd@Polymer@$CoFe_2O_4$ katalizörü yapmak için birlikte çöktürme yöntemi kullanıldı. XRD analizi, Pd@Polymer@$CoFe_2O_4$ katalizörünün kristal yapısını ortaya çıkardı ve bileşimini ve saflığını doğruladı. SEM ve EDX analizleri sırasıyla numunenin morfolojisi ve element bileşimi hakkında ayrıntılı bilgi sağladı. Faz Co, Fe ve Pd elementlerini içerir. XRD analizi, kristal boyutu 3,2 nm olan tek fazlı bir nanoürün sentezini doğruladı. VSM ölçümleri ürünün üstün manyetik özelliklerini gösterdi; bu, ürünün manyetik ayırma proseslerinde veya manyetik olarak tahrik edilen reaksiyonlarda katalizör olarak potansiyel uygulamalara sahip olduğunu göstermektedir. Katalitik çalışmalar Pd@Polymer@$CoFe_2O_4$'nın metil turuncu (MO), metilen mavisi (MB) ve 4-nitrofenol (4-NP) gibi organik boyaların indirgenmesini katalize edebildiğini gösterdi. Üstelik manyetik katalizör birkaç döngüden sonra yeniden kullanım özellikleri gösterdi. Bu nedenle Pd@Polymer@$CoFe_2O_4$, organik kirleticilerin atık su arıtımına uygulanması için potansiyel bir adaydır.

Anahtar kelimeler: Boya bozunumu, Heterojen kataliz, Jel-polimer fırça, Manyetik partikül, Metal nanopartikül

ACKNOWLEDGMENT

I would like to thank First and foremost, I thank God. I would also like to thank my esteemed supervisor, Assoc. Prof. Dr. Adem ZENGIN, for teaching and assisting me with my studies.

I would like to also thank my second supervisor, Asst. Prof. Dr. Necdet KARAKOYUN, who educated me and assisted me in my studies.

I'd like to express my gratitude to my father and my mother, and my heartfelt thanks go to all of my family members.

I want to thank my wonderful wife, Dr. Sura Saleem KHALID, and my children. This thesis would not be feasible without their assistance.

I would like to also thank Van Yil University Scientific Research Projects Coordination Unit for financial support (grant number FYL-2022-10115).

	2023
	Mohammed SHALLAL

CONTENTS

Page

ABSTRACT i
ÖZET iii
ACKNOWLEDGMENT v
CONTENTS vii
LIST OF TABLES xi
LIST OF FIGURES xiii
SYMBOLS AND ABBREVIATIONS xvii
1. INTRODUCTION 1
2. LITERATURE REVIEW 7
2.1 Polymers 13
2.1.1 Polymer Composition 13
2.1.1.1 Branching 14
2.1.2 Polymers Chemical Properties 14
2.1.2.1 Intermolecular Forces 14
2.1.2.2 Polymer Properties 15
2.1.2.3 Polymers and Environmental Pollution 16
2.1.3 Definition of Nanometer Scale 16
2.1.4 Properties of Nanomaterials 16
2.1.4.1 Mechanical Properties 17
2.1.4.2 Melting Point 17
2.1.4.3 Magnetic Properties 17
2.1.4.4 Electrical Properties 17
2.1.4.5 Chemical Properties 18
2.1.4.6 Biological Properties 18
2.2 Pd/Polymer/$CoFe_2O_4$ 18
2.3 Applications of Polymer-Metal Nanocomposites 19
2.3.1 Catalysis 19
2.3.2 Homogeneous and Heterogenized Catalyst 20
2.3.3 Nanocatalysis and Magnetic Nanoparticles 20

3. MATERIALS AND METHODS 23
3.1 Materials 23
3.1.1 Used Instruments 23
3.1.1.1 Cuvette 23
3.1.1.2 UV-Visible Spectroscopy 24
3.1.1.3 Zeiss Gemini SEM (scanning electron microscope) 25
3.1.2 Used Chemicals 26
3.1.2.1 4-NiteoPhenol Dye 26
3.1.2.2 Methylene blue dye 28
3.1.2.3 Methyl Orange Dye 29
3.2 Catalytic studies 30
3.3 Method 31
3.3.1 Synthesis of $CoFe_2O_4$ particles 31
3.3.2 Synthesis of magnetic gel brush (Polymer@ $CoFe_2O_4$) 31
3.3.3 Preparation of Pd^0 deposited magnetic gel brush (Pd/PAAmGB@Fe_3O_4) . 32
4. RESULTS 33
4.1 Characterization 33
4.1.1 SEM Analysis 33
4.1.2 EDX Analysis 35
4.1.2.1 $CoFe_2O_4$ 35
4.1.2.2 $CoFe_2O_4$@Polymer 36
4.1.2.3 $CoFe_2O_4$ @Polymer@Pd 36
4.1.2.4 $CoFe_2O_4$ @Polymer@Pd Mapping: 37
4.1.3 XRD Analysis 37
4.1.4 VSM Analysis 39
4.1.5 XPS Analysis 40
4.2 UV–Visible Spectroscopy 42
4.2.1 (4-NitroPhenol Dye) 42
4.2.1.1 (2 mg Pd@Polymer@$CoFe_2O_4$) 42
4.2.1.2 (1 mg Pd@Polymer@$CoFe_2O_4$) 43
4.2.1.3 (0.5 mg Pd@Polymer@$CoFe_2O_4$) 44
4.2.1.4 (2 mg/ml $CoFe_2O_4$@Pd, 0.2 mM 4-niteophenol, 60 mM $NaBH_4$) .. 45

4.2.1.5 (2 mg/ml Polymer@$CoFe_2O_4$, 0.2 mM 4-niteophenol, 60 mM $NaBH_4$) 47
4.2.1.6 (2 mg/ml $CoFe_2O_4$, 0.2 mM 4-niteophenol, 60 mM $NaBH_4$) 48
4.2.1.7 Recyclability of Pd@Polymer@$CoFe_2O_4$, 4-NP 49
4.2.2 Methylene Blue Dye 50
4.2.2.1 (2 mg Pd@Polymer@$CoFe_2O_4$) 50
4.2.2.2 (1 mg Pd@Polymer@$CoFe_2O_4$)..... 51
4.2.2.3 (0.5 mg Pd@Polymer@$CoFe_2O_4$)..... 53
4.2.2.4 (2 mg/ml $CoFe_2O_4$ @Pd, 0.2 mM MB, 60 mM $NaBH_4$) 54
4.2.2.5 (2 mg/ml Polymer@$CoFe_2O_4$, 0,2 mM MB, 60 mM $NaBH_4$) 56
4.2.2.6 (2 mg/ml $CoFe_2O_4$, 0,2 mM MB, 60 mM $NaBH_4$) 57
4.2.2.7 Recyclability of Pd@Polymer@$CoFe_2O_4$, MB 58
4.2.3 Methyl Orange Dye..... 59
4.2.3.1 (2 mg Pd@Polymer@$CoFe_2O_4$)..... 59
4.2.3.2 (1 mg Pd@Polymer@$CoFe_2O_4$)..... 60
4.2.3.3 (0.5 mg Pd@Polymer@$CoFe_2O_4$)..... 61
4.2.3.4 (2 mg/ml $CoFe_2O_4$ @Pd, 0.2 mM MO, 60 mM $NaBH_4$) 62
4.2.3.5 (2 mg/ml Polymer@$CoFe_2O_4$, 0,2 mM MO, 60 mM $NaBH_4$)..... 64
4.2.3.6 (2 mg/ml $CoFe_2O_4$, 0.2 mM MO, 60 mM $NaBH_4$) 65
4.2.3.7 Recyclability of Pd@Polymer@$CoFe_2O_4$, MO 66
4.2.4 The Kinetic Study 68
5. DISCUSSION AND CONCLUSION..... 69
5.1 4-Nitrophenol.....69
5.2 Methylene Blue..... 72
5.3 Methyl Orange 72
6. CONCLUSION..... 75
REFERENCES..... 77
EXTENDED TURKISH SUMMARY..... 83
CURRICULUM VITAE 93

LIST OF TABLES

Table 4.1 2 mg of Pd@Polymer@$CoFe_2O_4$with 0.05 mM of 4-niteophenol dye 43
Table 4.2 1 mg of Pd@Polymer@$CoFe_2O_4$with 0.05 mM of 4-niteo phenol dye 44
Table 4.3 0.5 mg of Pd@Polymer@$CoFe_2O_4$with 0.05 mM of 4-niteo phenol dye 45
Table 4.4 2 mg/ml of Pd@$CoFe_2O_4$ with 0.2 mM of 4-niteo phenol dye 46
Table 4.5 2 mg/ml of $CoFe_2O_4$ @Polymer with 0.2 mM of 4-nitrophenol dye 47
Table 4.6 2 mg/ml of $CoFe_2O_4$ with 0.2 mM of 4-nitrophenol dye..... 48
Table 4.7 The effectiveness of the Pd@Polymer@$CoFe_2O_4$ catalyst for 4-niteophenol dye degradation..... 50
Table 4.8 2 mg of Pd@Polymer@$CoFe_2O_4$ with 0.2 mM of Methylene blue dye..... 51
Table 4.9 1 mg of Pd@Polymer@$CoFe_2O_4$ with 0.2 mM of Methylene blue dye..... 52
Table 4.10 0.5 mg of Pd@Polymer@$CoFe_2O_4$ with 0.2 mM of Methylene blue dye.... 53
Table 4.11 2 mg of $CoFe_2O_4$ @Pd with 0.2 mM of Methylene blue dye..... 55
Table 4.12 2 mg/ml of Polymer@$CoFe_2O_4$ with 0.2 mM of Methylene blue dye 56
Table 4.13 2 mg/ml of $CoFe_2O_4$ with 0.2 mM of Methylene blue dye 57
Table 4.14 The effectiveness of the Pd@Polymer@$CoFe_2O_4$ catalyst for Methylene blue dye degradation..... 58
Table 4.15 2 mg of Pd@Polymer@$CoFe_2O_4$with 0.2 mM of Methyl Orange dye 59
Table 4.16 1 mg of Pd@Polymer@$CoFe_2O_4$ with 0.2 mM of Methyl Orange dye 61
Table 4.17 0.5 mg of Pd@Polymer@$CoFe_2O_4$with 0.2 mM of Methyl Orange dye 62
Table 4.18 2 mg of $CoFe_2O_4$ @Pd with 0.2 mM of Methyl Orange dye..... 63
Table 4.19 2 mg of Polymer@$CoFe_2O_4$ with 0.2 mM of Methyl Orange dye 64
Table 4.20 2 mg/ml of $CoFe_2O_4$ with 0.2 mM of Methyl Orange dye 66
Table 4.21 The effectiveness of the Pd@Polymer@$CoFe_2O_4$ catalyst for Methyl Orange dye degradation..... 67

LIST OF FIGURES

Figure 1.1 Several approaches for the removal or degradation of organic pollutants..... 3
Figure 2.1 Diagrammatic representation of the "grafting to" and "grafting from" methods. Grafted Polymer chains are indicated by blue lines..... 12
Figure 2.2 Propylene monomer and the repeating unit that makes up a polypropylene13
Figure 2.3 Protein Polymer unit 14
Figure 2.4 A horizontal row of 13 hydrogen atoms equal to approximately one nanometer..... 16
Figure 3.1 The cuvette used in experiment..... 24
Figure 3.2 UV–visible spectrophotometry. 25
Figure 3.3 Zeiss Gemini SEM 26
Figure 3.4 The chemical structure of 4-Niteophenol..... 27
Figure 3.5 4-Niteophenol..... 27
Figure 3.6 Chemical structure of methylene blue 28
Figure 3.7 Methylene blue..... 29
Figure 3.8 The chemical structure of Methylene Orange..... 30
Figure 3.9 Methylene Orange..... 30
Figure 4.1 Scanning electron microscopy (SEM) images, (a, b) $CoFe_2O_4$, (c, d) Polymer@$CoFe_2O_4$ 33
Figure 4.2 Scanning electron microscopy (SEM) images (E) Pd@Polymer@$CoFe_2O_4$ the particles on Pd at Polymer shell, (F) Pd@Polymer@$CoFe_2O_4$ the particles on Pd at Polymer shell under Mag 400.00 kx. 34
Figure 4.3 Energy-dispersive X-ray (EDX) spectra of the $CoFe_2O_4$ nanoparticles..... 35
Figure 4.4 Energy-dispersive X-ray (EDX) spectra of the $CoFe_2O_4$@Polymer..... 36
Figure 4.5 Energy-dispersive X-ray (EDX) spectra of the Pd@Polymer@$CoFe_2O_4$..... 36
Figure 4.6 Scanning electron microcopy (SEM)–energy-dispersive X-ray spectroscopy (EDX) mapping of the $CoFe_2O_4$ @Polymer@Pd. 37
Figure 4.7 The XRD diffraction patterns of as prepared $CoFe_2O_4$ nanoparticles..... 39
Figure 4.8 Vibrating-sample magnetometer (VSM) diagram showing (a) $CoFe_2O_4$, (b) Polymer@$CoFe_2O_4$, (c) Pd@Polymer@$CoFe_2O_4$..... 39
Figure 4.9 High-resolution XPS spectra of catalyst Pd@Polymer@$CoFe_2O_4$ 41

Figure 4.10 X-ray photoelectron spectroscopy (XPS) spectra of (a) C1s, (b) Co2p, (c) Fe2p, (d) N1s, (e) O1s and (f) Pd3d. 42
Figure 4.11 (a) 2 mg of Pd@Polymer@$CoFe_2O_4$ with 4-nitrophenol dye, (b) Time-dependent UV–Vis absorption spectra for the reduction of 4-NP. 43
Figure 4.12 (a) 1 mg of Pd@Polymer@$CoFe_2O_4$with 4-NP, (b) Time-dependent UV–Vis absorption spectra for the reduction of 4-NP. 44
Figure 4.13 (a) 0.5 mg of Pd@Polymer@$CoFe_2O_4$with of 4-NP, (b) Time- dependent UV–Vis absorption spectra for the reduction of 4-NP 45
Figure 4.14 2 mg/ml of $CoFe_2O_4$@Pd with 0.2 mM of 4-niteo phenol dye. 46
Figure 4.15 Absorption time dye using concentration 2 mg/ml of Polymer@$CoFe_2O_4$ with 0.2 mM of 4-niteo phenol dye. 47
Figure 4.16 Absorption time dye using concentration 2 mg/ml of $CoFe_2O_4$ with 0.2.. 49
Figure 4.17 The percentage of the Pd@Polymer@$CoFe_2O_4$ catalyst for 4-nitrophenol dye degradation. 50
Figure 4.18 (a) 2 mg of Pd@Polymer@$CoFe_2O_4$with MB, (b) Time-dependent UV–Vis absorption spectra for the reduction of MB. 51
Figure 4.19 (a) 1 mg of Pd@Polymer@$CoFe_2O_4$ with MB, (b) Time-dependent UV– Vis absorption spectra for the reduction of MB. 52
Figure 4.20 (a) 0.5 mg of Pd@Polymer@$CoFe_2O_4$ with MB, (b) Time-dependent UV–Vis absorption spectra for the reduction of MB. 54
Figure 4.21 Absorption time dye using concentration 2 mg of Pd@$CoFe_2O_4$ with 0.2 mM of Methylene blue dye..... 55
Figure 4.22 2 mg/ml of Polymer@$CoFe_2O_4$ with 0.2 mM of Methylene blue dye..... 56
Figure 4.23 2 mg/ml of $CoFe_2O_4$ with 0.2 mM of Methylene blue dye. 57
Figure 4.24 The percentage of the Pd@Polymer@$CoFe_2O_4$ catalyst for Methylene blue dye degradation 58
Figure 4.25 (a) 2 mg of Pd@Polymer@$CoFe_2O_4$with MO, (b) Time-dependent UV–Vis absorption spectra for the reduction of MO. 60
Figure 4.26 (a) 1 mg of Pd@Polymer@$CoFe_2O_4$ with MO. (b) Time-dependent UV–Vis absorption spectra for the reduction of MO. 61
Figure 4.27 (a) 0.5 mg of Pd@Polymer@$CoFe_2O_4$with MO, (b) Time-dependent UV-Vis absorption spectra for the reduction of MO. 62

Figure 4.28 2 mg of $CoFe_2O_4$ @Pd with 0.2 mM of Methyl Orange dye 63
Figure 4.29 2 mg of Polymer@$CoFe_2O_4$ with 0.2 mM of Methyl Orange dye..... 65
Figure 4.30 2 mg/ml of $CoFe_2O_4$ with 0.2 mM of Methyl Orange dye..... 66
Figure 4.31 The percentage of the Pd@Polymer@$CoFe_2O_4$ catalyst for Methyl Orange dye degradation..... 67

SYMBOLS AND ABBREVIATIONS

Some symbols and abbreviations used in this thesis are presented below, along with their descriptions.

Abbreviations	Description
Br-PCL-Br	A Bromine-Terminated Triblock Copolymer
EY	Eosin Y
EDS	Energy Disperse Spectroscopy
FTIR	Fourier Transformed Infrared Spectroscopy
HCB	Hexachlorobenzene
HEMA	Hydroxyethyl Methacrylate
ICP	Inductively Coupled Plasma
LDH	Layer Double Hydroxide
MB	Methylene Blue
MO	Methyl Orange
MNPs	Metal Complexes Or Metal Nanoparticles
NP	Nanoparticle
PCL	Polycaprolactone
PHEMA gel	Poly(2-Hydroxyethyl Methacrylate)
PEGMA	Polyaethylenglycolum
Pd	Palladium
Pd-NPs	Palladium Nano Particles
PNIPAM	Poly(N-Isopropylacrylamide)
SI-ATRP	Surface-İnitiated, Photoinduced Atom Transfer Radical Polymerization
SEM	Electron Microscopy
4-NP	4-Nitrophenol
RhB	Rhodamine B
XRD	X-Ray Diffraction
VSM techniques	Value Stream Mapping
UV-Vis	Ultraviolet–Visible Spectroscopy

1. INTRODUCTION

Today's world is undergoing quick, continuous developments in science and technology across all sectors. Due to its focus on the shapes and characteristics of nanoparticles with dimensions on the nanoscale, nanoscience is one of the most well-known fields of science in the present day. Understanding and regulating the behavior of materials at dimensions of 1.100 nanometers or smaller is referred to as nanotechnology because these materials exhibit distinctive phenomena and features that may be used in novel applications for the smallest possible cost. Our contribution to this research is to examine the fabrication, characterization, and characterization of organic nanomaterials on metallic compounds with the aid of prior literature on nanotechnology. This is because there has been an increase in publication in recent decades with a lot of research on the fabrication and characterization of nanomaterials. Nanomaterials are created using a variety of physical, chemical, biological, and other techniques in a variety of shapes and dimensions, both top-to-bottom and bottom-to-top. The biochemical approach uses plant extracts on mineral compounds, making it simple, quick, and ecologically friendly. One of the most significant areas to which it made a contribution by curing malignant illnesses, accurately diagnosing diseases early, delivering pharmaceuticals with high accuracy, and minimizing collateral damage, nanotechnology is used in the industrial, agricultural, and medical fields. Cancer illnesses can be effectively treated using gold nanoparticles. By understanding what is happening in the field of chemistry regarding nanotechnology, what researchers have discovered about the manufacture and diagnosis of these materials, and the most significant areas in which this cutting-edge and promising technology has been used, we have benefited from earlier studies on the manufacture and bio diagnosis of nanomaterials. Future prospects and objectives for nanotechnology include treating diseases, enhancing the functionality of electronic devices by reducing their size and cost, creating environmentally friendly materials, and solving the majority of current issues that science is still unable to resolve (Sabry, 2020).

God has endowed man with creative thinking that enabled him to intervene to control the internal structure of matter, reformulate it, modify its elements, and rearrange its atoms, as matter is the main and first support in building human

civilization, so it represents the largest area in the research and experimental programs of scientists since man thought of using stones And rocks until it reaches the nanomaterials (Sabry, 2020; Behrens, 2011; Alloosh, 2020).

The issue of the use of nanotechnology has become very important due to the results achieved by these technologies that stunned the world and for this reason, it was used on a large scale, so that it became difficult to limit the areas of its use because it included many fields if not all fields, and we mention among them the fields of medicine, agriculture, industry in all Types, cosmetics, environment (Hawya, 2020).

It should be noted that the nanotechnology revolution owes its progress to the great development that occurred in diagnostic and characterization methods such as X-rays, infrared rays, electron microscopes, and atomic force microscopy, and led to the possibility of imaging and characterizing secondary particles with accuracy up to the atomic level, as well as studying the properties of materials' surfaces. And he opened a new field, which is the possibility of studying atoms, determining their locations, and moving them to the locations that the researcher wants ((Liu et al., 2018; Dawodu et al., 2019).

To remove dangerous compounds from wastewater, various procedures can be applied. Among these include adsorption, biological processing, solvent extraction, distillation, and chemical oxidation. These technologies are costly due to their high energy requirements, as shown in Figure 1.1 (Nagarajan and Venkata Narasimhan, 2019; Das et al., 2020)

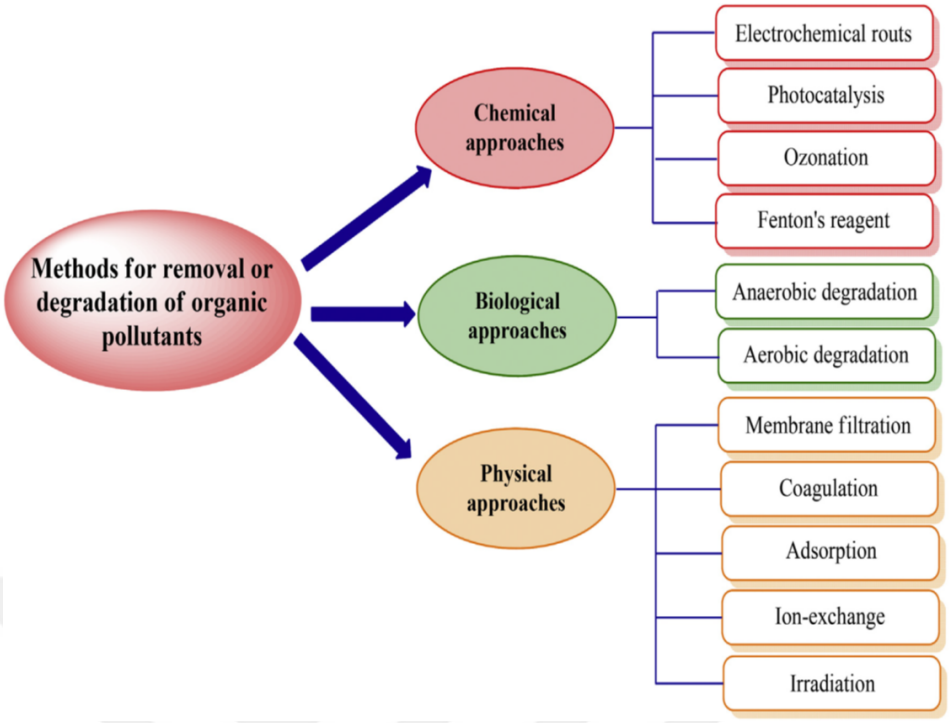

Figure 1.1 Several approaches for the removal or degradation of organic pollutants (Orooji et al., 2021)

Numerous research undertaken over the last several decades have proved the efficacy of heterogeneous or homogeneous catalysts in removing organic pollutants from the environment. Metal complexes or metal nanoparticles (MNPs) can be used to build heterogeneous or homogeneous catalysts for environmental applications (Wang et al., 2015; Bin-Jumah et al., 2020) The main disadvantage of homogeneous catalysts is that they must be kept separate from the reaction mixture. As a result, the use of heterogeneous catalysts has grown due to their numerous advantages, such as their high stability, insolubility in solvents, extensive availability of diverse supports, and, most importantly, their ability to be recycled and reused (Bin-Jumah et al., 2020).

Researchers have paid close attention to nanotechnology because of its wide range of applications. Actually, the word "nanotechnology" refers to sizes of particles ranged from 1 to 100 nm. Because of their unique nanoscale size, nanoparticles (NPs) have outstanding chemical and physical properties, such as high reactivity and high surface area to volume ratios. MNPs such as Au, Ag, Pd, and Cu NPs are examples of

MNPs that can be utilized to remove pollutants from the environment (Shaikh et al., 2020).

The fact that NPs aggregate in a reaction mixture, on the other hand, is a serious concern when using them in reactions. To get past this problem, MNPs can be utilized as catalytic support on the surface of a solid. A range of different chemicals can be used to facilitate the production of distinct heterogeneous catalysts or complexes, although synthetic and natural Polymers have gained appeal in recent years. Polymers, in other words, have a specific surface that makes them a good alternative for catalytic substrates, while their strong mechanical properties make them appropriate for long-term use (Mogha et al., 2017; Das et al., 2020).

However, due to its greater catalytic performance in contrast to the other pertinent metals, palladium (Pd) is especially utilized as a catalyst in numerous industrial processes (Corte et al., 2012). Significant effort has been made over the last ten years based on nanoscience concepts to create tiny metal nanoparticle that was durable and shown better catalytic action by raising the surface to volume ratio (Mogha et al., 2017; Das et al., 2020).

The three synthesis methods for nano-palladium that were most often used were electrochemical, chemical reduction, and radiation reduction processes (Hussain et al., 2015; Majumdar et al., 2016). The chemical reduction procedure, on the other hand, was frequently adopted because of its relatively quick rate of reaction, low cost, and convenience of use. Pd nanoparticles can be made utilizing biopolymers, according to a recent study (Tan et al., 2020; Filice et al., 2021). The active surface of nano-palladium particles was demonstrated to be governed by the Polymeric building blocks with their accessible functional groups, preventing the precipitation of inert black palladium.

Iron-based compounds are commonly utilized as catalysts in a wide range of chemical processes. The use of such systems has been increased by the addition of other simple magnetic NPs. Spinel ferrite, such as $CoFe_2O_4$, a well-known hard magnetic material, have a variety of diverse and technologically important materials due to their high saturation magnetization (Zhao et al., 2008), high coercivity (Maaz et al., 2007), strong anisotropy (Lima et al., 2015), thermal stability, and mechanical hardness.

In addition to their basic scientific interest, $CoFe_2O_4$ nanocomposites are the subject of extensive research due to their potential applications in magnetic storage

media, biosensing (Yardmc et al., 2012), catalysis (Tong et al., 2009; Rajput et al., 2013), superparamagnetic materials (Xu et al., 2013; Raghasudha et al., 2016), and medicinal applications.

Co-precipitation is one of the most extensively used processes for manufacturing ultrafine magnetic nanostructured ferrites of high purity due to its high yield and convenience of use (Vinosha et al., 2021; Chia et al., 2010). The co-precipitation method is a relatively simple and cost-effective technology that generates materials with good crystallinity, homogeneity, and acceptable textural qualities while requiring moderate temperatures (Chand et al., 2017).

In this work, a magnetically separable nano catalyst Pd@Polymer@$CoFe_2O_4$ was employed, and its catalytic activity in azo dye reduction processes and aromatic compound reduction was also examined.

2. LITERATURE REVIEW

To avoid pollution, the environmental concern caused by higher concentrations of industrial dyes must be resolved. Because of their biological and chemical durability, these dyes are extremely difficult to remove using typical degradation mechanisms. The current work presents an efficient strategy for removing these pollutants by co-precipitation. There is no substitute for these harmful nitro aromatic chemicals in human existence (apart from their usage in textile colors, medications, plastics, explosives, industrial solvents, and fungicidal agents) (Bhowmik et al., 2015). These compounds, such as 4-nitrophenol (4-NP), methylene blue (MB), and methyl orange (MO), may build up in food chain, pharmaceuticals, beverages, leather, printing, cosmetics, and food processing industries, and can be very dangerous to living organisms, causing serious damage to the kidney, liver, and central nervous system of humans, as well as causing various fatal diseases in animal blood (Mogha et al., 2017; Nagarajan and Venkatanarasimhan, 2019).

More hazardous chemicals are released into the environment as more parts of life become industrialized. Scientists are working hard to figure out how to get rid of these toxins in a sustainable way. Among the many possible ways, catalysts are a popular and efficient option. Catalytic reduction or catalytic degradation is a safe and effective method of removing contaminants. Because they efficiently remove impurities and pollutants, transition metal complexes (NPs) are useful for this. Metal catalysts based on Polymers have piqued the curiosity of researchers as efficient heterogeneous catalysts (Orooji et al., 2021).

Combining thermal breakdown and chemical reduction, a highly effective $MnFe_2O_2$ @SiO_2@Ag magnetic nanocatalyst was produced. In order to reduce organic pollutant dyes like Methyl Orange (MO), Methylene Blue (MB), Rhodamine B (RhB), and Eosin Y (EY), the catalytic performance of $MnFe_2O_2$ @SiO_2@Ag MRCs was investigated.

The conceivable process of dye reduction by the catalyst is described as an electron relay system. The catalyst absorbs electrons from the donor $BH4^-$ and transfers them to the dye molecules to begin the catalytic reduction, which is started by the Ag NPs relaying electrons from the donor $BH4^-$ to the dye molecules.

The hydride from $BH4^-$ may be trapped and adsorbed on the surface of the AgNPs when $NaBH_4$ is introduced to the reaction solution, transferring the hydride's electron to the AgNPs. The outcomes demonstrated the outstanding activity of the reduction azo dyes. It might make an ideal foundation for the development of incredibly effective magnetic catalysts for a variety of heterogeneous catalytic reduction applications (Kurtan et al., 2016).

Magnetite (Fe_3O_4) NPs were created using the hydrothermal technique. The size range of SiO_2 is between 320 to 950 nm. The superparamagnetic and catalytic activities of silver nanoparticles deposited on the surface of Fe_3O_4@SiO_2 nanospheres were measured. The photodegradation and reduction of methylene blue (MB) and 4-nitrophenol (4-NP) were examined using the Fe_3O_4@SiO_2/Ag Nanocatalyst in its as-prepared state. The photodegradation of MB took 14 minutes, while the decrease of 4-NP required 12 minutes. By boosting absorption in the visible light range and decreasing the bandgap, the deposition of Ag nanoparticles on the surface of the silicon dioxide core-shell boosted photocatalytic activity. Even after six cycles of usage, the Fe_3O_4@SiO_2/Ag MNCs generated retain nearly the same catalytic efficacy (Nabiet et al., 2021; Gürbüz et al., 2021).

Silver silica-coated magnetite nanospheres (Fe_3O_4@Ag/SiO_2) were created using sonication and their ability to remove Methylene Blue as a nanoadsorbent was examined. The equilibrium and kinetics of adsorption were studied using XRD, SEM, EDX, TEM, and FTIR. At pH 7.3, they were able to eliminate 99.6% of the methylene blue in batch mode testing. Five cycles were employed to regenerate Fe_3O_4@Ag/SiO_2 nanospheres. With the Langmuir isotherm model, the elimination process worked effectively (Jyoti et al., 2017) examined thermodynamic parameters and postulated spontaneous, endothermic, and probable adsorption of Methylene Blue under investigated experimental conditions.

A simple hydrothermal procedure was used to successfully manufacture a $CoFe_2O_4$ /CdS nanocomposite (with a particle diameter of 20 nm and a specific surface area of 39.329 m2/g). The $CoFe_2O_4$ /CdS nanocomposite was easily separated from aqueous solutions, according to magnetic tests. It was looked into how well the $CoFe_2O_4$ /CdS nanocomposite degraded methylene blue, rhodamine B, and methyl orange with the help of H_2O_2.

The breakdown of all dyes examined by the nanocomposite demonstrated excellent sonocatalytic activity; the colors were entirely eliminated in 3–9 minutes. (Farhadi and Siadatnasab, 2016).

A straightforward hydrothermal method is successfully employed to create $MnFe_2O_2$ nanoparticles and PAA/$MnFe_2O_2$ nanocomposites, which are then used to remove MB dye from an aqueous solution. XRD, FTIR, SEM, TEM, and VSM methods were used to characterize the end materials. The FTIR spectra unequivocally demonstrate that PAA is incorporated into the surface of the $MnFe_2O_2$ nanoparticles. Studies on MB adsorption reveal that a PAA coating can significantly increase the ability of $MnFe_2O_2$ nanoparticles to bind MB. This demonstrates that the PAA/$MnFe_2O_2$ nanocomposites that were created as-is are appropriate adsorbents for the commercial removal of MB dye (Wang et al., 2015).

A two-step technique was used to create the catalyst Fe_3O_4@Polystyrene@Ag (Fe_3O_4@PS@Ag). First, magnetic microspheres containing carboxyl groups (Fe_3O_4@PS-COOH) were successfully produced using the microemulsion Polymerization procedure. The Ag ions were then used to adsorb on the Fe_3O_4@PS microspheres' surface before being reduced there. To precisely determine the catalytic efficacy of the Fe_3O_4@PS@Ag catalyst, reduction operations including MB, RhB, and 4-NP were conducted in the presence of $NaBH_4$. Furthermore, a magnet could easily extract them from an aqueous solution, allowing the catalyst to be recovered and reused after the catalytic process. The findings suggested that the Fe_3O_4@PS@Ag catalyst has a strong catalytic performance, and these dyes can be reduced in a very short time (Revathi et al., 2020; Wang et al., 2021).

The manufacture, characterization, and degradation efficiency of new nickel/hydroxyapatite/cobalt ferrite (Ni/HAP/$CoFe_2O_4$) nanocomposites, including organic dyes, has been. The methylene blue and methyl orange organic dyes were broken down using the composite as both a heterogeneous catalyst and nanoadsorbent. when H_2O_2 is present however, considerable catalytic degradation of both dyes was seen. In the presence of hydrogen peroxide, the catalyst degraded methyl orange and methylene blue by about 90% and 99.1%, respectively, in 90 minutes.

The decolorization process includes the generation of reactive oxygen species (ROS), including hydroxyl and perhydroxyl radicals ($HO^{\bullet}$ and $HOO^{\bullet}$), and Fenton and Fenton-like reactions. The Ni/HAP/$CoFe_2O_4$ nanocomposite exhibited exceptional catalytic activity, stability, and superparamagnetic properties (Le et al., 2014; Das et al., 2020).

Metal oxide nanoparticles of the spinel type were created using co-precipitation. Monoethylene glycol (MEG) was utilized as a capping agent to stabilize the particles and prevent agglomeration. XRD and EDX analyses revealed that the nanocrystalline sample was very pure as manufactured. The SEM scans showed that the calcined sample had an irregular shape and variable structural morphology. SEM image examination determined the size of $CoFe_2O_4$ nanoparticles to be between 30 and 345 nm. As a result of the calcination technique, $CoFe_2O_4$ nanoparticles attracted the magnet and exhibited ferromagnetic characteristics (Demirelli et al., 2014; Dinçer et al., 2017).

The sol-gel and co-precipitate procedures were used to create $CoFe_2O_4$ and ZnO nanopowders. $CoFe_2O_4$ nanoparticles were employed as seeds in co-precipitation to form ZnO/$CoFe_2O_4$ and ZnO/$CoFe_2O_4$/Ag nanocomposites. The structure, morphology, and operation of the produced samples were examined using X-ray diffraction, field emission scanning electron microscopy, transmission electron microscopy, Fourier transform infrared spectroscopy, diffuse reflectance spectroscopy, and a vibration sample magnetometer. According to the microstructural investigation, the produced nanoparticles had spherical morphologies with an average particle size of 30-47 nm. The effect of nanocomposites on acid violet and acid brown degradation was investigated using UV radiation. In comparison to other samples, the $CoFe_2O_4$/ZnO nanocomposite displayed improved photocatalytic activity, with acid violet and acid brown degradation efficiencies of 76% and 63%, respectively. The improved photocatalytic activity of the $CoFe_2O_4$/ZnO hybrid may be attributed to the formation of a suitable internal structure between the two components. According to the magnetic data, hybrid nanopowders have ferrimagnetic characteristics, making them suitable for magnetic recovery (Ferdosi et al., 2018; Yang et al., 2021).

These dyes are very difficult to degrade due to their stable but complex aromatic molecular structure, but nowadays these organic dye molecules are e.g. adsorption (Lavanant et al., 2009; Bhandari and Knecht, 2012), membrane treatment (Haobin Ye

et al., 2021), biodegradation (Biesalski et al., 2002), photocatalysis and advanced oxidation processes have been studied to decompose it with various methods (Cao et al., 2013).

Polymer brushes are stretched Polymer chains formed by physical or covalent bonding on surfaces like gold, glass, mica, or colloidal particles. As Polymer concentration increases, hydrophobic and hydrophilic interactions increase, leading to an elongated conformation. This regularity and conformation enable the preparation of biocompatible, bioactive, hydrophobic, and hydrophilic surfaces by altering Polymer types and end groups (Deka et al., 2016).

The chemical adsorption method, on the other hand, is divided into three subheadings:

- Grafting method to the surface

In this method, the surface is functionalized with a Polymer end group and a suitable chemical group, then immersed in a Polymer solution. The Polymer is chemically adsorbed, resulting in low binding density Polymer brushes. The surface is modified with a monomeric unit molecule and immersed in a solution. Polymerization is initiated at a suitable temperature, resulting in more brushes than surface grafting (Bhandari and Knecht, 2012).

- Grafting method from the surface

In this method, the surface grafting method involves covalent bonding to the initiator surface and Polymerization after immersion in a solution containing monomers and initiators. This method produces denser, tightly stacked, and homogeneously dispersed Polymer brushes. The diffusion of monomers towards active-ended radicals on the surface affects grafting density, allowing for longer chain lengths in Polymer brushes. This method is widely used in various applications (Chen et al., 2006).

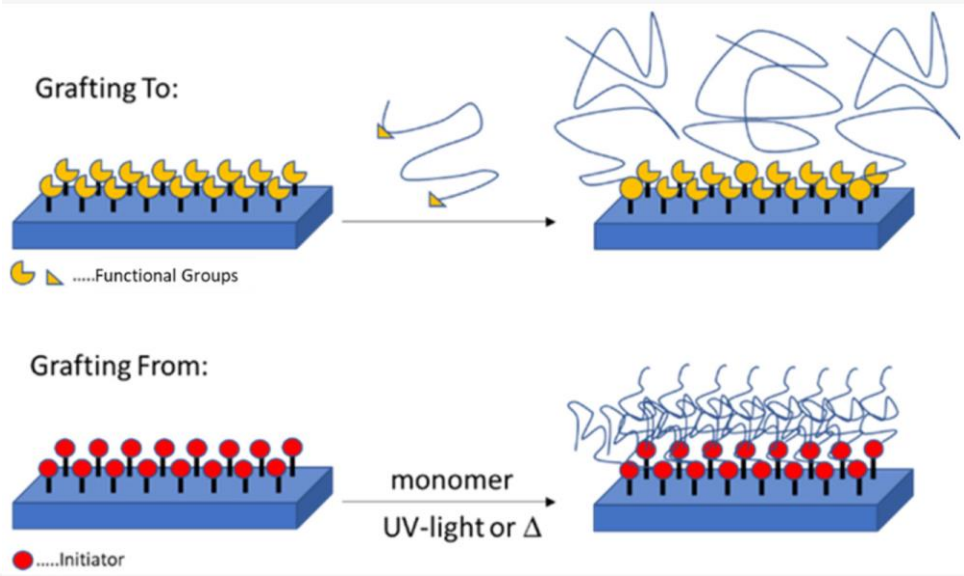

Figure 2.1 Diagrammatic representation of the "grafting to" and "grafting from" methods. Grafted Polymer chains are indicated by blue lines (Dyer, 2006)

Magnetic nanoparticles have numerous applications in magnetic fluids, MRI, catalysis, food, safety, and clinical settings. They require good stability to be effective. Diameters between 10-20 nm offer optimum stability, as they behave as single magnetic particles and exhibit superparamagnetic properties above the blocking temperature. However, particles in the 5-20 nm range have instability due to high energy, causing agglomeration and forming particles different from their original structure and diameter (Song et al., 2023).

In order to eliminate this situation, which is frequently encountered in the laboratory environment, the particles are modified with stabilizing protective groups during or after synthesis. Polymers such as poly (vinyl pyrrolidone), poly (ethylene glycol), surfactants such as oleic acid or sodium dodecyl sulfate, organic salts such as sodium citrate and layers such as silica, gold and silver are used as protective groups. Although such secondary modifications increase the response time of the particles to the magnetic field, they are more advantageous because they allow the particles to remain stable for a very long time (Rigoberto et al., 2004; Song et al., 2023).

2.1 Polymers

A Polymer is a substance with a high molecular weight that consists of repeated subunits. These substances may be natural or manufactured in origin, and they may be organic, inorganic, or mineral-organic (Biesalski et al., 2002)

Due to the special characteristics of Polymers, they now play a crucial and comprehensive role in daily life, including coatings, photoresists, fibers, plastics, ceramics, paper, adhesives, construction materials, soil components, plants, and living things. They are crucial in mechanical engineering, biology, computing, medicine, space exploration, human health, and environmental protection (Liu et al., 2018; Song et al., 2023).

Synthetic Polymers are more energy-efficient and lightweight, making them suitable for various applications. They are also used in engineering, such as gears, rollers, and structures. Polymers have a common name and structure, determined by the International Union of Pure and Applied Chemistry. Initials and brand names are used to identify most Polymers, such as polystyrene and Furrell-polyester, which are PET fibers made of polyethylene terephthalate (Astruc et al., 2005; Cai et al., 2017; Nagarajan and Venkatanarasimhan, 2019).

2.1.1 Polymer Composition

The components that repeat identically make up Polymer structures. These units themselves are composed of more compact molecules known as monomers, or monomers (plural of monomers). The monomers react with each other to form a Polymer as we see in Figure 2.2.

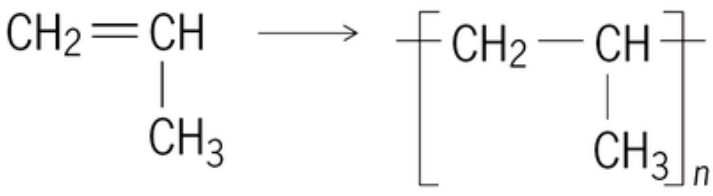

Figure 2.2 Propylene monomer and the repeating unit that makes up a polypropylene (Astruc et al., 2005)

With the exception of the terminal group in the polypropylene chain, it consists completely of this repeating unit. Numbers of such units (n) in the Polymer chain are called the degree of Polymerization or DP. Other Polymers, such as proteins, can be described by writing the approximate repeating unit as seen in Figure 2.3, where the nature of R is variable (replaced by an atom or group of atoms).

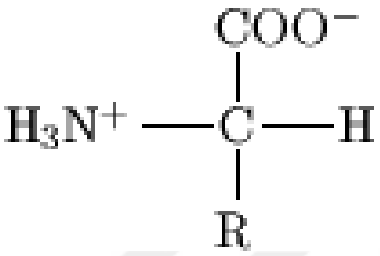

Figure 2.3 Protein Polymer unit (Astruc et al., 2005)

2.1.1.1 Branching

Polymer chain development can involve branching out. This happens when a chain wraps back and binds to an earlier segment of it during the Polymerization of free radicals. Small pieces are left behind as buds in the main carbon chain when this coil of carbon is disrupted. Branched chains are unable to align as precisely as without branches chains. As a result, there is less contact between the atoms in the various chains, which lowers the possibility of induction or the formation of permanent dipoles. Additionally, there are low-density sections of the chains. Evidence for this is the low melting points and weak tensile strength of the intermolecular forces are weak and can be easily broken (Alloosh, 2020).

2.1.2 Polymers Chemical Properties

2.1.2.1 Intermolecular Forces

The characteristics of Polymers are mostly determined by the attraction forces between their chains. Because the Polymer chains are so long, the attractive forces between the molecules are greater than the normal intermolecular forces. Long chains

are also amorphous (the way they are oriented is random). The shape of the Polymers can be visualized as if they are long, many, tangled strands. These intermolecular forces lead to high tensile forces and raise melting temperatures (Farhadi and Siadatnasab, 2016; Cao and Zuo, 2020).

Intermolecular forces can be seen by the dipoles between the monomers. Polymers containing amide groups can form hydrogen bonds with neighboring chains. Strong attraction exists between the negative oxygen ions in the C=O groups of one chain and the positive hydrogen atoms in the N-H groups of the opposite chain. These hydrogen bonds lead to an increase in the tensile strength and melting point of Kevlar. Polyesters have dipole-dipole bonding between oxygen atoms in C=O groups and hydrogen atoms in H-C groups. Dipole bonding is not as strong as hydrogen bonding, so the melting temperature and tensile strength of polyethylene are lower than Kevlar, but polyesters have higher elasticity (Cao and Zuo, 2020; Chishti et al., 2021).

Polyethylene generally does not have a bi-polarity. This reduces the electron density on one side of the Polymer chain, resulting in a small positive charge on that side. This charge is sufficient to attract the other Polymer chain. Van der Waals forces are very weak, therefore, polyethylene melts at lower temperature (Chishti et al., 2021).

2.1.2.2 Polymer Properties

Polymer characteristics can be determined using various laboratory methods, including large-angle X-ray scattering, small-angle X-ray scattering, and neutron scattering. Gel-transmission chromatography determines molecular weight, while Fourier transform and Fourier-dispersion infrared spectroscopy determine composition. Thermal properties, such as glass transition temperature, can be determined using differential scanning calorimetry and mechanical and motion analysis. Pyrolysis and analysis of small components are also techniques used to determine potential Polymer composition. The material used in banknotes is commemorative in some countries (Bashir et al., 2020).

2.1.2.3 Polymers and Environmental Pollution

Monomers are crucial materials for modern life due to their diverse uses and production options. However, they do not degrade naturally due to their unique ecosystem. When introduced to the environment, they cause contamination, which worsens daily. Polymers can be breeding grounds for rodents and insect pests, contribute to nature's deformation, and spread across seas and oceans, posing a hazard to fish. Disposal of these materials remains problematic, as burning them leads to air pollution and is not entirely effective. Examples include rubber tires burning, emitting thick smoke and bad smells, and polyvinyl chloride releasing harmful hydrogen chloride gas (Ali et al., 2021).

2.1.3 Definition of Nanometer Scale

It is a unit for measuring the lengths of very tiny objects that can only be seen under an electron microscope. Unit which used to express the dimensions of the diameters and measurements of atoms and molecules of substances, cells and microscopic particles such as bacteria. One nanometer equals one thousandth of a million (billionth) part of a meter contains a billion parts of a nanometer (nm), which is equal to 10 nanometers). For comparison, one nanometer is approximately equal to the length of a row of 13 hydrogen gas atoms if we imagine that they are stacked next to each other as seen in Figure 2.4.

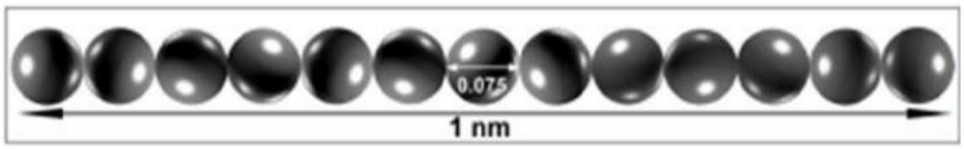

Figure 2.4 A horizontal row of 13 hydrogen atoms equal to approximately one nanometer (Hawya, 2020)

2.1.4 Properties of Nanomaterials

One may say that nanoparticles are a special class of sophisticated materials that can be created with internal granules that have diameters between 1 and 100

nanometers. Important pillar of the technologies of this century, and nanomaterials vary in terms of source, and they differ according to their source, they may be organic or inorganic materials, natural or synthetic (manufactured) (Balasubramanian et al., 2019; Cao and Zuo, 2020).

2.1.4.1 Mechanical Properties

The hardness value of metallic materials and their alloys increases, as well as their resistance to bear the different weights that fall on it, by minimizing the size of the material's grains and controlling the arrangement of its atoms (Balasubramanian et al., 2019; Yang et al., 2021).

2.1.4.2 Melting Point

The value of the melting temperature of the material is affected by reducing the dimensions of its granules, for example, the melting point of gold is 1064 degrees Celsius, and if we decrease the diameter of the gold granules, the melting point decreases by about 500 degrees Celsius (Shaikh et al., 2020).

2.1.4.3 Magnetic Properties

The size of the grains of the stuff out of which the magnet is formed have a sole bearing on the magnet's strength. The smaller the size of the secondary granules, the greater their outer surface area, and the more atoms on the surface, the greater the strength and intensity of the magnet (Balasubramanian et al., 2019).

2.1.4.4 Electrical Properties

The small sizes of nanomaterials have a positive effect on their electrical properties, as the ability of the materials to conduct electric current increases, as nanomaterials are used in the manufacture of microsensors and electronic chips in modern devices, which are of high technical specifications (Shaikh et al., 2020).

2.1.4.5 Chemical Properties

If the nanoparticles are homogeneous and of the same size, their interaction increases (Balasubramanian et al., 2019).

2.1.4.6 Biological Properties

The distribution of pharmaceuticals and therapeutic medications to the individual receiving them via membrane and veins is made easier by improving the appropriateness and bio compatibility of nanostructures and improving their capacity to permeate and penetrate biological barriers (Hawya, 2020).

2.2 Pd/Polymer/$CoFe_2O_4$

Organic colors derived from industrial waste endanger both human health and the environment. As a result, creating efficient solutions to breakdown organic in wastewater is critical for a civilization. Adsorption, chemical precipitation, biological mechanisms, and sophisticated oxidation processes have all been used to degrade organic dyes. Catalysts based on transition metal oxides (e.g., Fe, Co, and Cu) have received a lot of them are cheap, environmentally friendly, magnetically reusable, and display visible light reactions. Because of its outstanding stability, separation, and catalytic activity, spinel-type cobalt ferrite ($CoFe_2O_4$) has been extensively researched for organic dye degradation (Cao and Zuo, 2020).

So far, several methods for synthesizing $CoFe_2O_4$ have been proposed. However, to obtain the final products, such methods typically involve complicated procedures such as long reaction times, repeated washing, and calcination. For practical applications, a simple and efficient synthesis process is required. A solution combustion synthesis (SCS) method for manufacturing oxide nanomaterials with a high yield has been devised to manufacture magnetic $CoFe_2O_4$ nanoparticles. This process is essentially a redox reaction between fuels and oxidizers that is exothermic (Cao and Zuo, 2020; Cai et al., 2021).

Metal nitrates are commonly used as oxidizers, and glycine, citric acid, urea, and other fuels are used as fuels. Furthermore, the energy produced by exothermic reactions can be used to power the reaction system. Furthermore, the equipment used in this process is simple and inexpensive. A material's magnetic characteristics are greatly influenced by particle size and production method. Products may have a variety of unwanted phases, which impair their magnetic characteristics. With the benefits and characteristics of SCS, pure $CoFe_2O_4$ nanoparticles can be prepared in a single step without further processing (Costantini et al., 2010; Cao and Zuo, 2020).

2.3 Applications of Polymer-Metal Nanocomposites

2.3.1 Catalysis

It is extensively employed as the core of many chemical processes, from scientific research in university laboratories to economic research in industry laboratories, and catalysis is becoming more and more significant in chemical reactions. The role of the catalyst in chemistry, especially in organic synthesis, is crucial because it can effectively and sustainably synthesize commodities while also considerably promoting chemical processes and reactions. It is difficult to create new, sustainable chemical processes for the synthesis of natural products, medications, and physiologically active substances without the use of catalysis. A catalyst makes sure a chemical process consumes less energy, like heat (Kazemi et al., 2018; Orooji et al., 2021).

Catalysis is one of the most important areas of MNP use. NPs are highly selective catalysts and are in organic synthesis, the chemical industry, and other industries. On the surface of the catalyst, heterogeneous catalytic processes are known to occur. This indicates that in the case of monometallic MNPs, the central section of the catalyst particle is not involved in the catalytic process and can be replaced with another metal. In compared to monometallic PGM-MNPs, the synthesis of core@shell catalyst MNPs constituted of a low-cost metal corecoated with a thin PGM-shell can significantly reduce the total cost of the catalyst (Sabry, 2020; Alonso et al., 2022).

Catalysts and catalytic processes have received a lot of study recently, with the goal of discovering useful uses pharmaceutical and fine chemical. Catalysis has played an important enhancing and developing organic synthesis, particularly in medicinal chemistry, and has become one of the most commercially and environmentally significant technologies to date. The modern period of organic synthesis is moving toward innovative tactics that emphasize or focus on the concept of green chemistry, particularly the use of sustainable catalysts (Kazemi et al., 2018; Orooji et al., 2021; Alonso et al., 2022).

2.3.2 Homogeneous and Heterogenized Catalyst

Chemists concur that Homogeneous catalysis is a type of catalysis where the catalyst is in the same phase as the reactants, allowing for adjustable chemo-, region-, and enantioselectivity. This type of catalysis offers high selectivities, higher yield, higher turnover numbers, and easy optimization through ligand and metal modification. However, separating homogeneous catalysts from the desired products or reaction medium is a challenging task, requiring costly techniques and metal contamination control. Additionally, it is incompatible with green chemistry principles in modern catalysis. To address these issues, scientists have developed innovative, environmentally friendly, and efficient heterogonous catalytic systems (Kazemi et al., 2018; Orooji et al., 2021).

2.3.3 Nanocatalysis and Magnetic Nanoparticles

Nanotechnology focuses on molecular structure changes, focusing on objects smaller than 100 nm. It is a significant achievement in chemistry, particularly in nanocatalysis, a field that uses nanomaterials (averaging 1-100 nm in size) as catalysts in various catalysis applications. This technological revolution has led to significant advances in catalysis (Cai et al., 2021; Kongor et al., 2021).

Tailoring parameters like size, shape, and morphology can significantly improve nanocatalysts' catalytic activity, selectivity, and stability. Particle size and support for catalyst dispersion are crucial factors influencing nanocatalysis effectiveness.

Separating catalysts using centrifuges or filtering processes is challenging, laborious, and long-consuming (Kaang et al., 2018; Cao and Zuo, 2020; Kongor et al., 2021).

3. MATERIALS AND METHODS

The original value of this study (scientific quality, difference and innovation, how to eliminate any deficiency or how it will solve, which problem and what kind of original contribution it will make methodologically/conceptually/theoretically to the relevant science/technology fields, etc.) should be explained in details as follow.

In the study, a gel-brush combination will be made on magnetic particles for the first time. The magnetic nature of the material will enable magnetic separation, and will provide a lot of functionality in the separation of the catalyst both in the purification stage and in the catalytic reaction. As a result of the use of controlled living Polymerization in the preparation of gel-brush, it is a great advantage that the architectural structure and layer thickness of the gel-brush can be controlled only by changing the synthesis conditions.

It is thought that as a result of doping metal nanoparticles on the gel-brush, the stability of the particles will be higher than when doping metals to simple organic molecules. It is thought that this situation will increase the catalytic efficiency.

Since it is basically a Polymeric support material, it will cause an increase in the number of particles per unit area and the catalytic efficiency will be high. As a result, as a result of the comprehensive literature review (WOS 2015-2021), it was determined that the material to be used in the proposed study was not used in a catalytic reaction before. Therefore, the study is considered to be original.

3.1 Materials

3.1.1 Used Instruments

3.1.1.1 Cuvette

A cuvette, which translates to "little vessel" in French, is a small tube-like container with straight sides and a circular or square cross-section that is used in laboratories. It is formed of a clear, transparent substance like plastic, glass, or fused quartz and is sealed at one end as seen in Figure 3.1. Cuvettes are made to store samples

for spectroscopic analysis, which involves passing a beam of light through the sample to determine its absorbance, transmittance, fluorescence intensity, fluorescence polarization, or lifetime. The spectrophotometer is used to make this measurement (Edwerd, 2020; Cuvette - Wikipedia, 2022).



Figure 3.1 The cuvette used in experiment, (Cuvette - Wikipedia, 2022)

3.1.1.2 UV-Visible Spectroscopy

UV spectroscopy or UV–visible spectrophotometry (UV–VIS or UV/VIS) refers to reflectance or absorption spectroscopy in the nearby visible and entire, neighboring ultraviolet parts of the electromagnetic spectrum. This methodology is frequently employed in a variety of practical and theoretical applications since it is reasonably affordable and simple to execute. The sample must only be a chromophore and absorb in the UV-Visible range. Fluorescence spectroscopy is enhanced by absorption spectroscopy. In addition to the measurement wavelength, variables of interest include absorbance (A), transmittance (%T), and reflectance (%R), as well as how they change over time (Shaikh et al., 2020; Abdul Wahid, 2023).



Figure 3.2 UV–visible spectrophotometry

The amount of discrete UV or visible light wavelengths that are absorbed by or transmitted through a sample in contrast to a reference or blank sample is measured by a method called UV-Vis spectroscopy. This feature, which may reveal information about what is in the sample and at what concentration, is influenced by the makeup of the sample. Let's first think about the characteristics of light because the spectroscopic method depends on its utilization (Decher et al., 1992; Abdul Wahid, 2023).

3.1.1.3 Zeiss Gemini SEM (Scanning Electron Microscope)

The Zeiss Gemini is a line of scanning electron microscopes (SEMs) produced by Carl Zeiss, a German manufacturer of optical and optoelectronic equipment. These advanced instruments are used for high-resolution imaging of nanoscale samples. They feature innovative technology like field emission electron sources, variable pressure operation, high-resolution imaging, EDS for elemental analysis, and EBSD for crystallographic information.

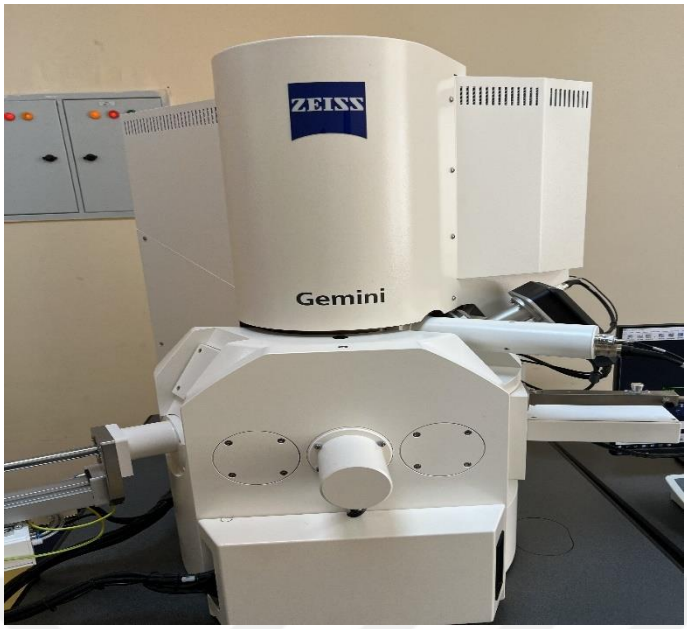

Figure 3.3 Zeiss Gemini SEM (scanning electron microscope)

3.1.2 Used Chemicals

Magnetic composites of cobalt ferrite nanoparticles, Sodium borohydride ($NaBH_4$), Palladium (Pd), 4-Nitrophenol, Methylene Blue, Methyl Orange will be explained.

3.1.2.1 4-NitroPhenol Dye

The phenolic chemical 4-nitrophenol, commonly known as p-nitrophenol or 4-hydroxynitrobenzene, has a nitro group opposite the hydroxyl group on the benzene ring as shown in Figure 3.4. Two polymorphs of 4-nitrophenol can be seen when it is crystallized. Alpha particles are transparent pillars that are unstable at ambient temperature but stable when exposed to sunlight. The beta form is stable at room temperature and consists of yellow pillars as shown in Figure 3.5; when exposed to sunlight, it progressively turns red. Usually, these two types combine to make 4-nitrophenol. 4-nitrophenol is typically employed in the production of medicines (such as acetaminophen), fungicides, methyl and ethyl parathion insecticides, and dyes, as well as to darken leather (Abdollahi and Mohammadirad, 2014; Orooji et al., 2021).

A crystalline solid in the color range of white to light yellow is 4-nitrophenol. Contact may cause serious skin and eye irritation. By skin contact, it is only moderately toxic and poisonous when consumed (Baran and Nasrollahzadeh, 2021).

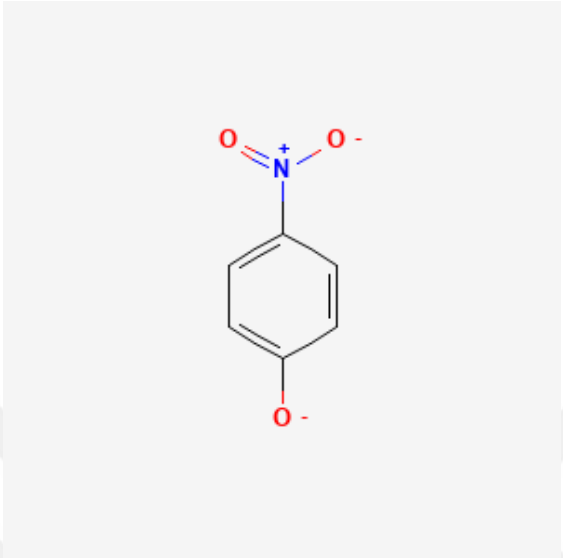

Figure 3.4 The chemical structure of 4-Nitrophenol (Baran and Nasrollahzadeh, 2021)



Figure 3.5 4-Nitrophenol

3.1.2.2 Methylene Blue Dye

The salt methylthionine chloride, also known as methylene blue, is employed as a medicine and a color. By chemically reducing the ferric iron in hemoglobin to ferrous iron, it is primarily used as a medicine to treat methemoglobinemia. The counterion of methylene blue is 3,7-bis (dimethyl amino) phenothiazin-5-ium, which is an organic chloride salt. An everyday dye with anti-inflammatory, anti-malarial, antidepressant, and cardioprotective effects. It functions as a monoamine oxidase (EC 1.4.3.4) inhibitor, acid-base indicator, fluorochrome, antidepressant, cardioprotective agent, cholinesterase (EC 3.1.1.8) inhibitor, histological dye, guanylate cyclase (EC 4.6.1.2) inhibitor, antioxidant, antimicrobial, neuroprotective agent, physical tracer, and antimalarial. A 3,7-bis(dimethyl amino)phenothiazin-5-ium is present (Wang et al., 2022).

One of the main basic dyes that is extensively used for coloring purposes is methylene blue (MB). This dye may irritate the skin, the digestive system, and the eyes in a way that is irreversible. MB is a regularly used chemical in dyeing operations and the textile industry that contributes to the pollution of textile effluent. Others have conducted research on the removal of the MB from aqueous solutions by the application of inexpensive materials (such as agricultural wastes), Figure 3.6, shows the chemical structure of MB (Sharifi Pajaie et al., 2018).

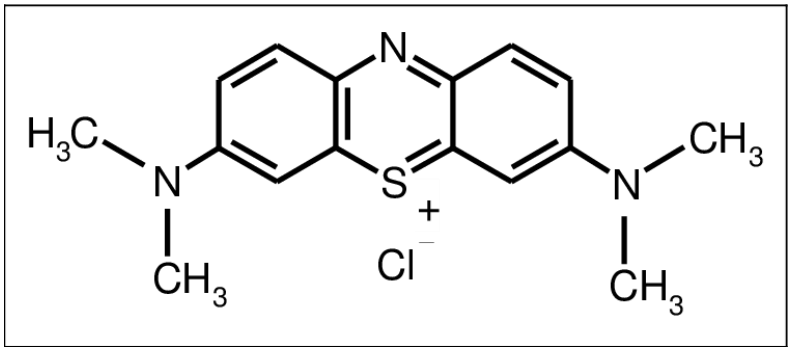

Figure 3.6 Chemical structure of methylene blue (Pajaie et al., 2018)

Methylene blue does not exist as a trihydrate, but rather as a number of distinct hydrates, according to a new study. The Working Group pointed out that "methylene blue" is the sole term used frequently in scientific literature, regardless of hydration state. Commercial methylene blue is frequently offered as the hydrate due to its

hygroscopic nature, but it is occasionally misrepresented as the trihydrate as shown in Figure 3.7 (Kurtan et al., 2016).



Figure 3.7 Methylene Blue (Cai et al., 2021)

As a biological stain and disinfectant, methylene blue is utilized. Methylene blue is marketed to end users as an aquarium fungicide in addition to its use as a disinfectant. Methylene blue has most recently been employed in photo electrochromic imaging, as a redox mediator, as an intercalator in nano porous materials, and as an optical probe in biophysical systems. Methylene blue is used to tone up silk colors as well as dye paper and office supplies. "Methylene blue active substances" are anionic surfactants that are identified using methylene blue in analytical chemistry. Additionally, pH and redox indicator reagents use methylene blue (Cai et al., 2021).

3.1.2.3 Methyl Orange Dye

The azo class of dyes includes the carcinogenic dye methyl orange (MO). It is both a chemically water-stable anionic dye and an anionic dye. As a result, its removal from wastewater using traditional methods of filtration is challenging. Because it makes water less light-permeable, its presence in water affects how aquatic plants respond to photosynthesis. Adsorption was frequently used to remove MO from wastewater using adsorptive means (Mogha et al., 2017; Wang et al., 2022).

Methyl Orange is a pH indicator that is often used in titration due to its distinct and visible color variation at various pH levels. In acidic and basic media, methyl orange exhibits red and yellow colors, respectively. It is typically utilized in titration of strong acids in weak bases that reach the equivalence point at a pH of 3.1- 4.4 because it changes color at the pKa of a mid strength acid that reaches the equivalence point at a

pH of 3.1-4.4. Methyl orange has a distinct end point but lacks the entire spectrum of color shift of a universal indication. Methyl orange transforms from red to orange to yellow as the acidity of the solution decreases, while the opposite happens as the acidity of the solution increases. Figure 3.8, shows the chemical structure of Methyl orange (Cai et al., 2021).

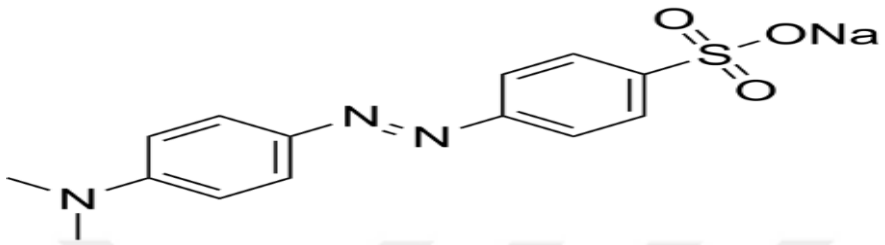

Figure 3.8 The chemical structure of Methylene Orange (Ahmad et al., 2020)



Figure 3.9 Methylene Orange (Labidi, 2023)

3.2 Catalytic studies

The catalytic efficiencies of the prepared Pd@Polymer@$CoFe_2O_4$ complex in the reduction/degradation reactions of 4-NP, MO, and MB substrates were investigated in the presence of $NaBH_4$ in aqueous media. For this purpose, the optimum reaction conditions were determined first by scanning the amount of $NaBH_4$, the substrate concentration, and the amount of catalyst. In this experimental study, the concentrations of the Pd@Polymer@$CoFe_2O_4$ catalyst were varied at 2 mg, 1 mg, and 0.5 mg. It was

observed that these concentrations resulted in the shortest reaction time for dye degradation. Consequently, the application of pseudo-first-order kinetics allowed for the estimation of rate constants. The obtained results indicate that the catalytic decolorization of the dyes can be described by the first-order kinetic model, expressed as in equation below:

$$\ln(C_0/C_t) = K \times t \quad (3.1)$$

Here, C_0 represents the initial concentration, C_t represents the concentration at time t, and K represents the apparent constant rate (Tercan, 2022).

3.3 Method

3.3.1 Synthesis of $CoFe_2O_4$ particles

$CoFe_2O_4$ particles were synthesized by a facile solvothermal method (Zhou, et al., 2011), In brief, 1.6 CoCl2.6H2O, 2.0 g FeCl3.6H2O and 4.8g sodium acetate were dissolved in 60.0 mL of ethylene glycol and the mixture was stirred vigorously for 30 min at room temperature. Then, the mixture was transferred to a 100 mL Teflon-lined stainless-steel reactor and heated to 200 °C for 8 h. After cooling to room temperature, the black product was washed with plenty of water and ethanol, respectively and dried in a vacuum oven at 60°C.

3.3.2 Synthesis of magnetic gel brush (Polymer@ $CoFe_2O_4$)

For the preparation of magnetic gel via surface-initiated Polymerization, $CoFe_2O_4$ particles were first modified with MPS. Then, 100 mg of Fe_3O_4 particles were dispersed in 50 mL of ethanol by ultrasonic treatment for 15 min at room temperature. After this, 250 µL of MPS was added to the mixture, and the mixture was stirred for 18 h at room temperature under nitrogen protection. After the reaction, the particles were collected with a simple magnet and washed with plenty of ethanol. Lastly, the product was dried in a vacuum oven.

To fabricate gel brush-grafted magnetic particles, a mixture of AAM (18 mmol), MBBAm (0.36 mmol), and AIBN (0.18 mmol) was prepared in 20 mL DMF, and 100

mg of $CoFe_2O_4$ particles were dispersed into the mixture. Then, the mixture was sealed with a rubber septum and bubbled with nitrogen for 30 minutes in an ice-bath. The Polymerization was started at 60 °C and continued for 8 h. After Polymerization, the particles were collected with a magnet and washed with DMF, H2O, and ethanol. In the last step, the particles were dried in a vacuum oven.

3.3.3 Preparation of Pd^0 deposited magnetic gel brush (Pd/PAAmGB@Fe_3O_4)

For this, 50 mg of Polymer@$CoFe_2O_4$ was dispersed in 10 ml of H_2O via ultrasonic treatment for 15 minute at room temperature, and 12.8 mg of $K2PdCl_4$ was added to the dispersion. The mixture was stirred with a mechanical stirrer at 600 rpm for 1 h at room temperature, and then an aqueous solution of $NaBH_4$ (4.0 mg/ml) was added drop by drop to reduce Pd^{2+} to Pd^0. The mixture was stirred at room temperature for 2 h and after the reaction, the product was collected by a magnet and washed with plenty of water. Lastly, the particles were dried in a vacuum oven and stored in a vacuum desiccator until needed.

4. RESULTS

4.1 Characterization

4.1.1 SEM Analysis

Scanning Electron Microscope (SEM) analyses were conducted to examine the morphological and structural characteristics of catalysts designed for the removal of dye contaminants from water sources. The SEM images obtained from these analyses and their interpretations are provided below.

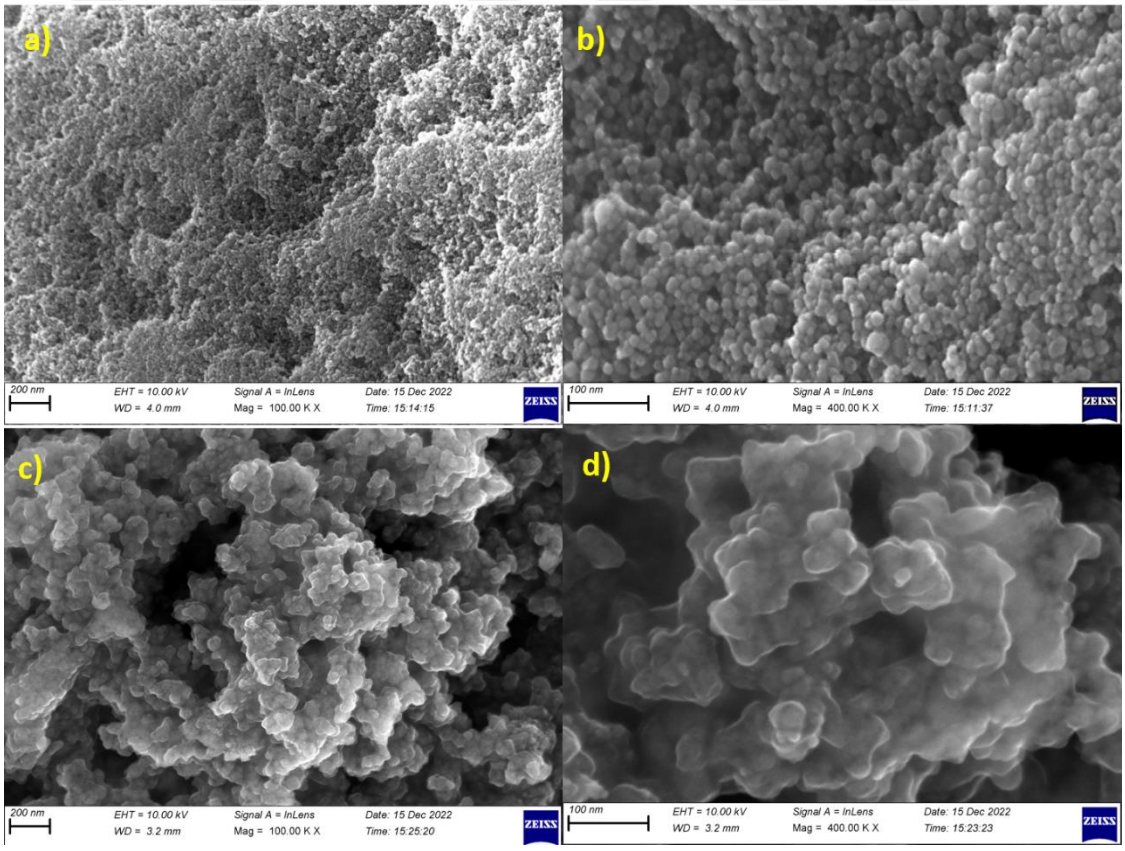

Figure 4.1 Scanning electron microscopy (SEM) images, (a, b) $CoFe_2O_4$, (c, d) Polymer@$CoFe_2O_4$

SEM was used to investigate the shape and structure of the as-prepared $CoFe_2O_4$ particles. Figure 4.1, shows the shape of the bulk $CoFe_2O_4$ particles. The particles appear to be broadly aggregated. The main reason for this phenomenon is the high

surface activity and strong magnetism of the $CoFe_2O_4$ nanoparticles. The particles are still formed as small balls with a limited radial distribution. As for Figure 4.1, it shows the microstructure and morphology of the Polymer covered with cobalt ferrite nanoparticles. Particle sizes measure approximately 32 nm and There are gaps between these molecules, which enhances the porosity of the catalyst and facilitates its participation in reactions. This indicates that the composite (Polymer@$CoFe_2O_4$) has a high affinity for nanoparticles, resulting in a homogeneous and protective coating. This coating has the potential to improve the stability and utility of nanoparticles in a variety of applications.

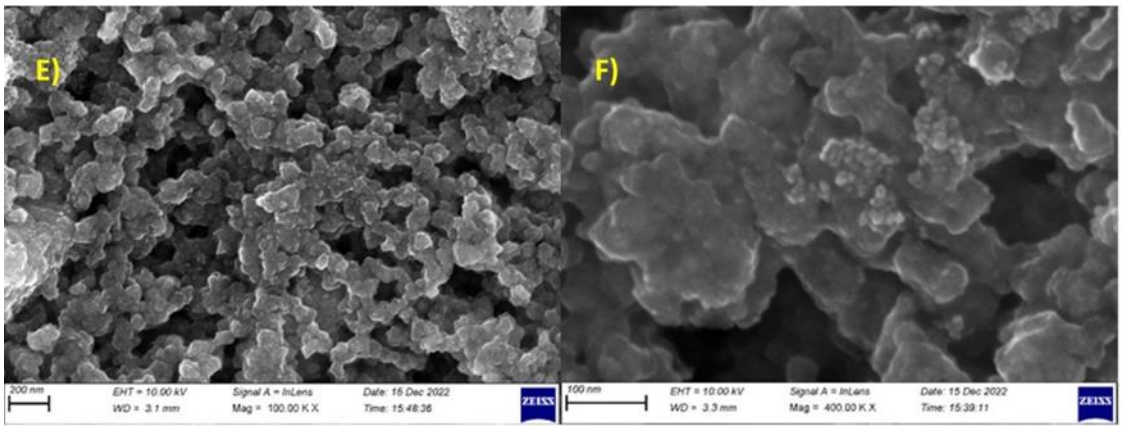

Figure 4.2 Scanning electron microscopy (SEM) images (E) Pd@Polymer@$CoFe_2O_4$ the particles on Pd at Polymer shell, (F) Pd@Polymer@$CoFe_2O_4$ the particles on Pd at Polymer shell under Mag 400.00 kx

Figure 4.2, which depicts both the morphology and microstructure of the catalyst (Pd@Polymer@$CoFe_2O_4$), reveals the presence of Pd particles adhering to the Polymer. It is also clear that the Pd nanoparticles are compatible with the Polymer matrix, which can help to avoid particle detachment and increase catalytic lifespan. This effect adds to the structural and thermal stability of the Pd@Polymer@$CoFe_2O_4$ catalyst.

4.1.2 EDX Analysis

EDX analysis is an analytical technique that measures the X-ray spectra of a sample to identify the elements and their weight percentages. The graphs below show the elemental compositions of the catalysts created as part of the research.

4.1.2.1 $CoFe_2O_4$

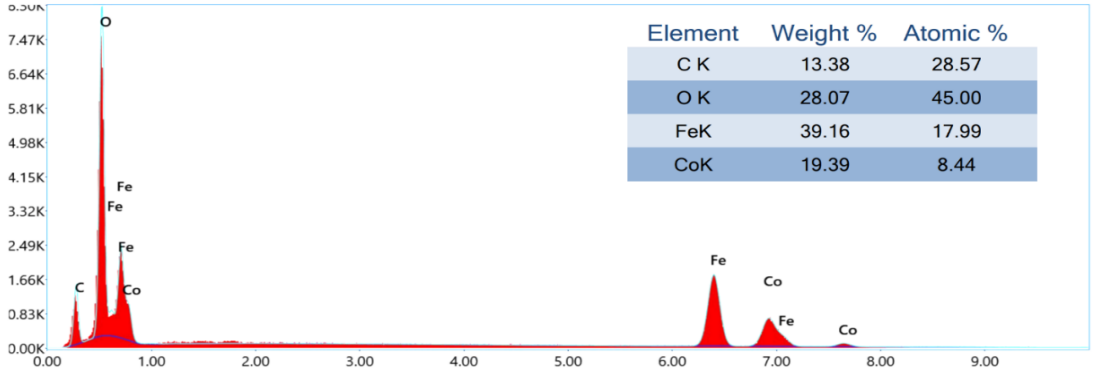

Element	Weight %	Atomic %
C K	13.38	28.57
O K	28.07	45.00
FeK	39.16	17.99
CoK	19.39	8.44

Figure 4.3 Energy-dispersive X-ray (EDX) spectra of the $CoFe_2O_4$ nanoparticles

The elemental composition of the $CoFe_2O_4$ catalyst is shown in Figure 4.3. The EDX graph shows the elemental composition of the samples. Shown in the graph are the peaks corresponding to the elements carbon (C), iron (Fe), oxygen (O), and cobalt (Co). The graph shows the weight ratios and the atomic ratios of these samples. Accordingly, it was determined that the samples consisted of 13.38% C, 39.16% Fe, 28.07% O, and 19.39% Co by weight. In terms of atomic percentage, it contains 28.57% C, 17.99% Fe, 45% O, and 8.44% Co. These results confirm that the samples are related to the formula $CoFe_2O_4$. In addition, the width and shape of the peaks in the graph reflect the crystal structure and purity of the material. Narrow and symmetrical peaks indicate a high degree of crystallinity and minimal impurities.

4.1.2.2 $CoFe_2O_4$@Polymer

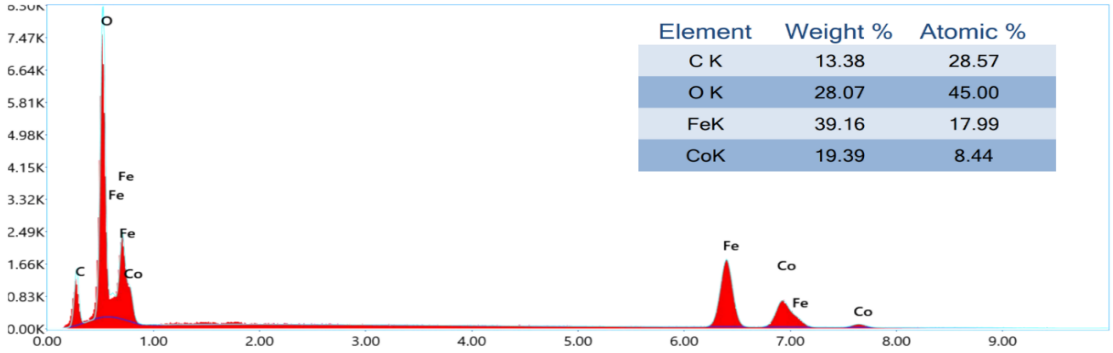

Figure 4.4 Energy-dispersive X-ray (EDX) spectra of the $CoFe_2O_4$@Polymer

As seen in Figure 4.4, shows the elemental composition of Polymer@$CoFe_2O_4$. The corresponding peaks for oxygen (O), cobalt (Co), iron (Fe), and carbon (C) are clearly visible in the graph. Atomic ratios and weight values are shown for these samples. Thus, the sample values for the weight ratios were calculated as 25.18% Fe, 25.34% O, 13.29% Co, and 36.10% C. Furthermore, the sample values for the atomic percentages were 30.15% O, 4.28% Co, and 8.55%. Fe, and 57.02% C. These results indicate that $CoFe_2O_4$ nanoparticles have been incorporated into the Polymer matrices.

4.1.2.3 $CoFe_2O_4$ @Polymer@Pd

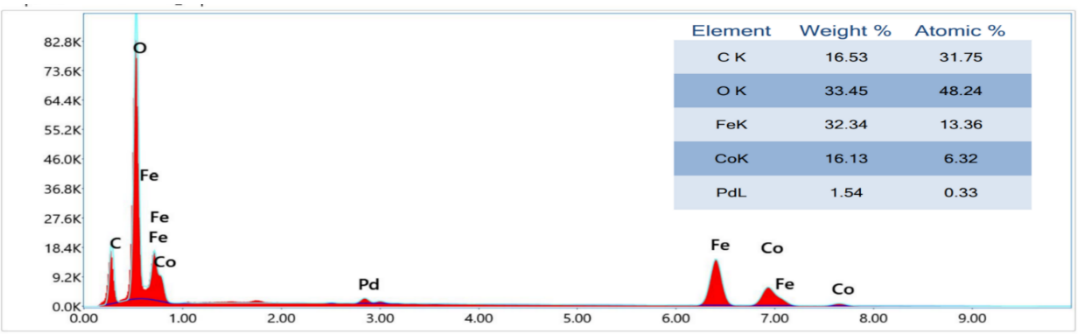

Figure 4.5 Energy-dispersive X-ray (EDX) spectra of the Pd@Polymer@$CoFe_2O_4$

As seen in Figure 4.5, shows the elemental structure of the Pd@Polymer@$CoFe_2O_4$ catalyst. In the graph, the peaks corresponding to the elements iron (Fe), cobalt (Co), and palladium (Pd) are visible. Besides the peaks, the weight and

atomic ratios of these samples are provided. These results indicate the incorporation of $CoFe_2O_4$ nanoparticles into Polymer matrices and their encapsulation with Pd.

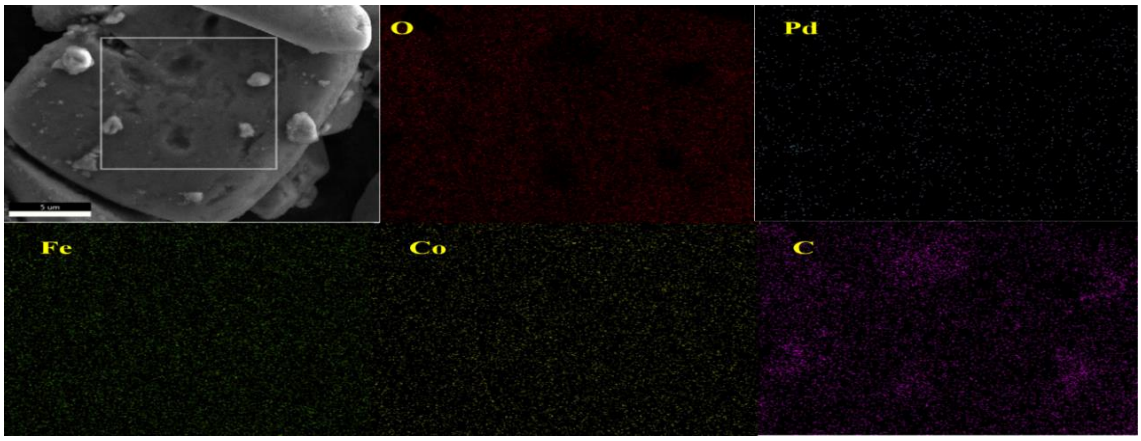

Figure 4.6 Scanning electron microcopy (SEM)–energy-dispersive X-ray spectroscopy (EDX) mapping of the $CoFe_2O_4$ @Polymer@Pd

4.1.2.4 $CoFe_2O_4$ @Polymer@Pd mapping:

$CoFe_2O_4$ nanoparticles are gathered together in the mapping picture of the catalyst with a 5-micrometer scale bar. These nanoparticles are cobalt (Co) and iron (Fe) oxides with catalytic activity. Red signifies oxygen (O), a critical ingredient in the $CoFe_2O_4$ nanoparticle structure for catalytic reactions. A dark picture indicates a nanoparticle palladium (Pd) coating. Pd increases surface area and reaction centers, preserves crystal structure, and prevents impurities, boosting catalytic activity. A green picture shows iron (Fe) in nanoparticles, which catalyzes A yellow picture shows cobalt (Co) in nanoparticles, supporting their catalytic activity. A purple picture shows carbon (C), a Polymer matrix component of $CoFe_2O_4$ nanoparticles. The Polymer stabilizes and disperses. The Polymer matrix equally distributes $CoFe_2O_4$ nanoparticles and coats them with Pd. This distribution increases surface area and reaction centers, boosting catalytic activity. The Pd coating prevents impurities and maintains nanoparticle crystal structure.

4.1.3 XRD Analysis

XRD analysis was conducted to compare the crystal structures of Pd@Polymer@$CoFe_2O_4$, Polymer@$CoFe_2O_4$, and $CoFe_2O_4$ catalysts. XRD is a

technique that measures the scattering of X-rays to determine the crystal structure of a material. The XRD analysis graph for the catalysts is shown in Figure 4.7.

X-ray diffraction patterns of the $CoFe_2O_4$ @Polymer@Pd, $CoFe_2O_4$ @Polymer, and $CoFe_2O_4$ are presented in Figure 4.7. The black line in the graph represents the Pd@Polymer@$CoFe_2O_4$ catalyst. $CoFe_2O_4$ nanoparticles are embedded within a Polymer matrix and coated with Pd nanoparticles. Peaks at (2θ = 30.28, 35.66, 36.69, 42.12, 44.95, 54.95, 57.18, and 63.95) No peaks related to the Polymer phase are observed because the Polymer has an amorphous structure that does not scatter X-rays. The peaks of this catalyst are quite sharp and narrow, indicating that both $CoFe_2O_4$ and Pd nanoparticles possess high crystallinity, The crystallite size of the nanocomposite particles as 8.5 ± 1nm.

The red line in the graph represents the Polymer@$CoFe_2O_4$ catalyst. In this catalyst, only $CoFe_2O_4$ nanoparticles are embedded within the Polymer matrix. The XRD graph of this catalyst shows only peaks associated with the $CoFe_2O_4$ phase. These peaks resemble those of the black line but appear with lower intensity and broader width. This suggests that the $CoFe_2O_4$ nanoparticles in this catalyst are smaller in size and possess lower crystallinity.

The blue line in the graph represents the $CoFe_2O_4$ nanoparticles. only $CoFe_2O_4$ nanoparticles are present. The XRD graph of this catalyst is similar to both the black and red lines but appears with higher intensity and narrower width. This indicates that the $CoFe_2O_4$ nanoparticles in this catalyst are larger in size and have higher crystallinity.

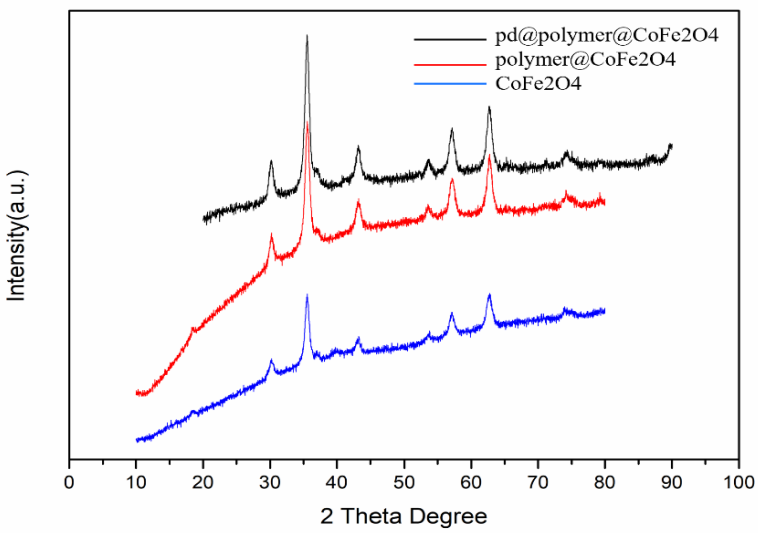

Figure 4.7 The XRD diffraction patterns of as prepared $CoFe_2O_4$ nanoparticles

4.1.4 VSM Analysis

A technique for displaying the magnetic characteristics of materials is the VSM (Vibrating Sample Magnetometer) graph. The applied magnetic field intensity (H) and material magnetization (M) are shown on the graph's x- and y-axes, respectively. The magnetic properties of the material are reflected in the Figure 4.8.

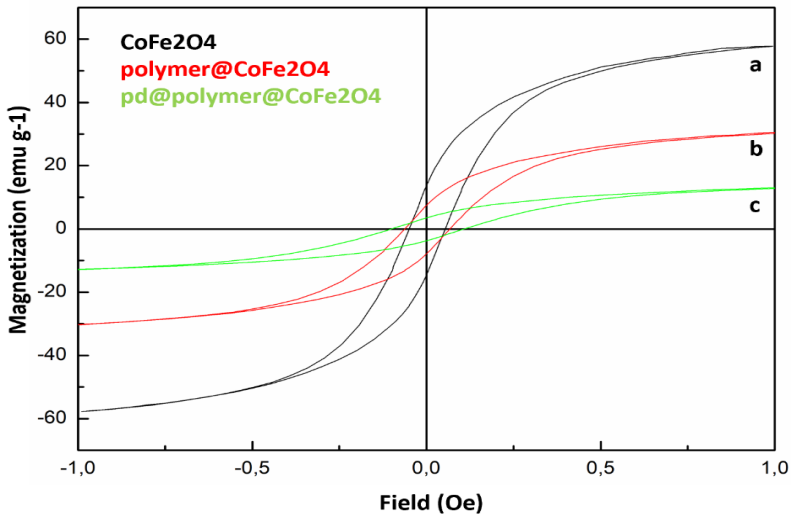

Figure 4.8 Vibrating-sample magnetometer (VSM) diagram showing (a) $CoFe_2O_4$, (b) Polymer@$CoFe_2O_4$, (c) Pd@Polymer@$CoFe_2O_4$

The magnetic properties of three materials, namely (a) $CoFe_2O_4$, (b) Polymer@$CoFe_2O_4$, and (c) Pd@Polymer@$CoFe_2O_4$, were studied at room temperature using a vibration sample magnetometer (VSM), as shown in Figure 4.8. The results are shown below:

$CoFe_2O_4$ has the highest coercivity of 0.5 kOe, requiring a strong external magnetic field for full demagnetization. Polymer@$CoFe_2O_4$ has a lower coercivity of 0.3 kOe, making it easier to demagnetize. Pd@Polymer@$CoFe_2O_4$ has the lowest coercivity of 0.1 kOe, making it the easiest material to demagnetize.

The remanent magnetization value of $CoFe_2O_4$ is reported to be 58.2 emu/g^{-1}, indicating its ability to maintain a substantial magnetization in the absence of an external magnetic field. The remanent magnetization of Polymer@$CoFe_2O_4$ is observed to be 30.1 emu/g^{-1}, which is lower than that of $CoFe_2O_4$. This suggests that a non-magnetic Polymer matrix has been applied as a coating over the $CoFe_2O_4$ nanoparticles, resulting in a reduction in magnetic saturation. Furthermore, Pd@Polymer@$CoFe_2O_4$ exhibits the lowest remanent magnetization value of 11.8 emu/g^{-1}, indicating that the presence of Pd nanoparticles on the Pd@Polymer@$CoFe_2O_4$ surface contributes to the decrease in saturation magnetization. Hence, the aforementioned findings provide a straightforward and effective method for the isolation and reutilization of the Pd@Polymer@$CoFe_2O_4$ nanocatalyst by the use of an external magnetic field.

4.1.5 XPS Analysis

X-ray photoelectron spectroscopy (XPS) was used to characterize the surface chemical composition of the as-prepared $CoFe_2O_4$ /Polymer/Pd composite catalyst. The characteristic signals for C1s, Co2p, Fe2p, N1s, O1s and Pd3d were clearly detected in Figure 4.9.

In Figure 4.10, The C 1s spectra show binding energy at 285 eV, suggesting carbon chemical environments and hybridization states. assigned for (C-C). The sample contains carbon in different states. The Co2p spectra, which represent two peaks at 782.52 and 797.25, confirmed the $Co2^+$ oxidation state in the compound. The Fe2p spectrum consists of two peaks at 712.45 eV and 725 eV, indicating the valence state of $Fe3^+$ in the octahedral site. The N 1s spectrum shows a peak at 400.2 eV, indicating

diverse nitrogen chemical environments and functional groups on the surface. The O1s spectrum shows a peak at 531,50 eV, indicating oxygen binding energy in various chemical environments and assigned to (C-O-O). Besides, two peaks of Pd 3d at 336.1 and 341.2 eV correspond to $3d_{3/2}$ and $3d_{5/2}$ of the metallic form of Pd (Pd^0) and The presence of these peaks confirmed that Pd^{2+} was mainly reduced to metallic Pd, potentially relevant to catalytic activity.

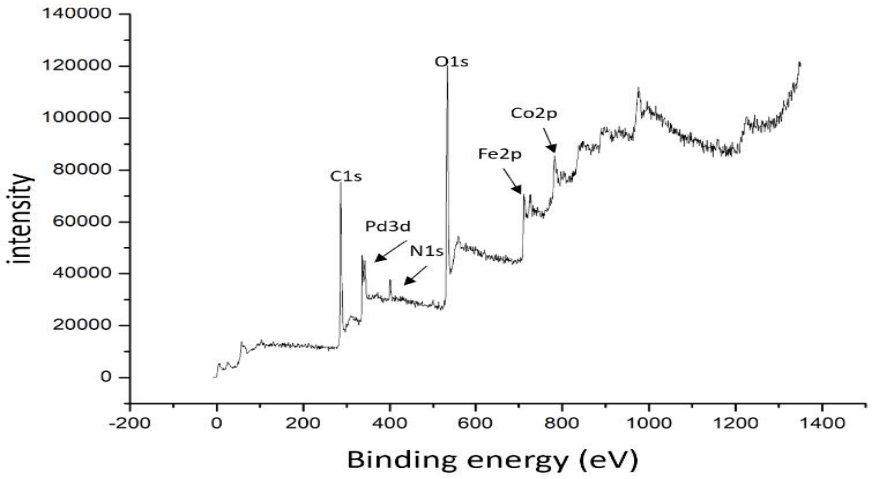

Figure 4.9 High-resolution XPS spectra of catalyst Pd@Polymer@$CoFe_2O_4$

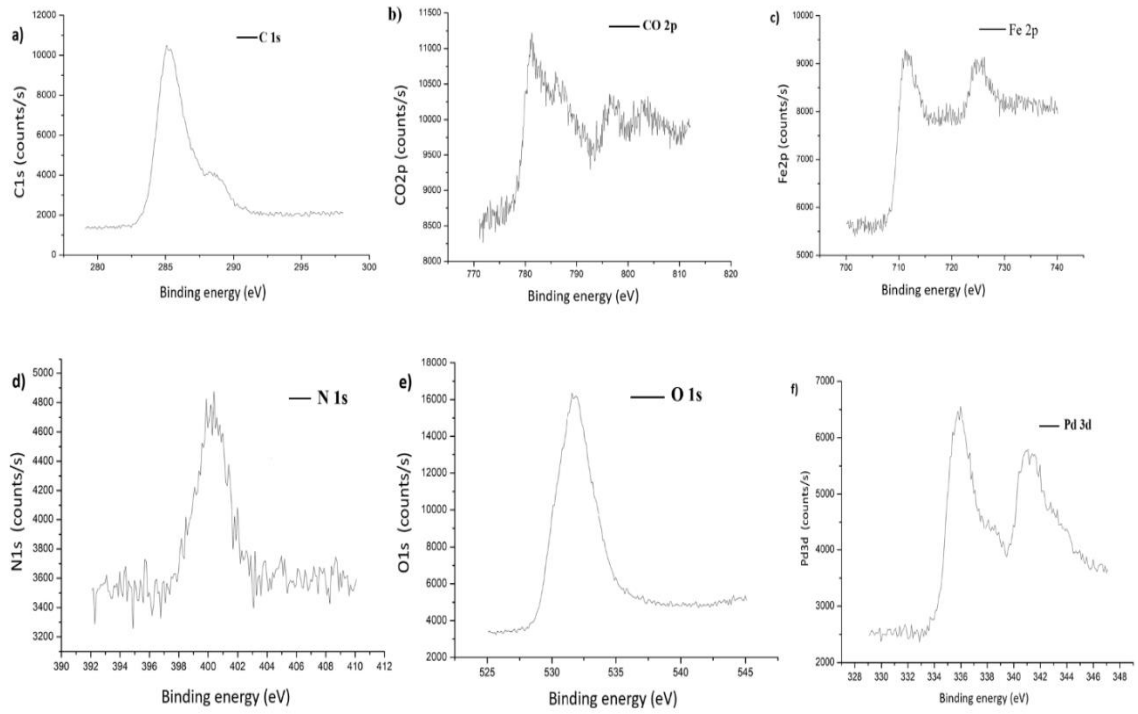

Figure 4.10 X-ray photoelectron spectroscopy (XPS) spectra of (a) C1s, (b) Co2p, (c) Fe2p, (d) N1s, (e) O1s and (f) Pd3d

4.2 UV–Visible spectroscopy

4.2.1 (4-Nitrophenol Dye)

4.2.1.1 (2 mg Pd@Polymer@$CoFe_2O_4$)

This catalyst (Pd@Polymer@$CoFe_2O_4$) was used in an amount of (2 mg) and added to a mixture of 4-nitrophenol dye (0.05 mM) and $NaBH_4$ in an amount of (1.89 mg) in a cuvette tube. The Pd@Polymer@$CoFe_2O_4$catalyst significantly increased the solubility of 4-nitrophenol dye, a dye that decomposed over time. The absorbance of the dye initially was 2.760, but it decreased over time, indicating the reaction progressed. The negative deviations in the absorbance values indicate the dye's decrease over time. The reaction rate was correlated with the rapid decomposition of 4-nitrophenol, particularly within the first 20 seconds. The Pd@Polymer@$CoFe_2O_4$catalyst facilitated the rapid reduction of the 4-nitrophenol dye, and the reaction was completed within 0.6

minutes, demonstrating the reaction's effectiveness and rapid decomposition with 4-nitrophenol rapidly decomposing, as shown in Table 4.1, and Figure 4.11.

Table 4.1 2 mg of Pd@Polymer@$CoFe_2O_4$with 0.05 mM of 4-niteophenol dye

2 mg Pd@Polymer@$CoFe_2O_4$, 0.05 mM 4-NP, 1.89 mg $NaBH_4$			
Time (s)	Time (minutes)	Absorbents	In
0	0	2.760	0
5	0.083333	2.400	-0.13976
10	0.166667	1.700	-0.4846
20	0.333333	1.300	-0.75287
30	0.5	0.960	-1.05605
40	0.666667	0.6	-1.52606
50			

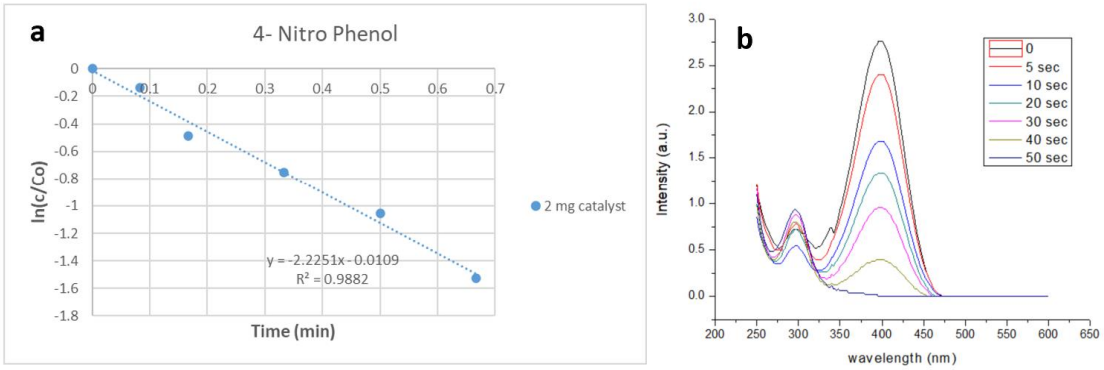

Figure 4.11 (a) 2 mg of Pd@Polymer@$CoFe_2O_4$ with 4-nitrophenol dye, (b) Time-dependent UV–Vis absorption spectra for the reduction of 4-NP

4.2.1.2 (1 mg Pd@Polymer@$CoFe_2O_4$)

This catalyst was used (Pd@Polymer@$CoFe_2O_4$) in an amount of 1 mg added to a cuvette tube containing 4-nitrophenol dye at a concentration of 0.05 mM and $NaBH_4$ in an amount of 1.89 mg. The Pd@Polymer@$CoFe_2O_4$catalyst significantly increased the solubility of 4-nitrophenol dye in the presence of $NaBH_4$. The dye's absorbance initially measured at 2.610 but decreased over time, indicating the dye had decomposed, The increasing reaction rate was correlated with the rapid decomposition of 4-

nitrophenol, and the color disappeared in 2 minutes. This suggests the catalyst's ability to facilitate the rapid reduction of 4-nitrophenol dye, as shown in Table 4.2, and Figure 4.12.

Table 4.2 1 mg of Pd@Polymer@$CoFe_2O_4$with 0.05 mM of 4-niteo phenol dye

1 mg Pd@Polymer@$CoFe_2O_4$, 0.05 mM 4-NP, 1.89 mg $NaBH_4$			
Time (s)	Time (minutes)	Absorbents	In
0	0	2.610	0
20	0.333333	2.025	-0.25378
40	0.666667	1.545	-0.52433
60	1	1.110	-0.85499
80	1.333333	0.660	-1.37487
100	1.666667	0.435	-1.79176
120	2	0.24	-2.38647

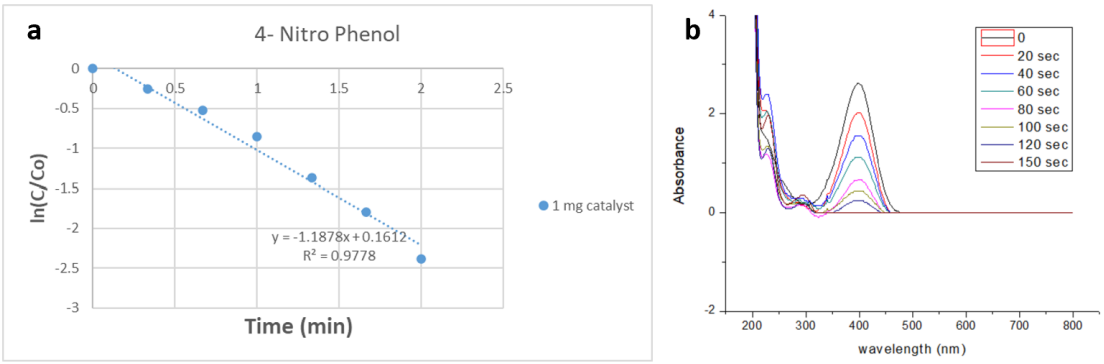

Figure 4.12 (a) 1 mg of Pd@Polymer@$CoFe_2O_4$with 4-NP, (b) Time-dependent UV–Vis absorption spectra for the reduction of 4-NP

4.2.1.3 (0.5 mg Pd@Polymer@$CoFe_2O_4$)

This catalyst (Pd @ Polymer @ $CoFe_2O_4$) was added in an amount of (0.5 mg) to a mixture of 4-nitrophenol dye with a concentration of (0.2 mM) and $NaBH_4$ in an amount of (60 mM) with the addition of (1.95 ml) distilled water in a cuvette tube. This mixture was entered into a UV-vis spectroscopy device to decompose the dye. At different times, starting from (0, 30, 60, 120, 150, 180, 210) seconds, the color disappeared in a time of 3 minutes. This finding indicates that the reaction occurred

rapidly and effectively, with 4-nitrophenol rapidly decomposing. as shown in Table 4.3, and Figure 4.13.

Table 4.3 0.5 mg of Pd@Polymer@$CoFe_2O_4$with 0.05 mM of 4-niteo phenol dye

0.5 mg/ml Pd@Polymer@$CoFe_2O_4$, 0.2 mM 4-NP, 60 mM $NaBH_4$			
Time (s)	Time (minutes)	Absorbents	In
0	0	2.61	0
30	0.5	2.025	-0.25378
60	1	1.11	-0.85499
120	2	0.663	-1.37033
150	2.5	0.435	-1.79176
180	3	0.24	-2.38647
210			

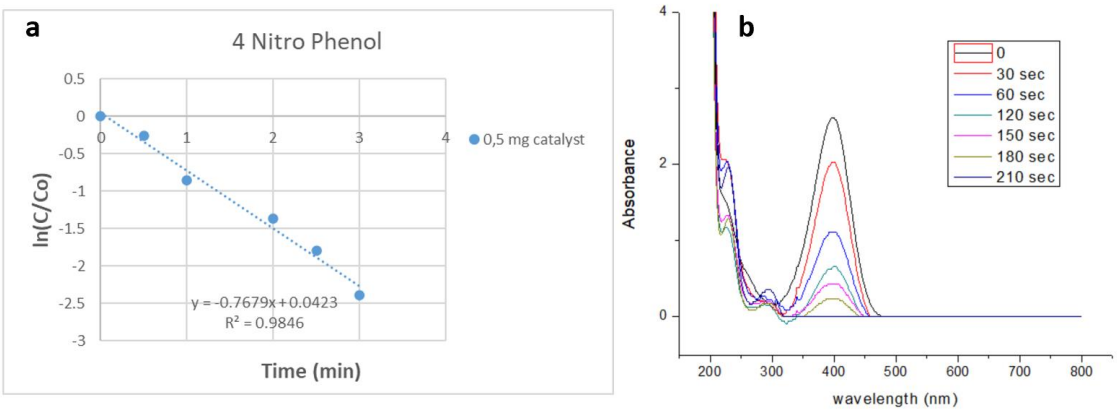

Figure 4.13 (a) 0.5 mg of Pd@Polymer@$CoFe_2O_4$with of 4-NP, (b) Time- dependent UV–Vis absorption spectra for the reduction of 4-NP

4.2.1.4 (2 mg/ml $CoFe_2O_4$@Pd, 0.2 mM 4-niteophenol, 60 mM $NaBH_4$)

This catalyst ($CoFe_2O_4$ @Pd) was used in an amount of (2 mg) for 4-nitrophenol dye, whose concentration was (0.2 mM), and then $NaBH_4$ (60 mM) was mixed with (1.95 ml) of distilled water in a Cuvette tube. This mixture was introduced to a UV-vis spectroscopy device to decompose the dye at different times, starting from (0, 60, 90, 120, 150, 180, 240, 270, 300, 360, 420) seconds. The rapid reduction of the 4-nitrophenol dye by the $CoFe_2O_4$@Pd catalyst is evident from the data obtained at

different time intervals. The UV-vis spectroscopy device allowed for accurate measurement of the decomposition process, showing that the reaction was completed within 7 minutes, as seen in Table 4.4, and the yellow line in Figure 4.14.

Table 4.4 2 mg/ml of $Pd@CoFe_2O_4$ with 0.2 mM of 4-niteo phenol dye

2 mg/ml $Pd@CoFe_2O_4$, 0,2 mM 4-niteo phenol, 60 mM $NaBH_4$			
Time (s)	Time (minutes)	Absorbents	In
0	0	2.76	0
60	1	2.26	-0.19987
90	1.5	2.053	-0.29593
120	2	1.814	-0.4197
150	2.5	1.64	-0.52053
180	3	1.32	-0.7376
210	3.5	1.111	-0.90997
240	4	0.965	-1.05086
270	4.5	0.852	-1.1754
300	5	0.625	-1.48523
360	6	0.552	-1.60944
420	7	0.47	-1.77025

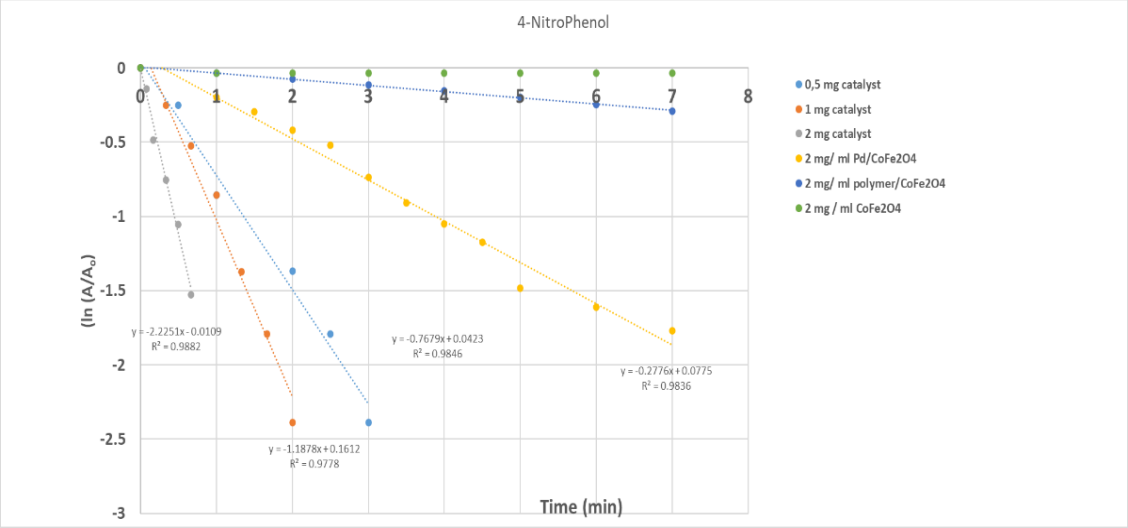

Figure 4.14 2 mg/ml of $CoFe_2O_4@Pd$ with 0.2 mM of 4-niteo phenol dye

4.2.1.5 (2 mg/ml Polymer@$CoFe_2O_4$, 0.2 mM 4-niteophenol, 60 mM $NaBH_4$)

This catalyst (Polymer@$CoFe_2O_4$) was used in an amount of (2 mg) for 4-nitrophenol dye, whose concentration was (0.2 mM), and then $NaBH_4$ (60 mM) was mixed with (1.95 ml) of distilled water in a Cuvette tube. This mixture was introduced to a UV-vis spectroscopy device to decompose the dye at different times starting from (0, 60, 90, 120, 150, 180, 240, 270, 300, 360, 420) seconds. Particularly, within 7 minutes, the absorbance value decreased. The dark blue line in the graph visually illustrates how the absorbance decreased over time, highlighting the progress of the reaction, as seen in Figure 4.15.

Table 4.5 2 mg/ml of $CoFe_2O_4$ @Polymer with 0.2 mM of 4-nitrophenol dye

2 mg/ml Polymer@$CoFe_2O_4$, 0.2 mM 4-nitro phenol, 60 mM $NaBH_4$			
Time (s)	Time (minutes)	Absorbents	In
0	0	2.76	0
60	1	2.66	-0.0369
120	2	2.56	-0.07522
180	3	2.46	-0.11507
240	4	2.36	-0.15657
300	5	2.26	-0.19987
360	6	2.16	-0.24512
420	7	2.06	-0.29252

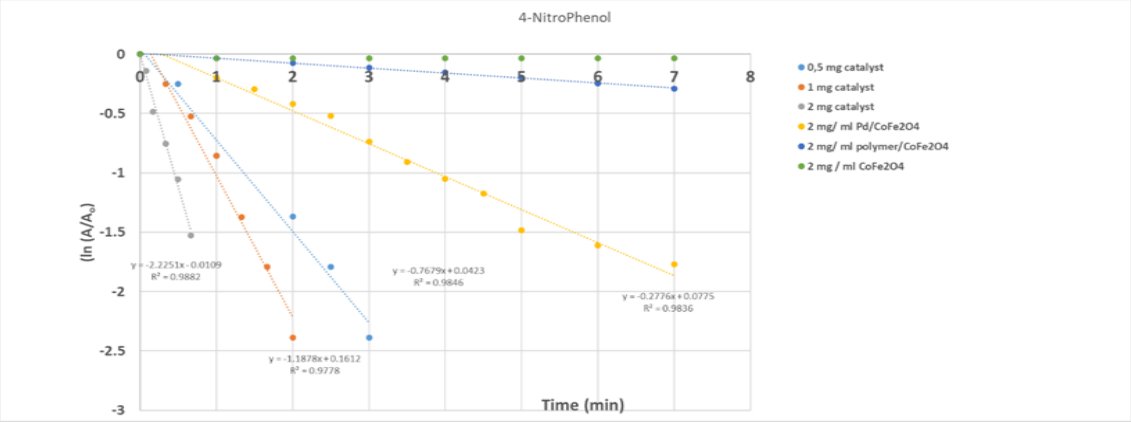

Figure 4.15 Absorption time dye using concentration 2 mg/ml of Polymer@$CoFe_2O_4$ with 0.2 mM of 4-niteo phenol dye

4.2.1.6 (2 mg/ml $CoFe_2O_4$, 0.2 mM 4-niteophenol, 60 mM $NaBH_4$)

Table 6, shows that $CoFe_2O_4$ was unsuccessful in boosting the 4-nitrophenol dye's solubility. The 4-nitrophenol dye's absorbance was measured at 2.76 at the start of the experiment, and during the course of the experiment (60 seconds, 120 seconds, etc.), the dye's absorbance value stayed essentially constant. This result suggests that the reaction did not proceed and that the $CoFe_2O_4$ catalyst was ineffective in enhancing the solubility of the 4-nitrophenol dye. The absorbance remained essentially constant throughout time, as seen by the green line in Figure 4.16, demonstrating that the reaction did not take place.

Table 4.6 2 mg/ml of $CoFe_2O_4$ with 0.2 mM of 4-nitrophenol dye

2 mg/ml $CoFe_2O_4$, 0.2 mM 4-niteophenol, 60 mM $NaBH_4$			
Time (s)	Time (minutes)	Absorbents	In
0	0	2.76	0
60	1	2.66	-0.036904557
120	2	2.66	-0.036904557
180	3	2.66	-0.036904557
240	4	2.66	-0.036904557
300	5	2.66	-0.036904557
360	6	2.66	-0.036904557
420	7	2.66	-0.036904557

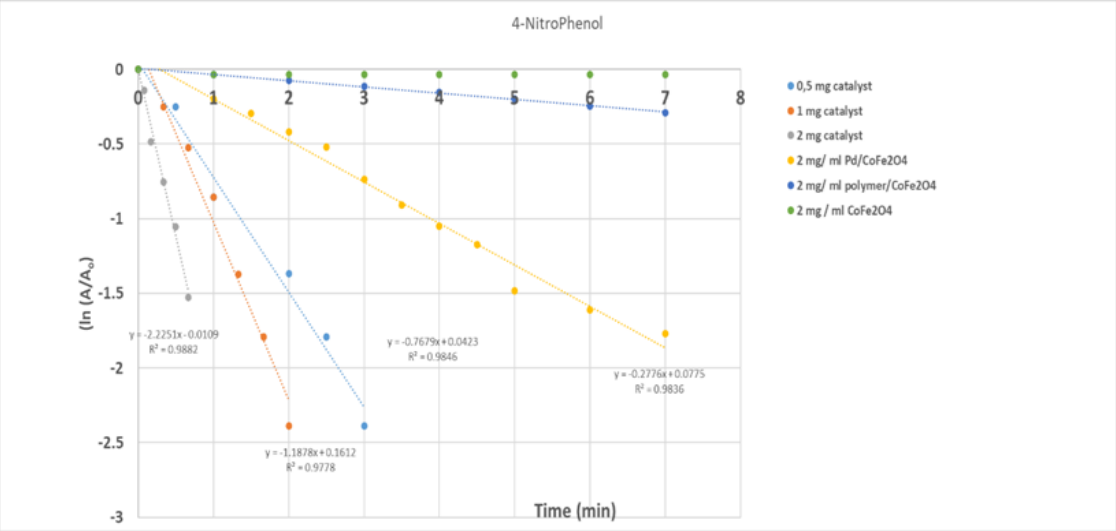

Figure 4.16 Absorption time dye using concentration 2 mg/ml of $CoFe_2O_4$ with 0.2 mM of 4-nitrophenol dye

4.2.1.7 Recyclability of Pd@Polymer@$CoFe_2O_4$, 4-NP

The experiment examines the performance of the Pd@Polymer@$CoFe_2O_4$ catalyst in reducing the solubility of 4-nitrophenol dye across five usage times. After each use, the catalyst was successfully separated and washed for reuse. Initially, the dye's absorbance was 2.76, dropping to 0.47 after the first catalyst use. This led to the decomposition of 2.29 units of the dye with 100% activity and conversion. In subsequent usages, the catalyst consistently reduced dye absorbance, albeit with slight efficiency decreases. Despite this, even after the fifth usage, the catalyst still exhibited activity 71.62%. Overall, the study demonstrates the catalyst's effective dye decomposition, its capacity for repeated use, and its sustained solubility-reducing ability, as seen in Table 4.7, and Figure 4.17.

Table 4.7 The effectiveness of the Pd@Polymer@$CoFe_2O_4$ catalyst for 4-niteophenol dye degradation

number of uses	start (ABS)	Remaining Amount of Substance (ABS)	Amount of Degraded Substance (ABS)	activity %	transformation %
1	2.76	0.47	2.29	100	100
2	2.76	0.53	2.23	97.37991	100
3	2.76	0.69	2.07	90.39301	100
4	2.76	0.91	1.85	80.78603	100
5	2.76	1.12	1.64	71.61572	100

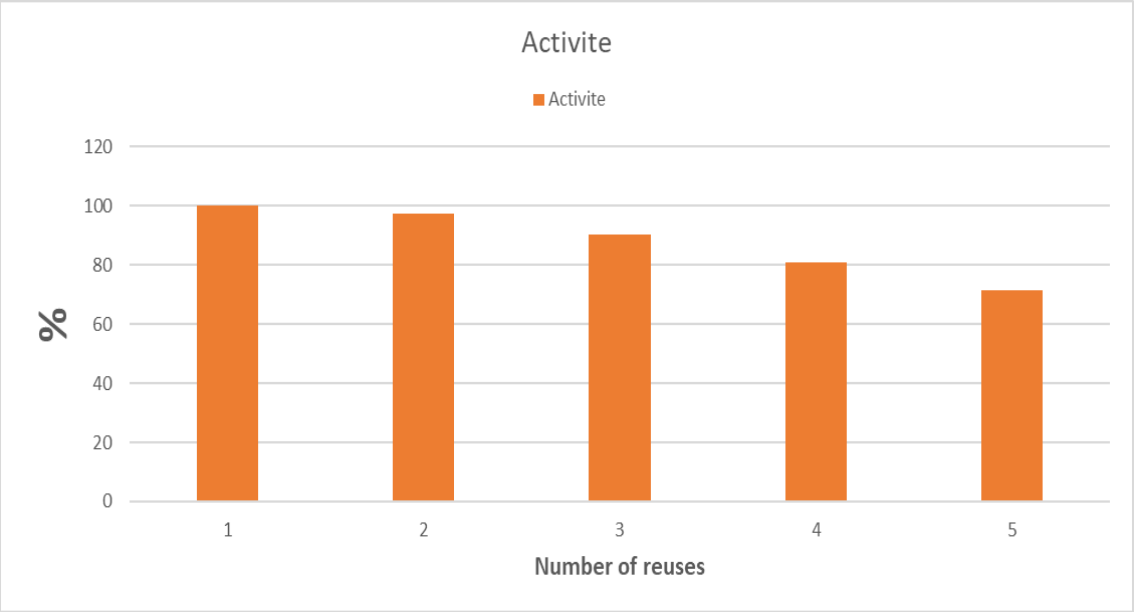

Figure 4.17 The percentage of the Pd@Polymer@$CoFe_2O_4$ catalyst for 4-nitrophenol dye degradation

4.2.2 Methylene Blue Dye

4.2.2.1 (2 mg Pd@Polymer@$CoFe_2O_4$)

This catalyst (Pd@Polymer@$CoFe_2O_4$) was used in an amount of (2 mg) for Methylene blue dye which concentration was (0.2 mM), then $NaBH_4$ (60 mM) was mixed with (1.95 ml) of distilled water in a Cuvette tube. The dye was initially measured at 3.259 absorbance, but over time, the absorbance value decreased. This

indicates that the dye decomposed over time, and the reaction progressed. The absorbance values were indicated with a negative deviation. The reaction was completed within 1.5 minutes, indicating that the reaction was rapid and effective, the dye was degraded quickly, as shown in Figure 4.18.

Table 4.8 2 mg of Pd@Polymer@$CoFe_2O_4$ with 0.2 mM of Methylene blue dye

Time (s)	Time (minutes)	Absorbents	In
0	0	3.259	0
5	0.083333	2.909	-0.11361
20	0.333333	1.956	-0.51052
30	0.5	1.228	-0.97603
60	1	0.487	-1.90091
90	1.5	0.237	-2.62112
100			

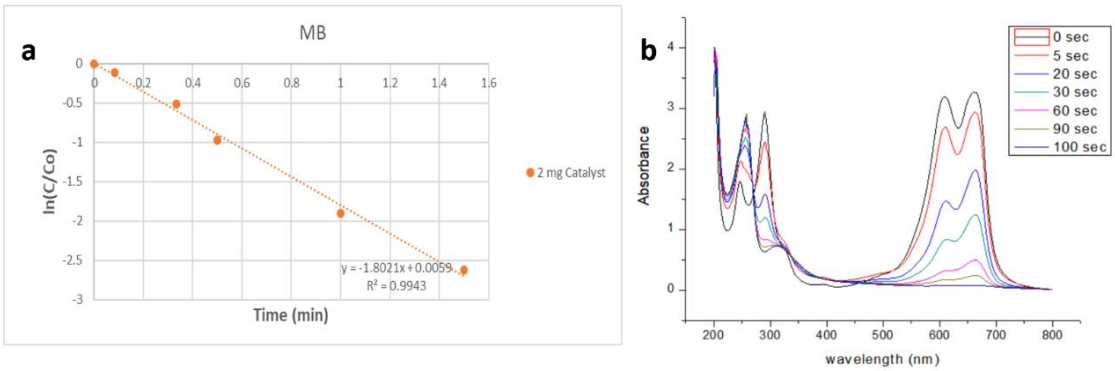

Figure 4.18 (a) 2 mg of Pd@Polymer@$CoFe_2O_4$with MB, (b) Time-dependent UV–Vis absorption spectra for the reduction of MB

4.2.2.2 (1 mg Pd@Polymer@$CoFe_2O_4$)

This catalyst (Pd@Polymer@$CoFe_2O_4$) was used in an amount of (1 mg) for MB dye with a concentration of (0.2 mM), and then $NaBH_4$ (60 mM) was mixed with (1.95 ml) of distilled water in a Cuvette tube. It has been observed that the Pd@Polymer@$CoFe_2O_4$ catalyst rapidly increased the solubility of methylene blue dye. the absorbance of methylene blue dye was measured as 3.259, and subsequently, over time (10 seconds, 30 seconds, etc.), this finding indicates that methylene blue dye degrades over time and the reaction progresses. The reaction was found to be completed

within precisely 4 minutes. This indicates that the reaction proceeds rapidly and effectively, as shown in Table 4.9, and Figure 4.19.

Table 4.9 1 mg of Pd@Polymer@$CoFe_2O_4$ with 0.2 mM of Methylene blue dye

1 mg Pd@Polymer@$CoFe_2O_4$, 0.2 mM MB, 60 mM $NaBH_4$			
Time (s)	Time (minutes)	Absorbents	In
0	0	3.259	0
10	0.166667	2.874	-0.12572
30	0.5	2.158	-0.41224
60	1	1.388	-0.85356
90	1.5	0.842	-1.3534
120	2	0.316	-2.33343
150	2.5	0.191	-2.8369
180	3	0.129	-3.22936
210	3.5	0.085	-3.64652
240	4	0.072	-3.81251

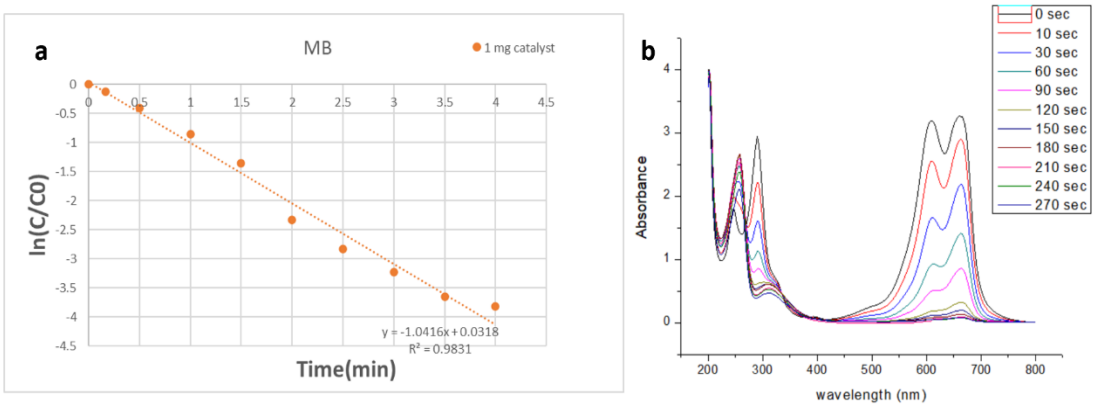

Figure 4.19 (a) 1 mg of Pd@Polymer@$CoFe_2O_4$ with MB, (b) Time-dependent UV–Vis absorption spectra for the reduction of MB

4.2.2.3 (0.5 mg Pd@Polymer@$CoFe_2O_4$)

The catalyst employed Pd@Polymer@$CoFe_2O_4$, with an amount of 0.5 mg. The MB dye utilized had a concentration of 0.2 mM, Subsequently, a mixture of $NaBH_4$ (60 mM) and (1.95 mL) of distilled water was prepared in a cuvette tube. This absorbance is noticed when the reaction takes place in the presence of $NaBH_4$. The measurement of the absorbance of methylene blue dye yielded a value of 3.31. The aforementioned suggests that the Methylene Blue dye underwent decomposition as time progressed. It is expected that the absorbance value will diminish to 0.321 after a duration of 6 minutes. Consequently, the dye will undergo full degradation, as shown in Table 4.10, and Figure 4.20.

Table 4.10 0.5 mg of Pd@Polymer@$CoFe_2O_4$ with 0.2 mM of Methylene blue dye

0.5 mg Pd@Polymer@$CoFe_2O_4$, 0,2 mM MB, 60 mM $NaBH_4$			
Time (s)	Time (minutes)	Absorbents	In
0	0	3.31	0
10	0.166667	3.28	-0.0091
20	0.333333	3.196	-0.03505
30	0.5	3.019	-0.09202
40	0.666667	2.716	-0.19779
50	0.833333	2.308	-0.36057
60	1	1.939	-0.53478
90	1.5	1.643	-0.70042
120	2	1.311	-0.92616
150	2.5	1.039	-1.15869
180	3	0.757	-1.47534
240	4	0.584	-1.7348
270	4.5	0.437	-2.02477
300	5	0.321	-2.33326
360	6		

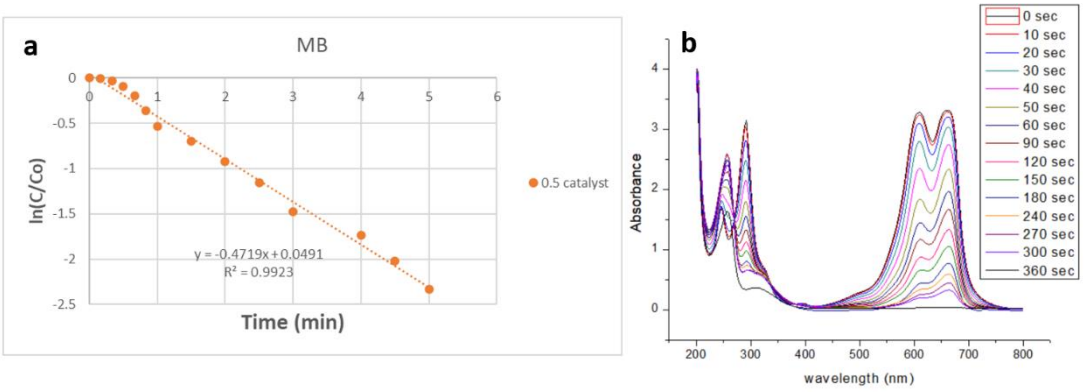

Figure 4.20 (a) 0.5 mg of Pd@Polymer@$CoFe_2O_4$ with MB, (b) Time-dependent UV–Vis absorption spectra for the reduction of MB

4.2.2.4 (2 mg/ml $CoFe_2O_4$ @Pd, 0.2 mM MB, 60 mM $NaBH_4$)

This catalyst ($CoFe_2O_4$ @Pd) at a concentration of 2 mg was used to remove the MB dye, whose concentration was 0.2 mM. Next, $NaBH_4$ (60 mM) was mixed with 1.95 ml of distilled water. This reaction occurs when $NaBH_4$ is present. The absorbance of methylene blue dye was measured at 3.31. These data indicate that methylene blue dye degrades over time. In addition, these values are given with a negative deviation, which shows that the color fades over time. After exactly 7 minutes, the reaction was complete. As shown in Figure 4.21, and Table 4.11, with the yellow line in the graph.

Table 4.11 2 mg of $CoFe_2O_4$ @Pd with 0.2 mM of Methylene blue dye

2 mg/ml $CoFe_2O_4$ @Pd, 0.2 mM MB, 60 mM $NaBH_4$			
Time (s)	Time (minutes)	Absorbents	In
0	0	3.31	0
60	1	3	-0.09834
90	1.5	2.53	-0.26873
120	2	2.014	-0.49683
150	2.5	1.7	-0.66632
180	3	1.32	-0.91932
210	3.5	1.111	-1.09169
240	4	0.865	-1.34197
270	4.5	0.752	-1.48197
300	5	0.625	-1.66695
360	6	0.452	-1.99102
420	7	0.347	-2.25538

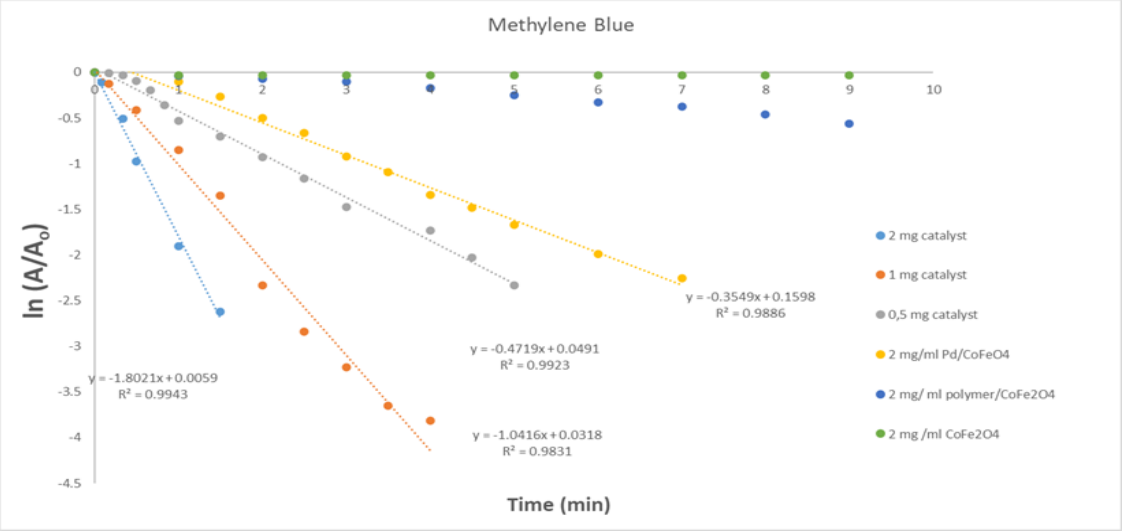

Figure 4.21 Absorption time dye using concentration 2 mg of Pd@$CoFe_2O_4$ with 0.2 mM of Methylene blue dye

4.2.2.5 (2 mg/ml Polymer@$CoFe_2O_4$, 0,2 mM MB, 60 mM $NaBH_4$)

Polymer@$CoFe_2O_4$ in the amount of (2 mg) was used to get rid of (0.2 mM) of methylene blue dye, and then (60 mM) of $NaBH_4$ and (1.95 ml) of distilled water were mixed. This reaction occurs in the presence of $NaBH_4$. This result indicates that the methylene blue dye degraded over time, progressing the reaction. The reaction was completed in exactly 9 minutes, as seen in Table 4.12, and Figure 4.22 (the blue line in the graph).

Table 4.12 2 mg/ml of Polymer@$CoFe_2O_4$ with 0.2 mM of Methylene blue dye

2 mg/ml Polymer@$CoFe_2O_4$, 0.2 mM MB, 60 mM $NaBH_4$			
Time (s)	Time (minutes)	Absorbents	In
0	0	3.31	0
60	1	3.18	-0.04007
120	2	3.08	-0.07202
180	3	2.98	-0.10502
240	4	2.78	-0.1745
300	5	2.58	-0.24916
360	6	2.38	-0.32985
420	7	2.28	-0.37277
480	8	2.08	-0.46458
540	9	1.88	-0.56568

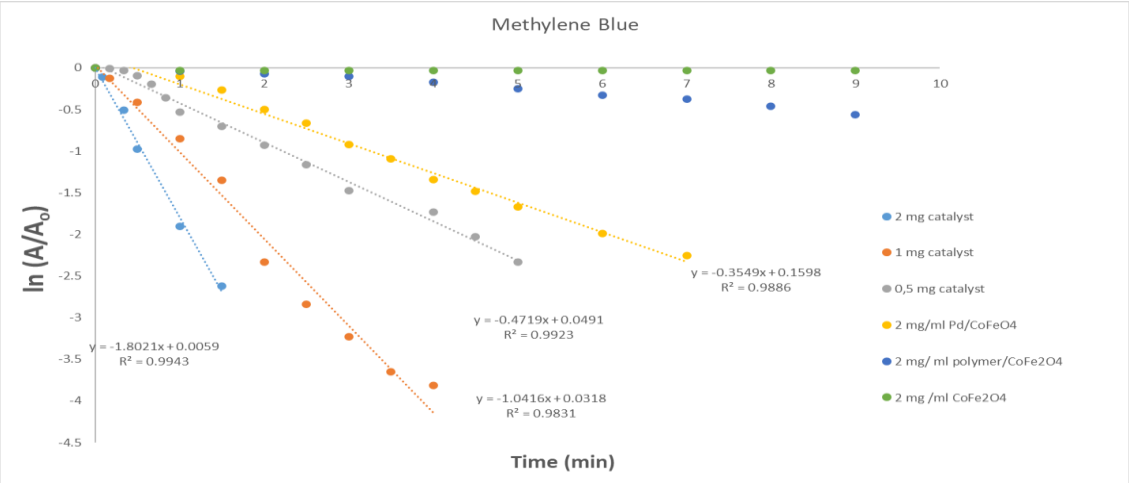

Figure 4.22 2 mg/ml of Polymer@$CoFe_2O_4$ with 0.2 mM of Methylene blue dye

4.2.2.6 (2 mg/ml $CoFe_2O_4$, 0,2 mM MB, 60 mM $NaBH_4$)

(0.2 mM) methylene blue dye was analyzed with (2 mg) of nanoparticles ($CoFe_2O_4$), and (1.95 ml) of distilled water was mixed with (60 mM) $NaBH_4$ in a cuvette. It has been shown that $CoFe_2O_4$ nanoparticles do not degrade methylene blue dye. It was found that the absorbance of methylene blue was 3.31. However, the dye absorption value remained constant during the reaction despite the passage of time, as shown in Table 4.13, and Figure 4.23 (Green line in the graph).

Table 4.13 2 mg/ml of $CoFe_2O_4$ with 0.2 mM of Methylene blue dye

2 mg/ml $CoFe_2O_4$, 0,2 mM MB, 60 mM $NaBH_4$			
Time(s)	Time (minutes)	Absorbents	In
0	0	3.31	0
60	1	3.21	-0.030677252
120	2	3.21	-0.030677252
180	3	3.21	-0.030677252
240	4	3.21	-0.030677252
300	5	3.21	-0.030677252
360	6	3.21	-0.030677252
420	7	3.21	-0.030677252
480	8	3.21	-0.030677252
540	9	3.21	-0.030677252

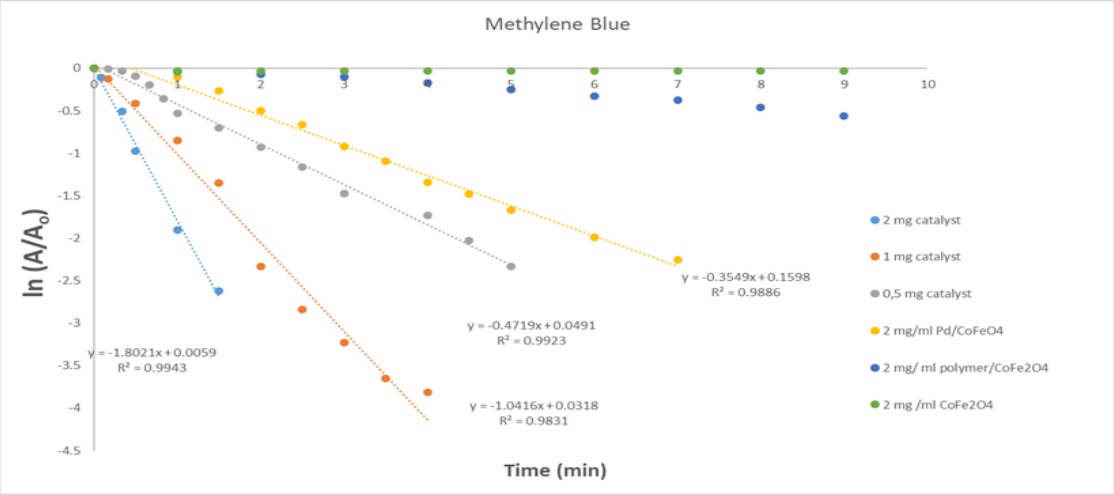

Figure 4.23 2 mg/ml of $CoFe_2O_4$ with 0.2 mM of Methylene blue dye

4.2.2.7 Recyclability of Pd@Polymer@$CoFe_2O_4$, MB

The study evaluated the performance of the Pd@Polymer@$CoFe_2O_4$ catalyst in reducing the solubility of methylene blue (MB) dye through five stages. After each stage, the catalyst is retrieved using a magnet, washed, and evaluated.

Initially, the catalyst showed promising results, significantly reducing MB adsorption and degradation. However, with each successive stage, a gradual decrease in potency is observed, which may indicate catalyst degradation or saturation. It is worth noting that despite the low activity rates (70.7%), the catalyst has consistently achieved a conversion rate of 100%, which confirms its continued catalytic potential, as illustrated in Table 4.14, and Figure 4.24.

Table 4.14 The effectiveness of the Pd@Polymer@$CoFe_2O_4$ catalyst for Methylene blue dye degradation

number of uses	start (ABS)	Remaining Amount of Substance (ABS)	Amount of Degraded Substance (ABS)	activity %	transformation %
1	3.259	0.237	3.022	100	100
2	3.259	0.375	2.884	95.43348776	100
3	3.259	0.786	2.473	81.83322303	100
4	3.259	0.91	2.349	77.72998015	100
5	3.259	1.12	2.139	70.78093977	100

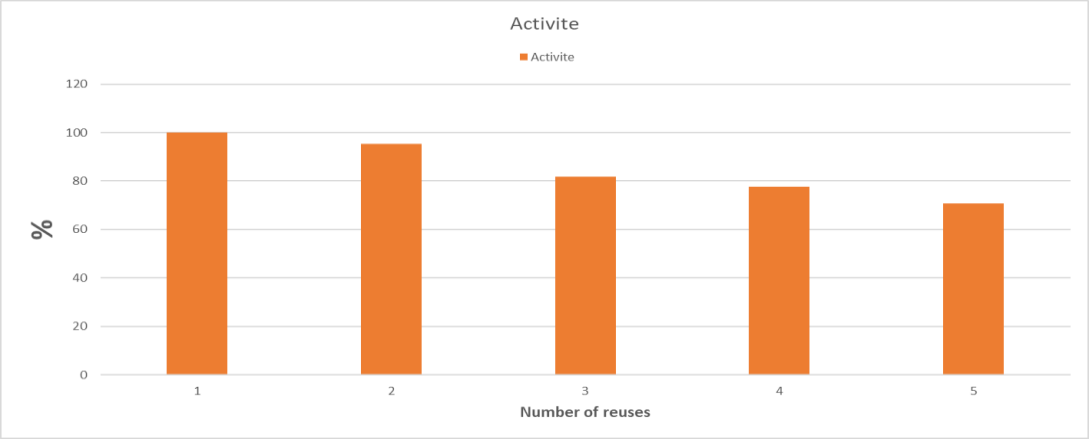

Figure 4.24 The percentage of the Pd@Polymer@$CoFe_2O_4$ catalyst for Methylene blue dye degradation

4.2.3 Methyl Orange Dye

4.2.3.1 (2 mg Pd@Polymer@$CoFe_2O_4$)

A catalyst composed of Pd@Polymer@$CoFe_2O_4$ was employed in a quantity of (2 mg) to break down methyl orange dye. The dye was present at a concentration of (0.2 mM), and a solution containing (60 mM) of $NaBH_4$ was mixed with (1.95 ml) of distilled water within a Cuvette tube. Initially, the absorbance of the methyl orange dye was measured at 2.66. As the reaction progressed, the absorbance values dropped: after 5 seconds, it decreased to 1.78; after 10 seconds, it dropped to 0.82; after 15 seconds, it reached 0.62; after 20 seconds, it fell to 0.4; and after 25 seconds, it diminished to 0.36. The data indicates a rapid decline in the solubility of the methyl orange dye, showcasing a substantial reduction in absorbance over time. The reaction was completed within a remarkably short span of 0.4 minutes (24 seconds), leading to a loss of color. The results suggest that the Pd@Polymer@$CoFe_2O_4$ catalyst played a pivotal role in swiftly and effectively facilitating the breakdown of the methyl orange dye, as evident from Table 4.15, and Figure 4.25.

Table 4.15 2 mg of Pd@Polymer@$CoFe_2O_4$with 0.2 mM of Methyl Orange dye

2 mg Pd@Polymer@$CoFe_2O_4$, 0.2 mM MO, 60 mM $NaBH_4$			
Time (s)	Time (minutes)	Absorbents	In
0	0	2.66	0
5	0.083333	1.78	-0.40171
10	0.166667	0.82	-1.17678
15	0.25	0.62	-1.45636
20	0.333333	0.4	-1.89462
25	0.416667	0.36	-1.99998

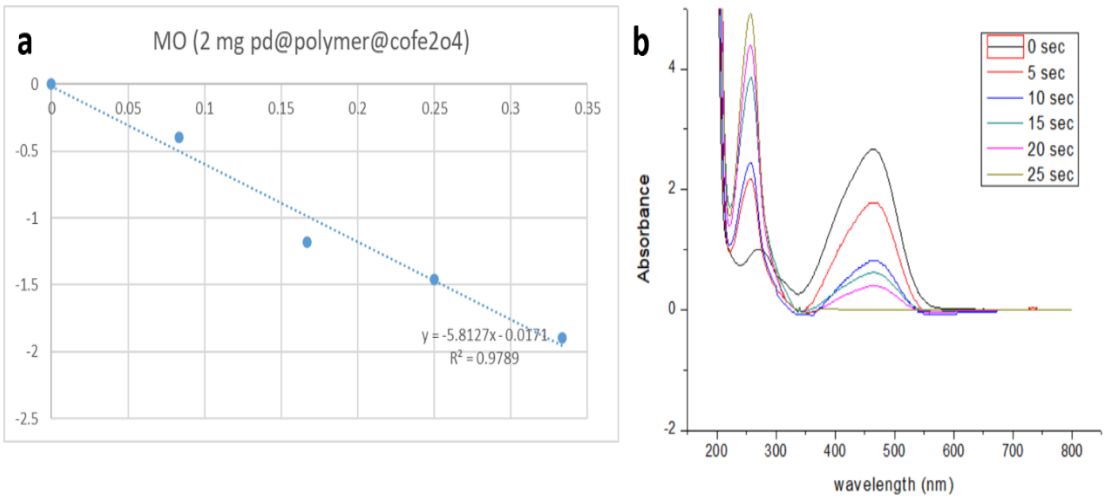

Figure 4.25 (a) 2 mg of Pd@Polymer@$CoFe_2O_4$with MO, (b) Time-dependent UV–Vis absorption spectra for the reduction of MO

4.2.3.2 (1 mg Pd@Polymer@$CoFe_2O_4$)

This catalyst was used Pd@Polymer@$CoFe_2O_4$ in an amount of (1 mg) to decompose the methyl orange dye. The concentration of the dye was (0.2 mM), and then (60 mM) of $NaBH_4$ was mixed in (1.95 ml) of distilled water in a Cuvette tube. It can be observed that initially, the absorbance of methyl orange dye was measured at 2.66. After 10 seconds, the absorbance of the dye decreased to 1.12; after 20 seconds, it decreased to 0.62; after 30 seconds, it decreased to 0.44; after 40 seconds, it decreased to 0.3; and after 50 seconds, it decreased to 0.14. However, at 1 minute (60 seconds), the absorbance of the dye reached 0. In this context, it can be stated that in this experiment, the Pd@Polymer@$CoFe_2O_4$ catalyst facilitated the rapid dissolution of methyl orange dye, and at the end of the reaction, it was observed that the dye had completely disappeared. This demonstrates that the catalyst effectively broke down the dye, and the reaction occurred rapidly, as shown in Table 4.16, and Figure 4.26.

Table 4.16 1 mg of Pd@Polymer@$CoFe_2O_4$ with 0.2 mM of Methyl Orange dye

1 mg Pd@Polymer@$CoFe_2O_4$, 0.2 mM MO, 60 mM $NaBH_4$			
Time (s)	Time (minutes)	Absorbents	In
0	0	2.66	0
10	0.166667	1.12	-0.865
20	0.333333	0.62	-1.45636
30	0.5	0.44	-1.79931
40	0.666667	0.3	-2.1823
50	0.833333	0.14	-2.94444
60	1	0	

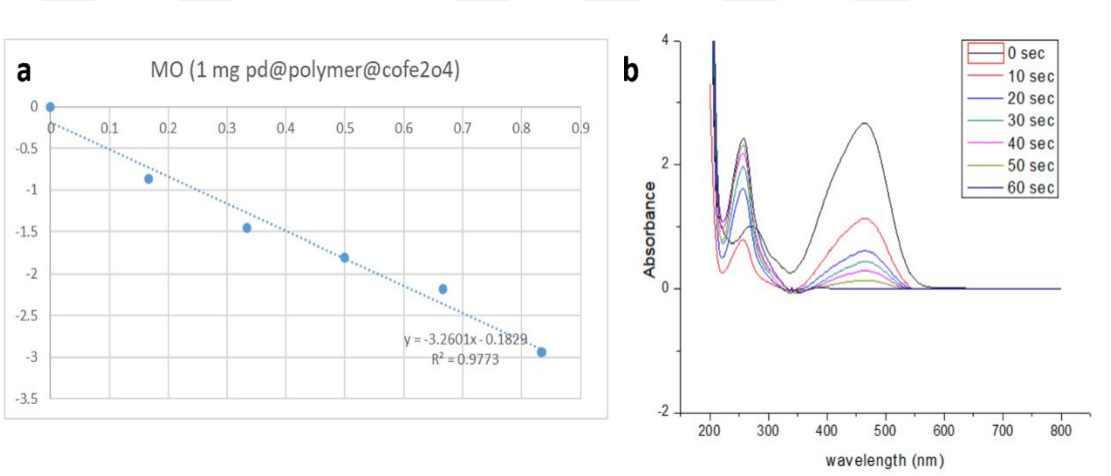

Figure 4.26 (a) 1 mg of Pd@Polymer@$CoFe_2O_4$ with MO. (b) Time-dependent UV–Vis absorption spectra for the reduction of MO

4.2.3.3 (0.5 mg Pd@Polymer@$CoFe_2O_4$)

This catalyst was used by Pd@Polymer@$CoFe_2O_4$ in an amount of (0.5 mg) to decompose the methyl orange dye. The concentration of the dye was (0.2 mM), and then (60 mM) of $NaBH_4$ was mixed in (1.95 ml) of distilled water in a Cuvette tube. Initially, the absorbance of methyl orange dye was measured at 2.64. After 10 seconds, the absorbance of the dye decreased to 1.8; after 20 seconds, it decreased to 1.45; after 30 seconds, it decreased to 1.12; after 40 seconds, it decreased to 0.96; and after 60 seconds, it decreased to 0.62. However, after 90 seconds, the absorbance of the dye dropped to 0.32, and after 2 minutes (120 seconds), the absorbance reached 0. This

indicates the complete dissolution of the dye. In this experiment, the Pd@Polymer@$CoFe_2O_4$ catalyst facilitated the rapid dissolution of methyl orange dye, and at the end of the reaction, it was observed that the dye had completely disappeared, as shown in Table 4.17, and Figure 4.27.

Table 4.17 0.5 mg of Pd@Polymer@$CoFe_2O_4$with 0.2 mM of Methyl Orange dye

0.5 mg Pd@Polymer@$CoFe_2O_4$, 0.2 mM MO, 60 mM $NaBH_4$			
Time (s)	Time (minutes)	Absorbents	In
0	0	2.64	0
10	0.166667	1.8	-0.39054
20	0.333333	1.45	-0.60676
30	0.5	1.12	-0.865
40	0.666667	0.96	-1.01915
60	1	0.62	-1.45636
90	1.5	0.32	-2.11776
120	2	0	#NUM!

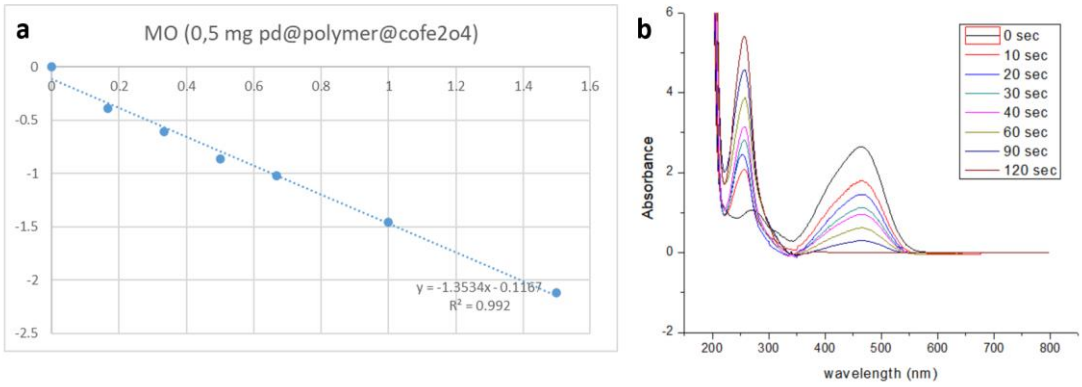

Figure 4.27 (a) 0.5 mg of Pd@Polymer@$CoFe_2O_4$with MO, (b) Time-dependent UV-Vis absorption spectra for the reduction of MO.

4.2.3.4 (2 mg/ml $CoFe_2O_4$ @Pd, 0.2 mM MO, 60 mM $NaBH_4$)

A (0.2 mM) concentrate of methyl orange dye was mixed with (2 mg) of this catalyst ($CoFe_2O_4$ @Pd). Next, (1.95 ml) of distilled water and (60 mM) $NaBH_4$ were mixed in a cuvette tube. It was found that the initial absorbance value of methyl orange,

2.66, decreased with time. Absorbance changes were determined for each time period and represented by negative numbers to quantify the reaction rate. The table shows how the amount of methyl orange decreases and degrades as the reaction proceeds. Absorption decreases rapidly at first, especially during the first 90 seconds, then decreases more slowly, after which the dye is gone within 6 minutes. As shown in Table 4.18, and Figure 4.28, the yellow line.

Table 4.18 2 mg of $CoFe_2O_4$ @Pd with 0.2 mM of Methyl Orange dye

2 mg/ml Pd/$CoFe_2O_4$ @Pd, 0.2 mM MO, 60 mM $NaBH_4$			
Time (s)	Time (minutes)	Absorbents	In
0	0	2.66	0
30	0.5	2.29	-0.14977
60	1	2.03	-0.27029
90	1.5	1.874	-0.35025
120	2	1.62	-0.4959
150	2.5	1.42	-0.62767
180	3	1.24	-0.76321
210	3.5	0.95	-1.02962
240	4	0.82	-1.17678
300	5	0.65	-1.40911
360	6	0.42	-1.84583

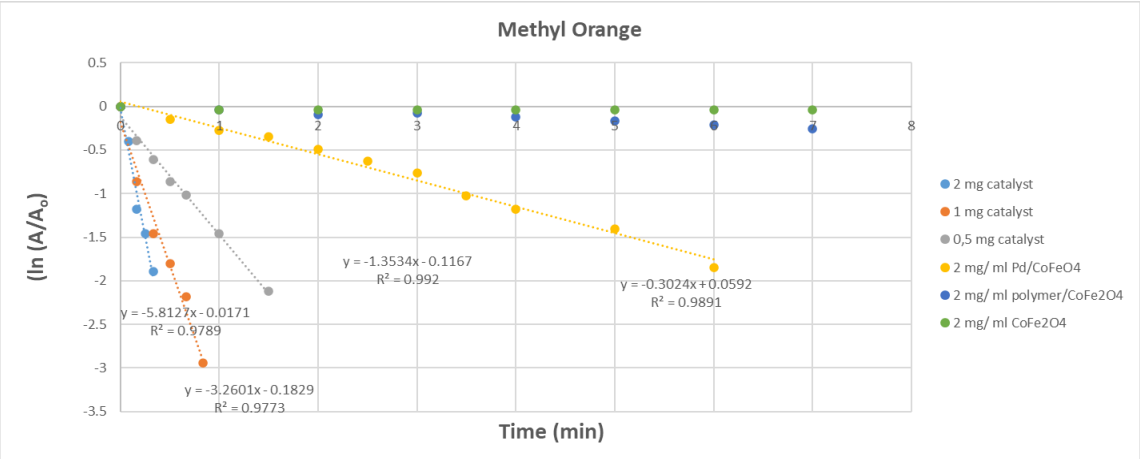

Figure 4.28 2 mg of $CoFe_2O_4$ @Pd with 0.2 mM of Methyl Orange dye

4.2.3.5 (2 mg/ml Polymer@$CoFe_2O_4$, 0,2 mM MO, 60 mM $NaBH_4$)

A catalyst (Polymer@$CoFe_2O_4$) was employed to facilitate the reduction of methyl orange dye using $NaBH_4$ as the reducing agent. The experiment was conducted with (2 mg) of the catalyst and a (0.2 mM) methyl orange dye solution. A mixture of $NaBH_4$ (60 mM) and 1.95 ml of distilled water was prepared in a Cuvette tube.

Initially, the solution's absorbance was measured at 2.66, and within 60 seconds, it decreased to 2.56. This drop in absorbance signified the initiation of the reduction process. As the reaction time progressed, the absorbance values exhibited a gradual decline. Specifically, after 6 minutes (360 seconds), the absorbance reached 2.16, indicating a substantial reduction in the methyl orange dye. At 7 minutes (420 seconds), the absorbance further decreased to 2.06, indicating that the reaction had reached a significant completion point.

Throughout the reaction, a consistent negative trend was observed in the absorbance values. This trend corresponded to the progressive color removal from the solution as the methyl orange dye underwent reduction. These findings are presented in Table 4.19, and illustrated by the blue line in Figure 4.29.

Table 4.19 2 mg of Polymer@$CoFe_2O_4$ with 0.2 mM of Methyl Orange dye

2 mg/ml Polymer@$CoFe_2O_4$, 0.2 mM MO, 60 mM $NaBH_4$			
Time (s)	Time (minutes)	Absorbents	In
0	0	2.66	0
60	1	2.56	-0.03832
120	2	2.43	-0.09043
180	3	2.46	-0.07816
240	4	2.36	-0.11966
300	5	2.26	-0.16296
360	6	2.16	-0.20822
420	7	2.06	-0.25562

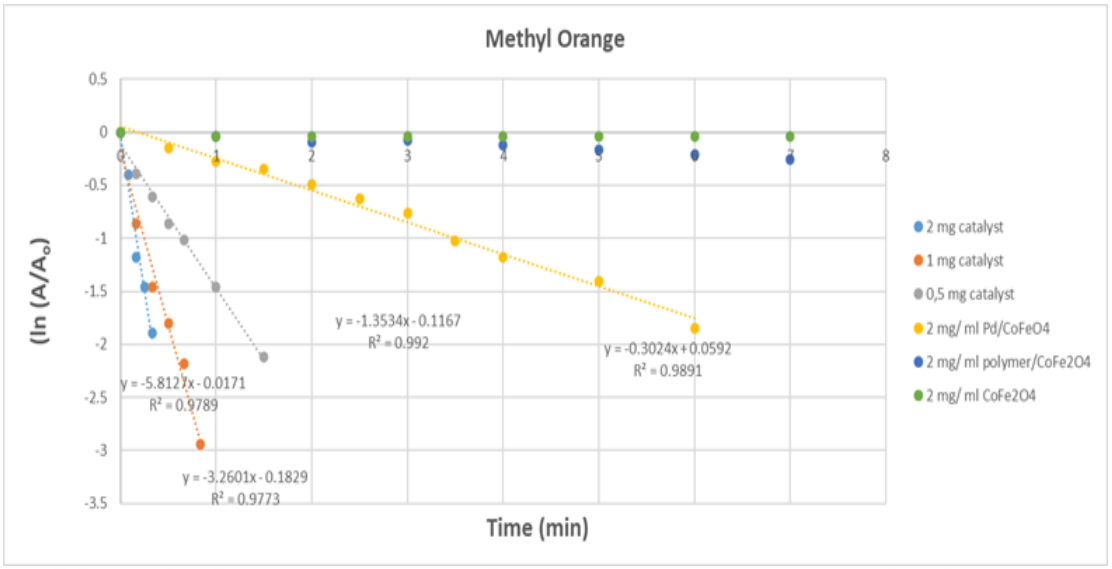

Figure 4.29 2 mg of Polymer@$CoFe_2O_4$ with 0.2 mM of Methyl Orange dye

4.2.3.6 (2 mg/ml $CoFe_2O_4$, 0.2 mM MO, 60 mM $NaBH_4$)

This nanoparticle ($CoFe_2O_4$) was utilized in a Cuvette tube in a concentration of (0.2 mM) for methyl orange dye, and then $NaBH_4$ (60 mM) was combined with (1.95 ml) of distilled water. The absorbance of the solution is initially 2.66, and it remains constant at 2.56 during the reaction time. During this procedure, no change in absorbance is seen. As indicated in Table 4.20, and the green line in Figure 4.30, the $CoFe_2O_4$ nanoparticle is unsuccessful at catalyzing the reduction reaction of methyl orange dye with $NaBH_4$.

Table 4.20 2 mg/ml of $CoFe_2O_4$ with 0.2 mM of Methyl Orange dye

2 mg/ml $CoFe_2O_4$, 0.2 mM MO, 60 mM $NaBH_4$			
Time (s)	Time (minutes)	Absorbents	In
0	0	2.66	0
60	1	2.56	-0.03832
120	2	2.56	-0.03832
180	3	2.56	-0.03832
240	4	2.56	-0.03832
300	5	2.56	-0.03832
360	6	2.56	-0.03832
420	7	2.56	-0.03832

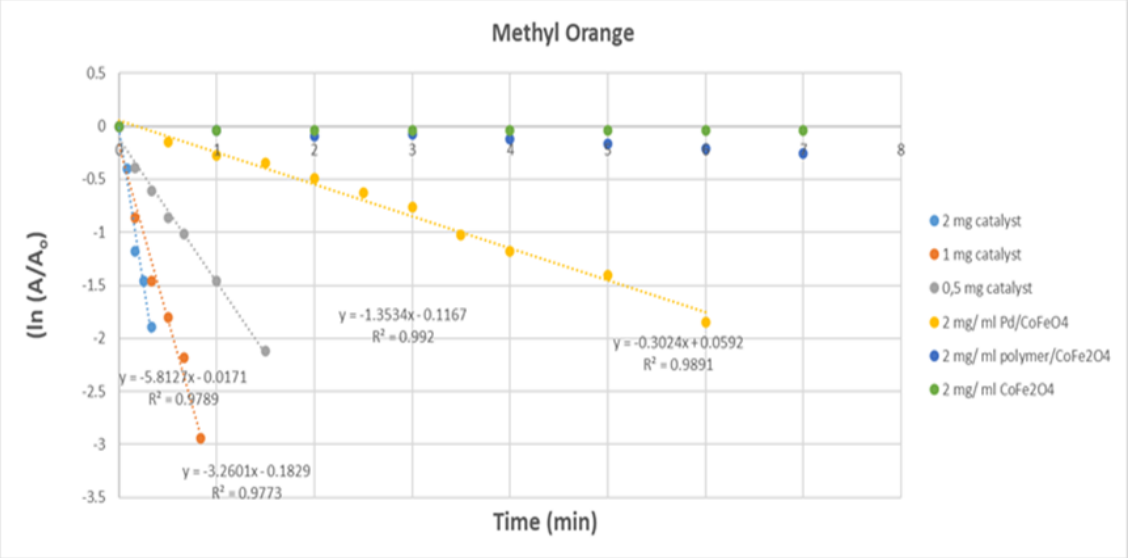

Figure 4.30 2 mg/ml of $CoFe_2O_4$ with 0.2 mM of Methyl Orange dye

4.2.3.7 Recyclability of Pd@Polymer@$CoFe_2O_4$, MO

The experiment involved the 5 times comparison for MO dye and their effectiveness on the Pd@Polymer@$CoFe_2O_4$ catalyst. Each time the catalyst was separated by an external magnet and washed with distilled water; Table 4.21 illustrates the catalyst's efficacy in dye degradation. Initially, at an absorbance of 2.66, the catalyst exhibited complete dye breakdown, achieving 100% conversion and activity. However,

in subsequent stages, while the catalyst's effectiveness remained relatively high, there was a gradual decline. This decline was marked by decreasing activity percentages. It is worth noting that despite the low activity rates (74.8%), the catalyst consistently maintained a 100% conversion rate, as shown in Figure 4.31.

Table 4.21 The effectiveness of the Pd@Polymer@$CoFe_2O_4$ catalyst for Methyl Orange dye degradation

Number of uses	start (ABS)	Remaining Amount of Substance (ABS)	Amount of Degraded Substance (ABS)	activity %	transformation %
1	2.66	0.47	2.19	100	100
2	2.66	0.53	2.13	97.26027	100
3	2.66	0.69	1.97	89.95434	100
4	2.66	0.91	1.75	79.90868	100
5	2.66	1.02	1.64	74.88584	100

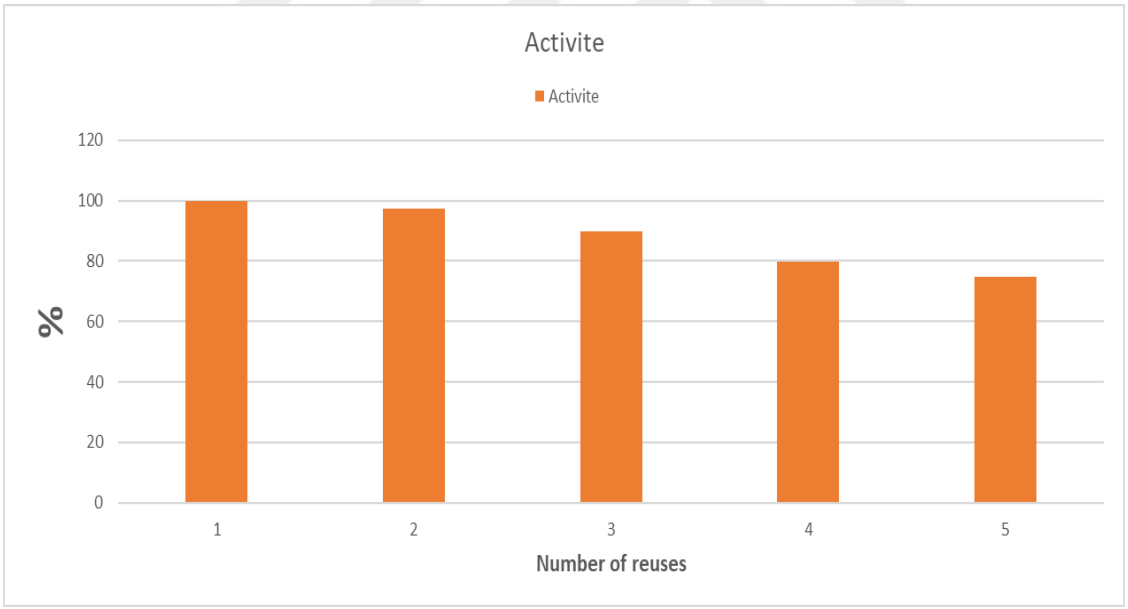

Figure 4.31 The percentage of the Pd@Polymer@$CoFe_2O_4$ catalyst for Methyl Orange dye degradation

4.2.4 The Kinetic Study

The table shows information about the decomposition of three different dyes by two different catalysts: $CoFe_2O_4$ @Polymer@Pd and CoFeO4@Pd. The dyes are 4-nitrophenol (4-NP), methylene blue (MB), and methyl orange (MO). Experiments were conducted with three different concentrations of catalyst: $CoFe_2O_4$ @Polymer@Pd: 2 mg, 1 mg, and 0.5 mg. The data includes R2 values and rate constants (K) for each combination of dye, catalyst, and concentration. For all dyes and both catalysts, the R2 values are relatively high, ranging from approximately 0.977 to 0.994. This shows that the pseudo-first-order kinetic model fits the experimental data well, which means that the decomposition reactions follow first-order kinetics, which is applied in equation (3.1). The rate constants (K) generally increase with higher catalyst concentrations. We can determine which dye decomposes the fastest for each catalyst based on their respective rate constants (K). A concentration of 2 mg was chosen because it has the lowest dye degradation time.

For Pd@Polymer@$CoFe_2O_4$ catalyst, methyl orange (K = 5.8127 min^{-1}) decomposes faster, followed by 4-nitrophenol (K = 2.2251 min^{-1}), then methylene blue (K = 1.8021 min^{-1}). For the CoFeO4@Pd catalyst, methyl orange (K = 3.2601 min^{-1}) also decomposes the fastest, followed by 4-nitrophenol (K = 1.1878 min^{-1}) and then methylene blue (K = 1.0416 min^{-1}). This observation indicates that the Pd@Polymer@$CoFe_2O_4$ catalyst shows a higher decomposition rate of methyl orange dye. Hence, it can be concluded that methyl orange shows the fastest degradation rate compared to the other colours examined.

5. DISCUSSION AND CONCLUSION

This thesis examines how efficiently a nanohybrid catalyst consisting of cobalt ferrite ($CoFe_2O_4$), Polymer, and palladium (Pd) can break down organic colors like methylene blue, methyl orange, and 4-nitrophenol using sodium borohydride ($NaBH_4$) as a reducing agent. Tests are done at room temperature. The aims are to create and describe the catalyst, analyze how effectively it degrades dye, understand the reaction kinetics and mechanism, evaluate its efficacy, and investigate potential applications. The objective of this study is to shed light on the behavior and efficacy of catalysts in the removal of pollutant dyes from wastewater, a topic that has garnered significant attention in the field of research.

SEM images as seen in Figure 4.1 reveal that the bulk $CoFe_2O_4$ particles exhibit an aggregated or clustered appearance. This clustering phenomenon is attributed to two main factors: high surface activity and the strong magnetism of the $CoFe_2O_4$ nanoparticles. Such nanoparticles tend to aggregate due to attractive forces between their surfaces and their magnetic properties. The images Figure 4.1 show the microstructure and morphology of $CoFe_2O_4$ nanoparticles that are coated with a Polymer material. These nanoparticles have an average size of around 32 nm. The presence of gaps between the coated particles enhances the porosity of the catalyst. The gaps create additional surface area and facilitate the diffusion of reactants and products during chemical reactions, potentially leading to improved reaction efficiency. and Figure 4.2 show Pd nanoparticles adhering to a Polymer in a catalyst structure called Pd@Polymer@$CoFe_2O_4$. This adherence ensures compatibility between the Pd nanoparticles and the Polymer matrix, preventing particle detachment and thereby increasing the catalyst's lifespan. Additionally, this adherence contributes to the overall structural and thermal stability of the catalyst (Karaoglu et al., 2013).

The EDX analysis reveals that the catalytic activity of $CoFe_2O_4$ nanoparticles varies depending on the modification method. As seen in Figure 4.3 and 4.4, $CoFe_2O_4$ nanoparticles have high crystallinity and minimal impurities, resulting in superior performance. However, when mixed with Polymer matrices, the proportion of carbon (C) increases, and iron (Fe) and cobalt (Co) decreases. This decrease in catalytic activity is attributed to the Polymer matrices, which reduce the surface area and reaction centers

of $CoFe_2O_4$ nanoparticles. Additionally, Polymer@$CoFe_2O_4$ nanocomposites exhibit lower catalytic activity compared to pure $CoFe_2O_4$ nanoparticles. In Figure 4.5, when $CoFe_2O_4$ nanoparticles are used within Polymer matrices and coated with Pd, catalytic activity increases. As a result, Pd@Polymer@$CoFe_2O_4$ nanocomposites exhibit higher catalytic activity (Sundaram and Murugesan, 2015).

In the X-ray diffraction (XRD) analysis of the $CoFe_2O_4$ @Polymer@Pd catalyst (black line), sharp and narrow peaks at specific 2θ values (30.28, 35.66, 36.69, 42.12, 44.95, 54.95, 57.18, and 63.95) indicate high crystallinity for both $CoFe_2O_4$ and Pd nanoparticles. Additionally, six peaks corresponding to indices (2 2 0), (3 1 1), (4 0 0), (4 2 2), (5 1 1), and (4 4 0) suggest a well-formed structure. Through this line profile fitting, the average crystallite size of 8.5 ±1 nm was determined (Demirelli et al., 2014). The crystalline size of the nanoparticles was determined using the Debye-Scherrer equation, $D_{XRD} = K \lambda / \beta \cos \theta$, where D stands for the nanoparticle size, K for the Scherrer constant (0.98), λ denotes the wavelength (1.54), and β denotes the full width at half maximum (FWHM). This catalyst exhibits the highest crystallinity among the tested materials, implying excellent structural integrity and catalytic activity (Karaoglu and Baykal, 2014).

The magnetic parameters of the $CoFe_2O_4$, Polymer@$CoFe_2O_4$, and Pd@Polymer@$CoFe_2O_4$ were determined via a vibrating sample magnetometer (VSM). $CoFe_2O_4$ has the highest coercivity (0.5 kOe) and remanent magnetization (58.2 emu/g^{-1}) values. This demonstrates the hard magnetism of $CoFe_2O_4$. The coercivity (0.3 kOe) and remanent magnetization (30.1 emu/g^{-1}) values of Polymer@$CoFe_2O_4$ are lower than those of $CoFe_2O_4$. This suggests that a non-magnetic Polymer matrix has been applied as a coating over the $CoFe_2O_4$ nanoparticles. The catalyst Pd@Polymer@$CoFe_2O_4$, which has the lowest coercivity (0.1 kOe) and remanent magnetization (11.8 emu/g^{-1}) values, makes it the softest magnet among them. indicating that the aforementioned findings provide a straightforward and effective method for the isolation and reutilization of the Pd@Polymer@$CoFe_2O_4$ nanocatalyst by the use of an external magnetic field. (Xuanduong et al., 2014).

XPS was utilized to evaluate the surface chemical composition of the as-prepared Pd@Polymer@$CoFe_2O_4$ composite catalyst. Figure 4.9, clearly showed C1s, Co2p, Fe2p, N1s, O1s, and Pd3d signals.

As seen in Figure 4.10, The 285 eV binding energy in C 1s spectra suggests carbon chemical environments and hybridization states. allocated to (C-C). The sample has several carbon states. Two peaks at 782.52 and 797.25 in the Co2p spectra validated the compound's Co^{2+} oxidation status (Nappini et al., 2015). The octahedral site's Fe^{3+} valence state is shown by two peaks at 712.45 and 725 eV in the Fe2p spectra (Yan et al.; 2015). An N 1s spectral peak at 400.2 eV indicates various nitrogen chemical environments and surface functional groups. The peak at 531,50 eV in the O1s spectrum indicates oxygen binding energy in diverse chemical conditions and is ascribed to (C-O-O) (Mohamed et al., 2015). Two peaks of Pd 3d at 336.1 and 341.2 eV correspond to $3d_{3/2}$ and $3d_{5/2}$ of the metallic form of Pd (Pd^0), confirming that $Pd2^+$ was mostly reduced to metallic Pd, which may be related to catalytic activity (Bin et al., 2020).

The catalytic performance of the compounds generated in this study was evaluated using three organic dyes, namely 4-NP, MB, and MO. The measurement of dye degradation over time is conducted using a UV–vis spectrophotometer.

5.1 4-Nitrophenol

The catalyst (Pd@Polymer@$CoFe_2O_4$) caused a colour change from yellow to colourless within 0.6, 2, and 3 minutes at concentrations of 2 mg, 1 mg, and 0.5 mg, respectively, exhibited an absorption peak at approximately 400 nm, (Park et al., 2009) and was stable at room temperature. As the concentration decreased, the rate of catalytic 4-NP degradation increased, resulting in accelerated degradation. The rate of colour change is dependent on the concentration of the catalyst, with greater concentrations resulting in a quicker rate (Panigrahi, et al., 2007)

The compound ($CoFe_2O_4$ @Pd) at a concentration of 2 mg decreased dye adsorption within 7 minutes, indicating that inadequate active catalytic sites slowed degradation. However, 2mg of $CoFe_2O_4$ @Polymer reduced dye adsorption within 7 minutes without colour loss, indicating that reduction reactions occur slowly in the absence of a Pd nanoparticles are excellent catalysts for hydrogenation reactions, when 2 mg of $CoFe_2O_4$ nanoparticles, there was no change in absorption. This indicates that the adsorbent surface is diverse.

5.2 Methylene Blue

$CoFe_2O_4$ @Polymer@Pd catalyst in concentrations 2mg, 1mg, and 0.5mg, the catalyst-decolorization efficiency reaction was tested with varied amounts. The most significant factor is MB dye colorlessness time. revealed an absorption peak at 660 nm, decolorizing quicker at 1.5, 4, and 6 minutes with higher catalyst doses. This pattern shows catalyst decolorization efficiency. The catalytic dose may reduce decolorization time due to active catalytic sites on the catalyst surface. More catalyst active sites interact with dye molecules, accelerating dye degradation. The 2 mg $CoFe_2O_4$@Pd molecule follows. It caused the MB dye to fade after 7 minutes. There may not be enough active catalytic sites to quickly breakdown the MB dye. While the $CoFe_2O_4$@Polymer catalyst took 9 minutes, the color did not fade. indicating that reduction reactions occur slowly in the absence of Pd nanoparticles, which are excellent catalysts for hydrogenation reactions. When applied alone, $CoFe_2O_4$ did not degrade the dye (Kurtan et al., 2016).

5.3 Methyl Orange

(Pd@Polymer@$CoFe_2O_4$) Catalyst amounts of 2 mg, 1 mg, and 0.5 mg were tested, revealed an absorption peak at 460 nm, decolorizing quicker at 0.4, 1, and 2 minutes. This pattern shows catalyst decolorization efficiency. The catalytic dose may reduce decolorization time due to active catalytic sites on the catalyst surface. More catalyst active sites interact with dye molecules, accelerating dye degradation.

The 2 mg $CoFe_2O_4$@Pd molecule follows. It caused the MO dye to fade after 6 minutes. There may not be enough active catalytic sites to quickly breakdown the MO dye. While the $CoFe_2O_4$@Polymer catalyst took 7 minutes, the color did not fade. indicating that reduction reactions occur slowly in the absence of Pd nanoparticles, which are excellent catalysts for hydrogenation reactions. When applied alone, $CoFe_2O_4$ did not degrade the dye (Kurtan et al., 2016).

A more comprehensive understanding of the catalytic activity of the catalyst may be obtained by examining the kinetics of the reduction process. In the conducted experiment, it was seen that the concentration of $NaBH_4$ exceeded that of azo dyes

significantly. Hence, the utilisation of pseudo-first-order kinetics enables the estimation of rate constants. The findings indicate that the catalytic decolorization of these azo dyes adheres to the first-order kinetic model, specifically described by the equation (3.1). In this equation, C_0 represents the initial concentration, C_t represents the concentration at time t, and k represents the apparent rate constant. The rate constants were determined for the decomposition of methyl orange (K = 5.8127 min^{-1}), 4-nitrophenol (K = 2.2251 min^{-1}), and methylene blue (K = 1.8021 min^{-1}), respectively. It is far more than the figures documented in the existing body of scholarly research (Lijuan et al., 2013).

The Pd@Polymer@$CoFe_2O_4$ catalyst has excellent dispersibility, enabling facile collection using a magnet. Consequently, this catalyst may be efficiently recycled after the catalytic process. The Pd@Polymer@$CoFe_2O_4$ catalyst exhibited sustained catalytic activity through numerous cycles, thereby confirming its stability. The absorption capacity exhibited a little decline during 5 successive iterations, with decreases of 71.6% for 4-NP, 70.7% for MB, and 74.8% for MO. The aforementioned observation underscores the catalyst's prospective practical use in efficiently mitigating organic dye pollution and its aptness for reuse and recycling.

This finding suggests that the $CoFe_2O_4$ @Polymer@Pd catalyst exhibits a greater rate of breakdown for the methyl orange dye. Therefore, it can be inferred that methyl orange exhibits the highest rate of deterioration in comparison to the other colours that were investigated.

6. CONCLUSION

The present work effectively synthesized a Pd@Polymer@$CoFe_2O_4$ magnetic nanocatalyst using a co-precipitation technique, which exhibited great effectiveness. Additionally, the data obtained demonstrated outstanding activity for the dyes 4-NP, MB, and MO. The Pd@Polymer@$CoFe_2O_4$ catalyst has a higher rate of breakdown for methyl orange dye. Based on the findings, it can be inferred that methyl orange exhibits the greatest rate of deterioration in comparison to the other hues that were investigated. Furthermore, this distinctive nanocatalyst may be effortlessly extracted from the reaction mixture by the use of magnetic external. Therefore, it shows promise as a suitable medium for the production of very effective magnetic catalysts for a range of heterogeneous catalytic reduction applications.

REFERENCES

Alonso, A., Macanás, J., Davies, G.L., Y. K. G. (2022). E*nvironmentally-Safe Polymer-Metal Nanocomposites with Most Favorable Distribution of Catalytically Active and Biocide Nanoparticles [Universitat Autònoma de Barcelona 2 Universitat, Politècnica de Catalunya]*. https://www.researchgate.net/publication/267782182_Environmentally-Safe_Polymer_Metal_Nanocomposites_with_Most_Favorable_Distribution_of_Catalytically_Active_and_Biocide_Nanoparticles

Abdollahi, M., Mohammadirad, A. (2014). 4-Nitrophenol. *Encyclopedia of Toxicology: Third Edition*, 3, 575–577.

Abdul, Wahid., (2023). *UV-Vis Spectroscopy: Principle, Instrumentation, and Applications - Instrumental Analysis - PSIBERG*. PSIBERG. https://psiberg.com/uv-vis-spectroscopy/

Ali, M. S., Al-Shukri, A. A., Maghami, M. R., Gomes, C. (2021). Nano and bio-composites and their applications: A review. *IOP Conference Series: Materials Science and Engineering*, 1067(1), 012093. https://doi.org/10.1088/1757-899x/1067/1/012093

Alloosh, M. T. (2020). Biosynthesis of nanoparticles and their applications for the control of agricultural pests: A review. *Arab Journal of Plant Protection*, 38(4), 267–280. https://doi.org/10.22268/AJPP-38.4.267280

Dyer, D.J. (2006). Photoinitiated Synthesis of Grafted Polymers. Adv. *Polym. Sci.* 197, 47–65.

Astruc, D., Lu, F., Aranzaes, J. R. (2005). Nanoparticles as recyclable catalysts: The frontier between homogeneous and heterogeneous catalysis. In *Angewandte Chemie - International Edition* (Vol. 44, Issue 48, pp. 7852–7872). Angew Chem Int Ed Engl. https://doi.org/10.1002/anie.200500766

Balasubramanian, S., Jeyapaul, U., Kala, S.M.J. (2019). Antibacterial Activity of Silver Nanoparticles Using Jasminum auriculatum Stem Extract. I*nternational Journal of Nanoscience*, 18(1). https://doi.org/10.1142/S0219581X18500114

Baran, T., Nasrollahzadeh, M. (2021). Pd/$CoFe_2O_4$ /chitosan: A highly effective and easily recoverable hybrid nanocatalyst for synthesis of benzonitriles and reduction of 2-nitroaniline. *Journal of Physics and Chemistry of Solids*, 149, 109772. https://doi.org/10.1016/j.jpcs.2020.109772

Barman, K., Chowdhury, D., Baruah, P. K. (2020). Bio-synthesized silver nanoparticles using Zingiber officinale rhizome extract as efficient catalyst for the degradation of environmental pollutants. *Inorganic and Nano-Metal Chemistry*, 50(2), 57–65. https://doi.org/10.1080/24701556.2019.1661468

Bashir, M. S., Jiang, X., Kong, X. Z. (2020). Porous polyurea microspheres with Pd immobilized on surface and their catalytic activity in 4-nitrophenol reduction and organic dyes degradation. *European Polymer Journal*, 129(January), 109652. https://doi.org/10.1016/j.eurpolymj.2020.109652

Behrens, S. (2011). Preparation of functional magnetic nanocomposites and hybrid materials: Recent progress and future directions. *Nanoscale*, 3(3), 877–892. https://doi.org/10.1039/c0nr00634c

Bhandari, R., Knecht, M. R. (2012). Isolation of template effects that control the structure and function of nonspherical, biotemplated Pd nanomaterials. *Langmutir*,

28(21), 8110–8119. https://doi.org/10.1021/la3015404
Bhowmik, T., Kundu, M. K., Barman, S. (2015). Ultra small gold nanoparticles-graphitic carbon nitride composite: An efficient catalyst for ultrafast reduction of 4-nitrophenol and removal of organic dyes from water. *RSC Advances*, 5(48), 38760–38773. https://doi.org/10.1039/c5ra04913j
Biesalski, M., Johannsmann, D., Rühe, J. (2002). Synthesis and swelling behavior of a weak polyacid brush. *Journal of Chemical Physics*, 117(10), 4988–4994. https://doi.org/10.1063/1.1490924
Bin-Jumah, M., Al-Abdan, M., Albasher, G., Alarifi, S. (2020). Effects of green silver nanoparticles on apoptosis and oxidative stress in normal and cancerous human hepatic cells in vitro. *International Journal of Nanomedicine*, 15, 1537–1548. https://doi.org/10.2147/IJN.S239861
Cai, K., Shen, W., Ren, B., He, J. J., Wu, S., Wang, W., Fu, Y., Xu, P., Huang, D., Zeng, G., Lai, C., Qin, L., Li, B., He, J. J., Yi, H., Cheng, M., Zhang, C., Rasheed, T., Nabeel, F., … Barman, S. (2021). Mussel-inspired preparation of temperature-responsive Polymer brushes modified layered double hydroxides@Pd/carbon dots hybrid for catalytic applications. *Journal of Molecular Liquids*, 23(2), 105958. https://doi.org/10.1016/j.clay.2020.105958
Cai, K., Shen, W., Ren, B., He, J., Wu, S., Wang, W. (2017). A phytic acid modified $CoFe_2O_4$ magnetic adsorbent with controllable morphology, excellent selective adsorption for dyes and ultra-strong adsorption ability for metal ions. *Chemical Engineering Journal*, 330, 936–946. https://doi.org/10.1016/j.cej.2017.08.009
Cao, X., Qi, D., Yin, S., Bu, J., Li, F., Goh, C. F., Zhang, S., Chen, X. (2013). Ambient fabrication of large-area graphene films via a synchronous reduction and assembly strategy. *Advanced Materials*, 25(21), 2957–2962. https://doi.org/10.1002/adma.201300586
Cao, Z., Zuo, C. (2020). Direct synthesis of magnetic $CoFe_2O_4$ nanoparticles as recyclable photo-fenton catalysts for removing organic dyes. *ACS Omega*, 5(35), 22614–22620. https://doi.org/10.1021/acsomega.0c03404
Chen, G., Huynh, D., Felgner, P. L., Guan, Z. (2006). Tandem chain walking Polymerization and atom transfer radical Polymerization for efficient synthesis of dendritic nanoparticles for bioconjugation. J*ournal of the American Chemical Society*, 128(13), 4298–4302. https://doi.org/10.1021/ja0573864
Chen, H., Zhong, A., Wu, J., Zhao, J., Yan, H. (2012). Adsorption behaviors and mechanisms of methyl orange on heat-treated palygorskite clays. *Industrial and Engineering Chemistry Research*, 51(43), 14026–14036. https://doi.org/10.1021/ie300702j
Chishti, A. N., Ni, L., Guo, F., Lin, X., Liu, Y., Wu, H., Chen, M., Diao, G. W. (2021). Magnetite-Silica core-shell nanocomposites decorated with silver nanoparticles for enhanced catalytic reduction of 4-nitrophenol and degradation of methylene blue dye in the water. *Journal of Environmental Chemical Engineering*, 9(2), 104948. https://doi.org/10.1016/j.jece.2020.104948
Christau, S., Genzer, J., Von Klitzing, R. (2015). Polymer brush/metal nanoparticle hybrids for optical sensor applications: From self-assembly to tailored functions and nanoengineering. *Zeitschrift Fur Physikalische Chemie*, 229(7–8), 1089–1117. https://doi.org/10.1515/zpch-2014-0573
Cookson, J. (2021). The preparation of palladium nanoparticles. P*latinum Metals Review*, 56(2), 83–98. https://doi.org/10.1595/147106712X632415

Costantini, F., Benetti, E. M., Tiggelaar, R. M., Gardeniers, H. J. G. E., Reinhoudt, D. N., Huskens, J., Vancso, G. J., Verboom, W. (2010). A brush-gel/metal-nanoparticle hybrid film as an efficient supported catalyst in glass microreactors. *Chemistry - A European Journal*, 16(41), 12406–12411. https://doi.org/10.1002/chem.201000948

Cuvette - Wikipedia. (2022). https://en.wikipedia.org/wiki/Cuvette

Das, K. C., Das, B., Dhar, S. S. (2020). Effective Catalytic Degradation of Organic Dyes by Nickel Supported on Hydroxyapatite-Encapsulated Cobalt Ferrite (Ni/HAP/$CoFe_2O_4$) Magnetic Novel Nanocomposite. *Water, Air, and Soil Pollution*, 231(2), 1–13. https://doi.org/10.1007/s11270-020-4409-1

Dawodu, F. A., Onuh, C. U., Akpomie, K. G., Unuabonah, E. I. (2019). Synthesis of silver nanoparticle from Vigna unguiculata stem as adsorbent for malachite green in a batch system. *SN Applied Sciences*, 1(4), 1–10. https://doi.org/10.1007/s42452-019-0353-3

Decher, G., Hong, J. D., Schmitt, J. (1992). Buildup of ultrathin multilayer films by a self-assembly process: III. Consecutively alternating adsorption of anionic and cationic polyelectrolytes on charged surfaces. *Thin Solid Films*, 210–211(PART 2), 831–835. https://doi.org/10.1016/0040-6090(92)90417-A

Deka, P., Deka, R. C., Bharali, P. (2016). Porous CuO nanostructure as a reusable catalyst for oxidative degradation of organic water pollutants. *New Journal of Chemistry*, 40(1), 348–357. https://doi.org/10.1039/c5nj02515j

Dey, C., De, D., Nandi, M., Goswami, M. M. (2020). A high performance recyclable magnetic CuFe2O4 nanocatalyst for facile reduction of 4-nitrophenol. *Materials Chemistry and Physics*, 242, 122237. https://doi.org/10.1016/j.matchemphys.2019.122237

Dolatkhah, A., Wilson, L. D. (2016). Magnetite/Polymer Brush Nanocomposites with Switchable Uptake Behavior Toward Methylene Blue. *ACS Applied Materials and Interfaces*, 8(8), 5595–5607. https://doi.org/10.1021/acsami.5b11599

Edwerd.h. (2020). Cuvette. *Chemed.Chem.Purdue.Edu*, 3(323), 98. http://chemed.chem.purdue.edu/genchem/lab/equipment/spec20/cuvette.html

Farhadi, S., Siadatnasab, F. (2016). $CoFe_2O_4$ /CdS nanocomposite: Preparation, characterisation, and application in sonocatalytic degradation of organic dye pollutants. *Cuihua Xuebao/Chinese Journal of Catalysis*, 37(9), 1487–1495. https://doi.org/10.1016/S1872-2067(16)62473-7

Fu, Y., Xu, P., Huang, D., Zeng, G., Lai, C., Qin, L., Li, B., He, J., Yi, H., Cheng, M., Zhang, C. (2019). Au nanoparticles decorated on activated coke via a facile preparation for efficient catalytic reduction of nitrophenols and azo dyes. *Applied Surface Science*, 473(August 2018), 578–588. https://doi.org/10.1016/j.apsusc.2018.12.207

Haobin Ye, B., Fong, L. H. N., Luo, J. M. (2021). Parasocial interaction on tourism companies' social media sites: antecedents and consequences. *Current Issues in Tourism*, 24(8), 1093–1108. https://doi.org/10.1080/13683500.2020.1764915

Hariri, S. (2021). Environmentally-Safe Polymer-MetalNanocomposites with Most FavorableDistribution of Catalytically Activeand Biocide Nanoparticles.

Hashim, A. A. (2020). A*dvances in Nanocomposite Technology* - Google Books. https://books.google.com.tr/books?hl=en&lr=&id=N9CPDwAAQBAJ&oi=fnd&pg=PR11&dq=advances+in+nanocomposite+technology.+Pdf&ots=Py3sTS3hKh&sig=lIPX2VH0AMyH_MheJwati9zQLI&redir_esc=y#v=onepage&q=advances in

nanocomposite technology.
Hawya, amal bu. (2020). The Impact Of The Use Of Nanotechnology On The Health And Safety Of Consumers *In The Algerian Consumption Law*, 2(4) ,1309–1293
Kaang, B. K., Han, N., Lee, H. J., Choi, W. S. (2018). Polyelectrolyte Brush-Grafted Polydopamine-Based Catalysts with Enhanced Catalytic Activity and Stability. *ACS Applied Materials and Interfaces*, 10(1), 1113–1124. https://doi.org/10.1021/acsami.7b15489
Karaoglu, E., Baykal, A. (2014). $CoFe_2O_4$ –Pd (0) Nanocomposite: Magnetically Recyclable Catalyst. *Journal of Superconductivity and Novel Magnetism*, 27(9), 2041–2047. https://doi.org/10.1007/s10948-014-2522-3
Kazemi, M., Ghobadi, M., Mirzaie, A. (2018). Cobalt ferrite nanoparticles ($CoFe_2O_4$ MNPs) as catalyst and support: Magnetically recoverable nanocatalysts in organic synthesis. *Nanotechnology Reviews*, 7(1), 43–68. https://doi.org/10.1515/ntrev-2017-0138
Kongor, A., Panchal, M., Athar, M., Vora, M., Makwana, B., Jha, P. C., Jain, V. (2021). Calix[4]pyrrole Stabilized PdNPs as an Efficient Heterogeneous Catalyst for Enhanced Degradation of Water-Soluble Carcinogenic Azo Dyes. *Catalysis Letters*, 151(2), 548–558. https://doi.org/10.1007/s10562-020-03304-x
Kurtan, U., Amir, M., Yildiz, A., Baykal, A. (2016). Synthesis of magnetically recyclable MnFe 2 O 4 @SiO 2 @Ag nanocatalyst: Its high catalytic performances for azo dyes and nitro compounds reduction. *Applied Surface Science*, 376, 16–25. https://doi.org/10.1016/j.apsusc.2016.02.120
Labidi, S. (2023). *The Role Of Digital Marketing Tools In Improving Banking Marketing Performance A Field Study On The National Bank Of Algeria -annaba- (Issue March)*. Annaba, Université Badji Mokhtar Annaba, Algeria.
Lavanant, L., Paripovic, D., Schu, N., Sugnaux, C., Tugulu, S., Klok, H. (2009). Polymer Brushes via Surface-Initiated Controlled Radical Polymerization: Synthesis, Characterization, Properties, and Applications. *Chem. Rev*, 109(11), 5437–5527.
Liu, Y., Zhang, K., Li, W., Ma, J., Vancso, G. J. (2018). Metal nanoparticle loading of gel-brush grafted Polymer fibers in membranes for catalysis. *Journal of Materials Chemistry A*, 6(17), 7741–7748. https://doi.org/10.1039/c8ta01231h
Methyl Orange -Wikipedia. (n.d.). Https://En.Wikipedia.Org/Wiki/Methyl_orange., Accessed 28 May 2022. Retrieved May 8, 2023, from https://en.wikipedia.org/wiki/Methyl_orange
Meydan, E., Demirci, S., Aktas, N., Sahiner, N., Ozturk, O. F. (2021). Catalytic performance of boron-containing magnetic metal nanoparticles in methylene blue degradation reaction and mixture with other pollutants. *Inorganic Chemistry Communications*, 126(January), 108474. https://doi.org/10.1016/j.inoche.2021.108474
Mogha, N. K., Gosain, S., Masram, D. T. (2017). Gold nanoworms immobilized graphene oxide Polymer brush nanohybrid for catalytic degradation studies of organic dyes. *Applied Surface Science*, 396, 1427–1434. https://doi.org/10.1016/j.apsusc.2016.11.182
Nagarajan, D., Venkatanarasimhan, S. (2019). Copper(II) oxide nanoparticles coated cellulose sponge—an effective heterogeneous catalyst for the reduction of toxic organic dyes. *Environmental Science and Pollution Research*, 26(22), 22958–22970. https://doi.org/10.1007/s11356-019-05419-0

Orooji, Y., Akbari, R., Nezafat, Z., Nasrollahzadeh, M., Kamali, T. A. (2021). Recent signs of progress in Polymer-supported silver complexes/nanoparticles for remediation of environmental pollutants. *Journal of Molecular Liquids*, 329, 115583. https://doi.org/10.1016/j.molliq.2021.115583

Qi, L., Zhang, K., Qin, W., Hu, Y. (2020). Highly efficient flow-through catalytic reduction of methylene blue using silver nanoparticles functionalized cotton. *Chemical Engineering Journal*, 388, 124252. https://doi.org/10.1016/j.cej.2020.124252

Rigoberto C. Advincula , William J. Brittain , Kenneth C. Caster, J. R. (2004). Polymer brushes : synthesis, characterization, applications. *WIKLY*, 483. https://www.wiley.com/engb/Polymer+Brushes%3A+Synthesis%2C+Characterization+and+Applications-p-9783527310333

Sabry, A. M. (2020). Materials developed by nanotechnology and their industrial applications in the field of product design. *International Design Journal, 10(3), 447–456.* https://doi.org/10.21608/IDJ.2020.96358

Shaikh, N. S., Shaikh, R. S., Kashid, S. (2020). In vitro bio-synthesis of silver nanoparticles using flower extract of parasitic plant Cascuta reflexa and evaluation of its biological properties. *Asian Journal of Nanoscience and Materials, 3*(2), 121–130. https://doi.org/10.26655/AJNANOMAT.2020.2.4

Sharifi Pajaie, S. H., Archin, S., Asadpour, G. (2018). Optimization of Process Parameters by Response Surface Methodology for Methylene Blue Removal Using Cellulose Dusts. *Civil Engineering Journal*, 4(3), 620. https://doi.org/10.28991/cej-0309121

Song, J., Vikulina, A. S., Parakhonskiy, B. V., Skirtach, A. G. (2023). Hierarchy of hybrid materials. Part-II: The place of organics-on-inorganics in it, their composition and applications. In *Frontiers in Chemistry* (Vol. 11, Issue APR, p. 179). Frontiers Media S.A. https://doi.org/10.3389/fchem.2023.1078840

Tercan, M. (2022). Use of Pd complex bearing 2-(thiophen-2-yl)1H-benzimidazole ligand as catalyst in reduction / degradation of multiple mixtures containing 4-NP, RhB and MB organic pollutants. *Yüzüncü Yıl Üniversitesi Fen Bilimleri Enstitüs*ü Dergisi, 28(1), 271–284. https://doi.org/10.53433/yyufbed.1167004

Wang, W., Dai, G., Yang, H., Liu, X., Chen, X., Meng, Z., He, Q. (2022). Highly efficient catalytic reduction of 4-nitrophenol and organic dyes by ultrafine palladium nanoparticles anchored on CeO2 nanorods. *Environmental Science and Pollution Research*, 29(6), 8242–8252. https://doi.org/10.1007/s11356-021-16276-1

Wang, Y., Gao, P., Wei, Y., Jin, Y., Sun, S., Wang, Z., Jiang, Y. (2021). Silver nanoparticles decorated magnetic Polymer composites (Fe_3O_4@PS@Ag) as highly efficient reusable catalyst for the degradation of 4-nitrophenol and organic dyes. *Journal of Environmental Management*, 278(P1), 111473. https://doi.org/10.1016/j.jenvman.2020.111473

Wang, Z., Kim, H. G. (2017). Can Social Media Marketing Improve Customer Relationship Capabilities and Firm Performance? Dynamic Capability Perspective. *Journal of Interactive Marketing*, 39, 15–26. https://doi.org/10.1016/j.intmar.2017.02.004

Yang, Y., Zhu, W., Cui, D., Lü, C. (2021). Mussel-inspired preparation of temperature-responsive Polymer brushes modified layered double hydroxides@Pd/carbon dots hybrid for catalytic applications. *Applied Clay Science*, 200(July 2020), 105958.

https://doi.org/10.1016/j.clay.2020.105958

Zhao, Y., Cao, B., Lin, Z., Su, X. (2019). Synthesis of $CoFe_2O_4$ /C nano-catalyst with excellent performance by molten salt method and its application in 4-nitrophenol reduction. *Environmental Pollution*, 254. https://doi.org/10.1016/j.envpol.2019.112961

Xuanduong, Le., Zhengping, Dong., Yansheng, Liu., Jin, Zhicheng; Huy, Thanh-Do; Le, Minhdong; Ma, Jiantai (2014). Palladium nanoparticles immobilized on core–shell magnetic fibers as a highly efficient and recyclable heterogeneous catalyst for the reduction of 4-nitrophenol and Suzuki coupling reactions. *J. Mater. Chem. A, 2(46),* 19696–19706.

Demirelli, M., Karaoğlu, E., Baykal, A., Sözeri, H., Uysal, E. (2014). Synthesis, characterization and catalytic activity of $CoFe_2O_4$ -APTES-Pd magnetic recyclable catalyst. *Journal of Alloys and Compounds*, 582(), 201–207.

Karaoglu, E., Summak, M. M., Baykal, A. … (2013). Synthesis and Characterization of Catalytically Activity Fe_3O_4–3-Aminopropyl-triethoxysilane/Pd Nanocomposite., 23(2), 409–417.

Xu, Z., Ding, L., Long, Y., Xu, L.G., Wang, L., Xu, C. (2011). Preparation and evaluation of superparamagnetic surface molecularly imprinted polymer nanoparticles for selective extraction of bisphenol A in packed food., 3(8), 1737–0.

Rehan, M., Mashaly, H, M., Mowafi, S., Abou El-Kheir, A.; Emam, Hossam E. (2015). Multi-functional textile design using in-situ Ag NPs incorporation into natural fabric matrix. *Dyes and Pigments,* 118, 9–17.

Park, S., Seo, J. G., J. C. Jung, S. H. Baeck, T. J. Kim, Y. M. Chung, S. H. Oh, I. K. *Song, Catal. Commun.* 2009, 10, 1762

Panigrahi, S., Basu, S., Praharaj, S., Pande, S., Jana, S., Pal, A., Ghosh, S. K., T. Pal, Phys, *J. Chem. C* 2007, 111, 4596.

EXTENDED TURKISH SUMMARY
(GENİŞLETİLMİŞ TÜRKÇE ÖZET)

BAZI ORGANİK BOYALARIN KATALİTİK BOZUNMASINA YÖNELİK MANYETİK JEL-POLİMER FIRÇA/METAL NANOPARÇACIK HİBRİT MALZEMELERİN HAZIRLANMASI

SHALLAL, Abdul Kareem Mohammed
Yüksek Lisans Tezi, Kimya Mühendisliği Anabilim Dali
Danışman: Doç. Dr. Adem ZENGIN
İkinci Danışman: Dr. Öğr. Üyesi Necdet KARAKOYUN
Eylül 2023, 88 sayfa

ÖZ

Bu çalışmada birlikte çökeltme yaklaşimi kullanilarak yeniden kullanilabilir bir Pd@Polymer@$Cofe_2O_4$ katalizörü oluşturuldu. Pd@Polymer@$Cofe_2O_4$ katalizörünün kristal yapısı, bileşimini ve saflığını doğrulayan XRD araştırması ile açıklandı. numunenin morfolojisi ve elementel yapısı sırasıyla SEM ve EDX çalışmaları ile kapsamlı bir şekilde açıklanmıştır. Fazda Co, Fe ve Pd elementleri mevcuttur. 3,2 nm kristal boyutuna sahip tek fazlı bir nanoürün oluşturulduğu XRD incelemesi ile doğrulandı. Ürünün olağanüstü manyetik yetenekleri, manyetik olarak tahrik edilen reaksiyonlarda veya manyetik ayırma yöntemlerinde katalizör olarak kullanılabileceği olasılığını artıran VSM testleri ile gösterilmiştir. Pd@Polymer@$Cofe_2O_4$'ün, metil turuncu (MO), metilen mavisi (MB) ve 4-nitrofenol (4-np) gibi organik boyaların indirgenmesini katalize edebildiği katalitik araştırmalarla gösterilmiştir. Çoklu döngülerden sonra manyetik katalizör yeniden kullanilabilir nitelikler de gösterdi. Bu nedenle Pd@Polymer@$Cofe_2O_4$, atık suyu temizlemek amacıyla organik kirleticilerin kullanılması için olası bir seçimdir.

1. MATERYAL VE YÖNTEM

Çalışmada ilk kez manyetik parçacıklar üzerinde jel-fırça kombinasyonu yapılacak. Malzemenin manyetik yapisi, manyetik ayırmayi mümkün kılacak ve katalizörün hem saflaştırma aşamasında hem de katalitik reaksiyonda ayrılmasında birçok işlevsellik sağlayacaktır. Jel firça üzerine metal nanopartiküllerin katkılanması sonucunda parçacıkların stabilitesinin, metallerin basit organik moleküllere katkılanmasına göre daha yüksek olacağı düşünülmektedir. Bu durumun katalitik verimliliği arttıracağı düşünülmektedir. Temel olarak polimerik destek malzemesi olduğundan birim alan başına düşen partikül sayısında artışa neden olacak ve katalitik verimi yüksek olacaktır.

Kobalt ferrit nanopartiküllerinin manyetik kompozitleri, Sodyum Borohidrit ($NaBH_4$), Paladyum (Pd), 4-Nitro fenol (4-NP), Metilen Mavisi (MB), Metil Portakal (MO).

Hazırlanan pd@polimer@cofe2o4 kompleksinin 4-np, mo ve mb substratlarının indirgeme/bozunma reaksiyonlarındaki katalitik etkinlikleri, sulu ortamda nabh4 varlığında araştırıldı. Bu amaçla öncelikle $NaBH_4$ miktari, substrat konsantrasyonu ve katalizör miktari taranarak optimum reaksiyon koşulları belirlendi. Bu deneysel çalişmada Pd@Polymer@$CoFe_2O_4$ katalizörünün konsantrasyonlari 2 mg, 1 mg ve 0,5 mg olarak değiştirildi. Bu konsantrasyonlarin boya bozunmasi için en kisa reaksiyon süresine neden olduğu gözlendi. Sonuç olarak, sözde birinci dereceden kinetiğin uygulanması hız sabitlerinin tahmin edilmesine olanak sağladı. Elde edilen sonuçlar, boyaların katalitik renk gideriminin, aşağidaki denklemde ifade edilen birinci dereceden kinetik modelle tanımlanabileceğini göstermektedir:

$$\ln(C_0/C_t) = K \times t \qquad (1.1)$$

Burada, $\boldsymbol{C_0}$ başlangıç konsantrasyonunu, $\boldsymbol{C_t}$ zamanındaki konsantrasyonu ve $\boldsymbol{K}$ görünür sabit hızı temsil eder.

$CoFe_2O_4$ parçacıkları kolay bir solvotermal yöntemle sentezlendi. Kısaca 1.6 $CoCl_2.6H_2O$, 2.0 g $FeCl_3.6H_2O$ ve 4.8 g sodyum asetat, 60.0 ml Etilen glikol içerisinde çözüldü ve karışım, oda sıcaklığında 30 dakika kuvvetlice karıştırıldı. Daha sonra karışım, 100 ml'lik teflon kaplı paslanmaz çelik bir reaktöre aktarıldı ve 8 saat süreyle 200 °C'ye ısıtıldı. Oda sıcaklığına soğutulduktan sonra siyah ürün sırasıyla bol su ve Etanol ile yıkandı ve 60 °C'deki vakumlu fırında kurutuldu.

Yüzeyle başlatılan polimerizasyon yoluyla manyetik jelin hazırlanması için $CoFe_2O_4$ parçacıkları ilk olarak MPS ile değiştirildi. daha sonra 100 mg Fe_3O_4 partikülü oda sıcaklığında 15 dakika ultrasonik işlemle 50 ml Etanol içerisinde dağıtıldı. daha sonra karışıma 250 µL MPS ilave edildi ve karışım oda sıcaklığında, nitrojen koruması altında 18 saat karıştırıldı. reaksiyonun ardından parçacıklar basit bir mıknatısla toplandı ve bol miktarda etanol ile yıkandı. son olarak ürün vakumlu fırında kurutuldu.

Bunun için 50 mg Polimer@$CoFe_2O_4$ oda sıcaklığında 15 dakika ultrasonik işlemle 10 ml H_2O içerisinde dağıtıldı ve dispersiyona 12,8 mg $K2PdCl_4$ eklendi. Karışım, oda sıcaklığında 1 saat boyunca 600 rpm'de mekanik bir karıştırıcı ile karıştırıldı ve daha sonra Pd^{2+}'nın Pd^0'a düşürülmesi için sulu bir $NaBH_4$ (4.0 mg/ml) çözeltisi damla damla ilave edildi. Karışım oda sıcaklığında 2 saat karıştırıldı ve reaksiyonun ardından ürün bir mıknatısla toplandı ve bol su ile yıkandı. Son olarak parçacıklar vakumlu bir fırında kurutuldu ve ihtiyaç duyulana kadar vakumlu desikatörde saklandı.

2. SONUÇLAR VE TARTIŞMA

SEM görüntüleri, $CoFe_2O_4$ parçacıklarının yüksek yüzey aktivitesi ve güçlü manyetizma nedeniyle kümelendiğini göstermektedir. Bu nanopartiküller çekici kuvvetler ve manyetik özellikler nedeniyle bir araya gelir. Bir polimer malzemeyle kaplanmış $CoFe_2O_4$ nanopartikülleri ortalama 32 nm boyuta sahiptir ve aralarındaki boşluklar, katalizörün gözenekliliğini artırarak kimyasal reaksiyonlar sırasında reaktanların ve ürünlerin difüzyonunu kolaylaştırır. Pd nanopartikülleri, Pd@Polimer@$CoFe_2O_4$ adı verilen katalizör yapısında bir polimere yapışarak, nanopartiküller ile polimer matrisi arasındaki uyumluluğu sağlar, partikül ayrılmasını önler ve katalizörün ömrünü arttırır. Bu yapışma aynı zamanda katalizörün genel yapısal ve termal stabilitesine de katkıda bulunur.

EDX analizi, $CoFe_2O_4$ nanopartiküllerinin katalitik aktivitesinin modifikasyon yöntemine bağlı olarak değiştiğini ortaya koymaktadır. $CoFe_2O_4$ nanopartikülleri yüksek kristalliğe ve minimum yabancı maddeye sahiptir, bu da üstün performans sağlar. Ancak Polimer matrislerle karıştırıldığında karbon (C) oranı artar, demir (Fe) ve kobalt (Co) oranı azalır. Katalitik aktivitedeki bu azalma, $CoFe_2O_4$ nanopartiküllerinin yüzey alanını ve reaksiyon merkezlerini azaltan Polimer matrislerine atfedilir. Ek olarak, Polymer@$CoFe_2O_4$ nanokompozitleri, saf $CoFe_2O_4$ nanopartiküllerine kıyasla daha düşük katalitik aktivite sergiler. $CoFe_2O_4$ nanopartikülleri Polimer matrisleri içerisinde kullanıldığında ve Pd ile kaplandığında katalitik aktivite artar. Sonuç olarak Pd@Polymer@$CoFe_2O_4$ nanokompozitleri daha yüksek katalitik aktivite sergiler.

Pd@Polimer@$CoFe_2O_4$ katalizörünün X-ışını kırınımı (XRD) analizinde, belirli 2θ değerlerinde (30.28, 35.66, 36.69, 42.12, 44.95, 54.95, 57.18 ve 63.95) keskin ve dar tepeler, her ikisi için de yüksek kristalliği gösterir. $CoFe_2O_4$ ve Pd nanopartikülleri. Ek olarak (2 2 0), (3 1 1), (4 0 0), (4 2 2), (5 1 1) ve (4 4 0) endekslerine karşılık gelen altı tepe noktası iyi biçimlenmiş bir yapıyı akla getirir. Bu çizgi profili uyumu sayesinde, 8,5 ±1 nm'lik ortalama kristalit boyutu belirlendi. Bu katalizör, test edilen malzemeler arasında en yüksek kristalliği sergiler ve bu da mükemmel yapısal bütünlük ve katalitik aktivite anlamına gelir.

$CoFe_2O_4$, Polimer@$CoFe_2O_4$ ve Pd@Polimer@$CoFe_2O_4$'nin manyetik parametreleri, titreşimli bir numune manyetometresi (VSM) aracılığıyla belirlendi.

$CoFe_2O_4$ en yüksek zorlayıcılık (0,5 kOe) ve kalıcı mıknatıslanma (58,2 emu/g^{-1}) değerlerine sahiptir. Bu, $CoFe_2O_4$'un sert manyetizmasını gösterir. Polymer@$CoFe_2O_4$'un koersivite (0,3 kOe) ve kalıcı mıknatıslanma (30,1 emu/g^{-1}) değerleri $CoFe_2O_4$'dan daha düşüktür. Bu, $CoFe_2O_4$ nanopartiküllerinin üzerine bir kaplama olarak manyetik olmayan bir Polimer matrisinin uygulandığını göstermektedir. En düşük koersivite (0,1 kOe) ve kalıcı mıknatıslanma (11,8 emu/g-1) değerlerine sahip olan Pd@Polymer@$CoFe_2O_4$ katalizörü, onu aralarında en yumuşak mıknatıs haline getirmektedir. yukarıda belirtilen bulguların, harici bir manyetik alan kullanılarak Pd@Polymer@$CoFe_2O_4$ nanokatalizörünün izolasyonu ve yeniden kullanımı için basit ve etkili bir yöntem sağladığını göstermektedir.

XPS, C1s, Co2p, Fe2p, N1s, O1s ve Pd3d sinyallerini açıkça gösteren, hazırlanan Pd@Polimer@$CoFe_2O_4$ kompozit katalizörünün yüzey kimyasal bileşimini değerlendirmek için kullanıldı. C1 spektrumundaki 285 eV bağlanma enerjisi, karbon kimyasal ortamlarını ve hibridizasyon durumlarını akla getirir. (C-C)'ye tahsis edilmiştir. Numunenin birkaç karbon durumu vardır. Co2p spektrumundaki 782.52 ve 797.25'teki iki tepe, bileşiğin Co^{2+} oksidasyon durumunu doğruladı. Oktahedral bölgenin Fe^{3+} değerlik durumu, Fe2p spektrumunda 712,45 ve 725 eV'de iki tepe noktasıyla gösterilir. 400,2 eV'deki bir N1s spektral zirvesi, çeşitli nitrojen kimyasal ortamlarını ve yüzey fonksiyonel gruplarını gösterir. O1 spektrumundaki 531,50 eV'deki zirve, çeşitli kimyasal koşullarda oksijen bağlama enerjisini gösterir ve (C-O-O)'ya atfedilir. 336.1 ve 341.2 eV'deki iki Pd3d zirvesi, Pd'nin (Pd^0) metalik formunun $3d_{3/2}$ ve $3d_{5/2}$'sine karşılık gelir; bu, Pd^{2+}'nın çoğunlukla metalik Pd'ye indirgendiğini doğrular; bu, katalitik aktiviteyle ilişkili olabilir.

Bu çalışmada üretilen bileşiklerin katalitik performansı, 4-NP, MB ve MO olmak üzere üç organik boya kullanılarak değerlendirildi. Zaman içindeki boya bozulmasının ölçümü, UV-vis spektrofotometresi kullanılarak gerçekleştirilir.

Katalizör (Pd@Polimer@$CoFe_2O_4$), 2 mg, 1 mg ve 0,5 mg konsantrasyonlarda 0,6, 2 ve 3 dakika içinde sarıdan renksiz bir renk değişimine neden oldu. Absorbsiyon zirvesi 400 nm civarındaydı ve oda sıcaklığında stabildi. Konsantrasyon azaldıkça, katalitik 4-NP bozunma hızı arttı ve bu da bozunmanın hızlanmasına neden oldu. Renk değişiminin hızı, katalizör konsantrasyonuna bağlıdır; daha yüksek konsantrasyonlar,

daha hızlı bir hıza neden olur. $CoFe_2O_4$ @Pd, 7 dakika içinde boya adsorpsiyonunu azalttı; bu, yetersiz aktif katalitik bölgelerin göstergesidir. Pd nanopartikülleri hidrojenasyon reaksiyonları için mükemmel katalizörlerdir ancak 2 mg $CoFe_2O_4$ nanopartikülleri kullanıldığında absorpsiyonda herhangi bir değişiklik gözlenmemiştir.

2 mg, 1 mg ve 0,5 mg konsantrasyonlarda Pd@Polimer@$CoFe_2O_4$ katalizörü kullanılarak, katalizör-renk giderme verimliliği reaksiyonu çeşitli miktarlarda test edildi. En önemli faktör MB boyasının renksizlik süresidir. 660 nm'de bir emilim zirvesi ortaya çıkardı ve daha yüksek katalizör dozlarıyla 1,5, 4 ve 6 dakikada renk giderimi daha hızlı oldu. Bu model, katalizörün renk giderme verimliliğini gösterir. Katalitik doz, katalizör yüzeyindeki aktif katalitik bölgelere bağlı olarak renk giderme süresini azaltabilir. Daha fazla katalizör aktif bölge boya molekülleri ile etkileşime girerek boya bozunmasını hızlandırır. Bunu 2 mg $CoFe_2O_4$@Pd molekülü takip eder. MB boyasının 7 dakika sonra solmasına neden oldu. MB boyasını hızlı bir şekilde parçalamak için yeterli aktif katalitik bölge bulunmayabilir. $CoFe_2O_4$@Polimer katalizörü 9 dakika sürerken renk solmadı. Hidrojenasyon reaksiyonları için mükemmel katalizörler olan Pd nanopartiküllerinin yokluğunda indirgeme reaksiyonlarının yavaş gerçekleştiğini gösterir. Tek başına uygulandığında $CoFe_2O_4$, boyayı bozmadı.

(Pd@Polimer@$CoFe_2O_4$) 2 mg, 1 mg ve 0,5 mg'lık katalizör miktarları test edildi, 460 nm'de bir absorpsiyon zirvesi ortaya çıktı, 0,4, 1 ve 2 dakikada renk giderimi daha hızlı oldu. Bu model, katalizörün renk giderme verimliliğini gösterir. Katalitik doz, katalizör yüzeyindeki aktif katalitik bölgelere bağlı olarak renk giderme süresini azaltabilir. Daha fazla katalizör aktif bölgesi boya molekülleri ile etkileşime girerek boya bozunmasını hızlandırır.

Bunu 2 mg $CoFe_2O_4$@Pd molekülü takip eder. MO boyasının 6 dakika sonra solmasına neden oldu. MO boyasını hızlı bir şekilde parçalamak için yeterli aktif katalitik bölge bulunmayabilir. $CoFe_2O_4$@Polimer katalizörü 7 dakika sürerken renk solmadı. Hidrojenasyon reaksiyonları için mükemmel katalizörler olan Pd nanopartiküllerinin yokluğunda indirgeme reaksiyonlarının yavaş gerçekleştiğini gösterir. Tek başına uygulandığında $CoFe_2O_4$, boyayı bozmadı.

Pd@Polymer@$CoFe_2O_4$ katalizörü mükemmel dağılabilirliğe sahiptir ve mıknatıs kullanarak kolay toplama sağlar. Sonuç olarak, bu katalizör, katalitik işlemden sonra verimli bir şekilde geri dönüştürülebilir. Pd@Polymer@$CoFe_2O_4$ katalizörü, çok sayıda döngü boyunca sürekli katalitik aktivite sergileyerek stabilitesini doğruladı. Absorbsiyon kapasitesi, birbirini takip eden 5 yineleme sırasında küçük bir düşüş sergiledi; 4-NP için %71,6, MB için %70,7 ve MO için %74,8'lik düşüşler görüldü. Yukarıda belirtilen gözlem, katalizörün organik boya kirliliğini etkili bir şekilde azaltmada olası pratik kullanımının ve yeniden kullanım ve geri dönüşüme uygunluğunun altını çizmektedir.

3. SONUÇ

Mevcut çalışma, büyük etkinlik sergileyen bir birlikte çökeltme tekniği kullanarak bir Pd@Polimer@$CoFe_2O_4$ manyetik nanokatalizörünü etkili bir şekilde sentezledi. Ek olarak, elde edilen veriler 4-NP, MB ve MO boyaları için olağanüstü aktivite gösterdi. Pd@Polimer@$CoFe_2O_4$ katalizörü, metil turuncu boya için daha yüksek bir parçalanma oranına sahiptir. Bulgulara dayanarak, incelenen diğer tonlarla karşılaştırıldığında metil turuncunun en yüksek oranda bozulma gösterdiği sonucuna varılabilir. Ayrıca, bu ayırt edici nanokatalizör, harici manyetik kullanımıyla reaksiyon karışımından zahmetsizce ekstrakte edilebilir. Bu nedenle, bir dizi heterojen katalitik indirgeme uygulaması için çok etkili manyetik katalizörlerin üretimi için uygun bir ortam olarak umut vaat etmektedir.

CURRICULUM VITAE

Personal Information

Name Surname : Mohammed AbdulKareem SHALLAL

Education Information

Undergraduate

University : Technological University/ Baghdad- Iraq

Faculty : College of Engineering

Department : Chemical Engineering

Graduation Year : 2004-2005

VAN YÜZÜNCÜ YIL UNIVERSITY
THE INSTITUTE OF NATURAL AND APPLIED SCIENCES
THESIS ORIGINALITY REPORT

Date 18 /10 /2023

Thesis Title: **PREPARATION OF MAGNETIC GEL-POLYMER BRUSH/METAL NANOPARTICLE HYBRID MATERIALS FOR CATALYTIC DEGRADATION OF SOME ORGANIC DYES**

The title of the mentioned my thesis, above having total (90) pages with cover page, introduction, main parts and conclusion, has been checked by me/my supervisor for originality by Turnitin computer program on the date of 18/10/2023 and its detected similary rate was 13% (thirteen percentage) according to the following specified filtering.

The applied filters are given below:

- Excluding the acceptance and approval page,
- Excluding Acknowledgments,
- Excluding table of contents,
- Excluding symbols and abbreviations,
- Excluding materials and methods,
- Excluding references,
- Excluding quotations,
- Excluding publications derived from the thesis
- Excluding the text parts less than 7 words (Limit match size to 7 words)

I read the Thesis Originality Report instruction of Van Yuzuncu Yil University for Obtaining and Using Similarity Rate for the thesis and I declare my thesis does not contain any plagiarism according to the maximum similarity rates specified in this directive; otherwise I accept all kinds of legal responsibility for any dispute arising in situations which are likely to be detected and I declare that the information I have given above is correct.

I submit it to your information.

Date and Signature

Name and Surname: Mohammed Shallal
Student ID: 20910001229
Department: Chemical Engineering
Program:
Status: (X) M.Sc ( ) Ph.D.

SUPERVISOR	**APPROVAL OF THE INSTITUTE**
Assoc. Prof. Dr. Adem ZENGIN SUITABLE	SUITABLE